



**PRC2 inhibition counteracts
the culture-associated loss of
engraftment potential of human
cord blood-derived hematopoietic
stem/progenitor cells**

**Die Inhibition des PRC2 wirkt
dem Kultur-bedingten Verlust
des Repopulationspotenzials
in humanen hämatopoetischen
Stammzellen/Vorläuferzellen aus
Nabelschnurblut entgegen**

Doctoral thesis for a doctoral degree
at the Julius-Maximilians-Universität Würzburg,
submitted by

Linda Varagnolo

from
Chioggia, Italy

Würzburg 2014





PRC2 inhibition counteracts
the culture-associated loss of
engraftment potential of human
cord blood-derived hematopoietic
stem/progenitor cells

Die Inhibition des PRC2 wirkt
dem Kultur-bedingten Verlust
des Repopulationspotenzials
in humanen hämatopoetischen
Stammzellen/Vorläuferzellen aus
Nabelschnurblut entgegen

Doctoral thesis for a doctoral degree
at the Julius-Maximilians-Universität Würzburg,
submitted by

Linda Varagnolo

from
Chioggia, Italy

Würzburg 2014

Submitted on: _____
Office stamp

Members of the *Promotionskommission*:

Chairperson:

Primary Supervisor: Prof. Dr. Albrecht Müller

Supervisor (Second): Prof. Dr. Ricardo Benavente

Date of Public Defence: _____

Date of receipt of certificate: _____

TABLE OF CONTENTS

1 SUMMARY	9
2 ZUSAMMENFASSUNG	11
3 ABBREVIATIONS	13
4 INTRODUCTION	16
4.1 Hematopoiesis	16
4.1.1 Hematopoietic stem cell	16
4.1.2 HSC transplantation (HSCT).....	18
4.1.3 Sources of HSCs for transplantation	19
4.1.4 Umbilical cord blood as source of HSCs	19
4.1.5 Expansion strategies	21
4.1.6 Cytokine-based <i>ex vivo</i> expansion.....	22
4.2 Epigenetics	23
4.2.1 Bivalent domains.....	24
4.2.2 Epigenetic regulation of hematopoiesis	25
4.2.3 EZH2 in hematopoiesis.....	27
4.3 Aim and experimental strategy	28
5 RESULTS	29
5.1 Morphological and immunophenotypic changes upon expansion of human CB-CD34 ⁺ cells.....	29
5.2 NSG transplantation of expanded CB-CD34 ⁺ cells with different cytokine combinations	31
5.3 Expansion of CB-CD34 ⁺ cells is accompanied by marginal changes of gene expression but significant alterations of global histone modification.....	33
5.4 Remodelling of H3K4me ³ and H3K27me ³ marks upon culture of CB-CD34 ⁺ cells	38
5.5 Clonogenic potential of EZH2 inhibitor-treated CB-CD34 ⁺ cells	53
5.6 EZH2 inhibition increases the engrafting potential of expanded CB-CD34 ⁺ cells	55
6 DISCUSSION	58
6.1 STFIA cocktail maintains the engrafting potential of CB-CD34 ⁺ cells	58
6.2 Global levels of H3K4me ³ and H3K27me ³ change upon expansion of CB-CD34 ⁺ cells.....	61
6.3 <i>Ex vivo</i> expansion of CB-CD34 ⁺ cells remodels the distribution of H3K4me ³ and H3K27me ³ histone modification marks.....	62

6.4 The treatment of STF-cultured CB-CD34 ⁺ cells with two different EZH2 inhibitors increases hematopoietic engraftment...	66
7 MATERIALS AND METHODS	69
7.1 Materials	69
7.1.1 Cell culture media and supplements	69
7.1.2 Antibodies	70
7.1.3 Primers	71
7.1.4 Kits and reagents	72
7.1.5 Consumables	73
7.1.6 Buffers and solutions	73
7.1.7 Animals	75
7.1.8 Equipment	76
7.1.9 Softwares	76
7.2 Methods	77
7.2.1 Informed consent and CB collection	77
7.2.2 Criteria for the storage of samples prior to processing	77
7.2.3 Isolation of CD34 ⁺ cells from CB	77
7.2.4 Culture of CD34 ⁺ cells	78
7.2.5 Immunostainings of fresh and cultured CD34 ⁺ cells	79
7.2.6 Inhibitor treatment	79
7.2.7 Colony-forming unit (CFU) assays	79
7.2.8 Hematoxylin & Eosin staining	80
7.2.9 Flow cytometry membrane staining	81
7.2.10 Intranuclear staining	81
7.2.11 FACS data analysis	82
7.2.12 RNA isolation	82
7.2.13 DNase treatment and cDNA synthesis	83
7.2.14 Primer design and quantitative realtime PCR	83
7.2.15 Global gene expression analysis (Microarray)	84
7.2.16 Western blot	85
7.2.17 Chromatin immunoprecipitation (ChIP) low cell number	85
7.2.19 NSG Mouse line	88
7.2.20 Primary and secondary NSG transplantation	88
7.2.21 Organs preparation and analysis of human cell engraftment	89
7.2.22 Statistical analysis	90
8 BIBLIOGRAPHY	91
9 ACKNOWLEDGMENTS	105
10 AFFIDAVIT	106
11 LIST OF PUBLICATIONS	108

1 SUMMARY

Cord blood hematopoietic stem cells (CB-HSCs) are an outstanding source for the treatment of a variety of malignant and non-malignant disorders. However, the low amount of cells collected per donor is often insufficient for treatment of adult patients. In order to make sufficient numbers of CB-HSCs available for adults, expansion is required. Different approaches were described for HSC expansion, however these approaches are impeded by the loss of engrafting potential during *ex vivo* culture. Little is known about the underlying molecular mechanisms. Epigenetic mechanisms play essential roles in controlling stem cell potential and fate decisions and epigenetic strategies are considered for HSC expansion. Therefore, this study aimed to characterize global and local epigenotypes during the expansion of human CB-CD34⁺, a well established CB progenitor cell type, to better understand the molecular mechanisms leading to the culture-associated loss of engrafting potential. Human CB-CD34⁺ cells were cultured using 2 different cytokine cocktails: the STF cocktail containing SCF, TPO, FGF-1 and the STFIA cocktail, which combines STF with Angiopoietin-like 5 (Angptl5) and Insulin-like growth factor-binding protein 2 (IGFBP2). The latter expands CB-HSCs *ex vivo*. Subsequently, the NOD-scid gamma (NSG) mouse model was used to study the engraftment potential of expanded cells. Engraftment potential achieved by fresh CB-CD34⁺ cells was maintained when CB-CD34⁺ cells were expanded under STFIA but not under STF conditions. To explore global chromatin changes in freshly isolated and expanded CB-CD34⁺ cells, levels of the activating H3K4me³ and the repressive H3K27me³ histone marks were determined by chromatin flow cytometry and Western blot analyses. For analysis of genome-wide chromatin changes following *ex vivo* expansion, transcriptome profiling by microarray and chromatin immunoprecipitation combined with deep sequencing (ChIP-seq) were performed. Additionally, local chromatin transitions were monitored by ChIP analyses on promoter regions of developmental and self-renewal factors. On a global level, freshly isolated CD34⁺ and CD34⁻ cells differed in H3K4me³ and H3K27me³ levels. After 7 days of expansion, CD34⁺ and CD34⁻ cells adopted similar levels of active and repressive marks. Expanding the cells without IGFBP2 and Angptl5 led to a higher global H3K27me³ level. ChIP-seq analyses revealed a cytokine cocktail-dependent redistribution of H3K27me³

profiles. Chemical inhibition of the H3K27 methyltransferase EZH2 counteracted the culture-associated loss of NSG engraftment potential. Collectively, the data presented in this study revealed that by adding epigenetically active compounds in the culture media we observed changes on a chromatin level which counteracted the loss of engraftment potential. H3K27me³ rather than H3K4me³ may be critical to establish a specific engraftment supporting transcriptional program. Furthermore, I identified a critical function for the Polycomb repressive complex 2-component EZH2 in the loss of engraftment potential during the *in vitro* expansion of HPSCs. Taken together this thesis provides a better molecular understanding of chromatin changes upon expansion of CB-HSPCs and opens up new perspectives for epigenetic *ex vivo* expansion strategies.

2 ZUSAMMENFASSUNG

Hämatopoetische Stammzellen aus Nabelschnurblut (CB-HSCs) sind eine bedeutende Quelle für die Behandlung einer Vielzahl maligner und nicht-maligner Erkrankungen. Allerdings ist die geringe Anzahl an Stammzellen, die von einem Spender gewonnen werden kann, meist nicht ausreichend für die Rekonstitution des hämatopoetischen Systems erwachsener Patienten. Um eine ausreichende Menge an CB-HSCs zu gewinnen, ist eine Expansion der Zellen erforderlich. Verschiedene Ansätze zur *ex vivo* Expansion von HSCs wurden beschrieben, allerdings waren diese Ansätze durch den Verlust des Repopulationspotentials während der *ex vivo* Kultivierung nicht umsetzbar. Über die zugrundeliegenden Mechanismen ist wenig bekannt. Epigenetische Mechanismen spielen eine entscheidende Rolle in der Kontrolle von Selbsterneuerung und Differenzierung von Stammzellen. Aus diesem Grund werden epigenetische Strategien zur HSC-Expansion in Betracht gezogen. Das Ziel dieser Studie war, globale und lokale Epigenotypen während der Expansion humaner CB-CD34⁺-Zellen (CB-Vorläuferzellen) zu charakterisieren. Diese Studien sollten zu einem besseren Verständnis der molekularen Mechanismen, welche zum Kultivierungs-assoziierten Verlust des Repopulationspotentials führen. Humane CB-CD34⁺-Zellen wurden in zwei verschiedene Zytokin-Cocktails kultiviert: Der sogenannte STF-Cocktail, welcher SCF, TPO und FGF-1 enthält und der STFIA-Cocktail, welcher STF mit Angptl5 und IGFBP2 kombiniert. Aus der Literatur war zu Beginn dieser Doktorarbeit bekannt, dass CB-HSCs *ex vivo* in STFIA, nicht aber in STF expandiert werden können. In Übereinstimmung mit diesem Befund zeigen die hier vorgestellten heterologen Transplantationsexperimente, dass das Repopulationspotential frischer CB-CD34⁺-Zellen nur erhalten blieb, wenn die Zellen unter STFIA, jedoch nicht, wenn sie unter STF-Bedingungen expandiert waren. Um die globalen Chromatinveränderungen frisch isolierter und expandierter Zellen zu untersuchen, wurden die Level der aktivierenden Histonmodifikation H3K4me³ und der repressiven H3K27me³-Modifikation durch Chromatin-Durchflusszytometrie und Western Blot Analyse bestimmt. Zur Analyse der genomweiten Chromatinveränderungen nach *ex vivo* Expansion wurden

Transkriptomprofile durch Mikroarray und Chromatin-Immunpräzipitation, in Kombination mit Deep-Sequencing (ChiP-Seq) durchgeführt.

Zusätzlich wurden lokale Chromatinveränderungen durch ChiP-Analysen an Promotorregionen von Entwicklungs- und Selbsterneuerungs-Faktoren analysiert. Auf globaler Ebene unterschieden sich frisch isolierte CD34⁺ und CD34⁻ Zellen in ihren H3K4me³ und H3K27me³ Leveln. Nach siebentägiger Expansion nahmen CD34⁺ und CD34⁻ Zellen ähnliche Level aktiver und repressiver Markierungen an. Die Expansion der Zellen ohne IGFBP2 und Angptl5 führte zu höheren globalen H3K27me³ Leveln. ChiP-seq Analysen zeigten eine Zytokin-Cocktail-abhängige Neuverteilung von H3K27me³ Mustern. Die chemische Inhibition der H3K27me-Transferase EZH2 wirkte dem Kultivierungs-assozierten Verlust des NSG Repopulationspotentials entgegen. Zusammenfassend zeigen diese Daten, dass durch die Zugabe von spezifischen Zytokinen in das Kulturmedium Veränderungen auf Chromatinebene verbunden sind, die dem kultivierungs-assozierten Verlust des Repopulationspotentials entgegen wirken. Diese Daten zeigen weiterhin, dass die durch die PRC2 Komponente EZH2 vermittelte H3K27me³, nicht jedoch die H3K4me³ Histonmodifikation ein kritischer Faktor für die Etablierung eines die Repopulation fördernden Transkriptionsprogrammes ist. Somit dient diese Arbeit einem besseren molekularen Verständnis der Chromatinveränderungen während der Expansion von CB-HSPCs und eröffnet eine Perspektive für neue epigenetische *ex vivo* Expansionsstrategien.

3 ABBREVIATIONS

%	percent
°C	degree Celsius
Angptl5	Angiopoietin-like 5
APC	Allophycocyanin
BFU-E	burst forming unit - erythroid
BM	bone marrow
bp	base pair
BSA	Bovine Serum Albumin
cDNA	complementary deoxyribonucleic acid
CFU	colony forming unit
ChIP	Chromatin immunoprecipitation
DAPI	4,6-diamidino-2-phenylindole
ddH ₂ O	double distilled water
DEPC	diethylpyrocabonate
DMEM	Dulbecco's Modified Eagles Medium
DMSO	dimethyl sulfoxide
DNA	Deoxyribonucleic acid
DNase	Deoxyribonuclease
dNTP	deoxynucleotide triphosphate
EDTA	ethylenediaminetetraacetic acid
ESC	embryonic stem cells
<i>et al.</i>	et alii (and others)
EtOH	Ethanol
EZH2	Enhancer of zeste 2
FACS	fluorescence activated cell sorting
FGF-1	Fibroblast growth factor-1

FL	Fetal liver tyrosine kinase-3 ligand
FITC	Fluorescein Isothiocyanate
FCS	Fetal Calf Serum
g	gram
GM	granulocyte, macrophage
GEMM	granulocyte, erythrocyte, macrophage, and megakaryocyte
GO	Gene Ontology
Gy	Grey
GvHD	graft-versus-host disease
h	hour
HLA	Human leukocyte antigen
Hox	Homeobox
HOXB4	Homeoprotein homeobox B4
HRP	HorseRadish Peroxidase
HSC	hematopoietic stem cells
HSPC	hematopoietic stem and progenitor cells
IGFBP2	Insulin-like growth factor-binding protein 2
IL-3	Interleukin-3
IL-6	Interleukin-6
k	kilo
Kb	kilo bases
l	liter
m	milli, [10^{-3}]
M	Molarity [mol/l]
max	maximum
min	minimum
min	minute
mRNA	messenger RNA
n	nano [10^{-9}]
NSG mice	NOD.Cg-Prkdc ^{scid} Il2rg ^{tm1Wjl} /SzJ mice
PB	peripheral blood
PBS	Phosphate Buffer Saline
PE	Phycoerythrin

PcG	Polycomp group
PCR	polymerase chain reaction
RNA	Ribonucleic Acid
rpm	revolutions per minute
rt	room temperature
SDS	Sodium Dodecyl Sulfate
s	second
SP	spleen
STF	Stem cell factor
TBE	Tris Borate EDTA
TE	Tris EDTA
TEMED	N,N,N',N'-Tetramethylethylenediamine
TNC	total nuclear cell
TPO	Thrombopoietin
TSS	transcriptional start site
Tris	Tris-(Hydroxymethyl)-Aminoethan
TrxG	Trithorax group
U	units
UCBT	umbilical cord blood transplantation
UV	ultra violet
μ	micro[10 ⁻⁶]

4 INTRODUCTION

4.1 Hematopoiesis

Blood is one of the most regenerative adult tissues in the human body. About 500 billion blood cells are generated per day from the adult bone marrow, in a process known as hematopoiesis (from the Greek 'haima': blood, and 'poiein': to make) (Doulatov *et al.*, 2012). Hematopoiesis is organized as a cellular hierarchy of stem, progenitor and mature cells (see Figure 1). Every mature blood cell derives from a common progenitor cell called hematopoietic stem cell (HSC) that is capable of entering the cell cycle and then either undergoes self-renewal or it differentiates into a multipotent progenitor cell (Adams *et al.*, 2006). HSCs are multipotent adult stem cells critical for life-long blood production. HSCs stand on the top of the hematopoietic hierarchy, composed of an organized sequence of cells and precursors that can differentiate into two main lineages, the lymphoid and the myeloid lineages (Arai *et al.*, 2007; Müller-Sieburg *et al.*, 2002). In mouse, primitive HSCs first originate at day 7,5 of gestation in the extra-embryonic yolk sack, and at day 10,5 they are found in an area around the dorsal aorta termed the aorta-gonad mesonephros (AGM) region (Müller *et al.*, 1994; Medvinsky *et al.*, 2011). HSCs then migrate to the fetal liver, where finally they are mobilized into bone marrow (BM) and spleen. From birth on the major hematopoietic tissue remains the bone marrow (Medvinsky *et al.*, 2011).

4.1.1 Hematopoietic stem cell

HSCs are defined by their abilities to self-renew and to produce differentiated blood cells (Orkin *et al.*, 2008). They are an extremely rare heterogeneous population of cells (Catlin *et al.*, 2011). Wang *et al.* reported that in humans only 1 in 3×10^6 cells in the BM is a transplantable HSC (Wang *et al.*, 1997). The first evidences providing the existence of blood-forming stem cells were published in the early 60s, when James Till and Ernest McCulloch discovered that the mouse BM contained highly proliferative progenitor cells that were able to give rise to clonogenic mixed colonies of hematopoietic cells within the spleen of irradiated hosts, the so

called colony forming units-spleen (CFU-S) (Till, McCulloch 1961). HSCs reside in the BM in a complex microenvironment termed niche. The BM niche is composed of stromal cells, extracellular matrix molecules, growth factors and cytokines (Arai *et al.*, 2005; Ehninger *et al.*, 2011). HSCs characteristics of self-renewal, proliferation and differentiation are driven by their niches. These special environments control HSC maintenance and differentiation. Most of the HSCs are quiescent, a process that is controlled by a combination of intrinsic and extrinsic cellular mechanisms (Purton *et al.*, 2009).

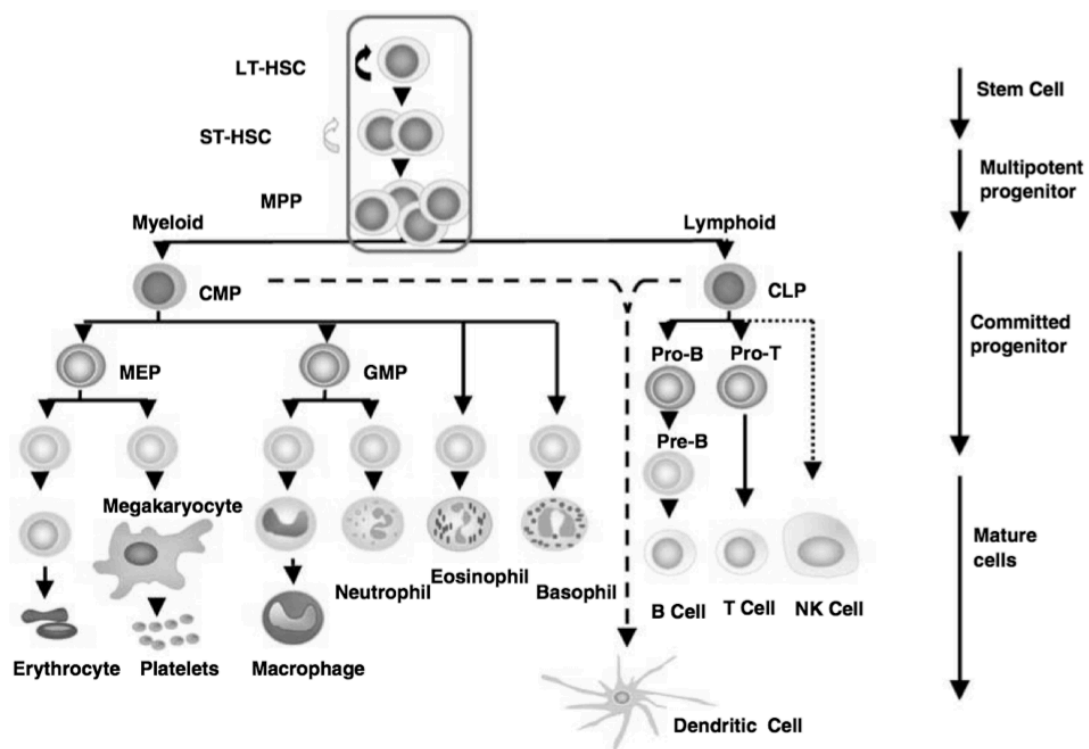


Figure 1: The hierarchy of hematopoietic cells. Shown is the hematopoietic system that starts with an HSC that balances between self-renewal and differentiation. HSCs generate *via* lineage committed progenitors all mature blood lineages. LT-HSC, long-term repopulating HSC; ST-HSC, short-term repopulating HSC; MPP, multipotent progenitor; CMP, common myeloid progenitor; CLP, common lymphoid progenitor; MEP, megakaryocyte/erythroid progenitor; GMP, granulocyte-macrophage progenitor (modified from Larsson *et al.*, 2005).

The genetic stability, integrity and regulation of HSCs are dependent on the nature of the interacting niche. For example in the endosteal niche, HSCs maintain their quiescence. In contrast activated HSCs reside in the so-called perivascular niche (Ehninger *et al.*, 2011; Wilson *et al.*, 2006). Moreover, HSCs are capable of two processes known as “mobilization” and “homing”, that involve sequential activation of adhesion molecules, in which HSCs

constantly move from the BM to the blood stream and *vice versa* (Lanzkron *et al.*, 1999; Orkin *et al.*, 2002). HSCs can be purified by the presence of specific surface markers that are characteristic for long-term/short-term repopulating-HSCs (LT-/ST-HSCs), and are distinguished from differentiated cells. CD34 was the first differentiation marker to be recognized on primitive human hematopoietic cells. CD34 is still a widely used marker to obtain enriched populations of human HSCs, as more than 99% of human HSCs are CD34⁺ (Civin *et al.*, 1984, Ishii *et al.*, 2011). Further analyses revealed that in human BM, HSCs are highly enriched within the Lin⁻CD34⁺CD38⁻CD90⁺CD45RA⁻CD49f⁺ population (Bhatia *et al.*, 1997; Notta *et al.*, 2011, Doulatov *et al.*, 2012). HSCs can only be identified *via* functional repopulation assays using long-term repopulation of a recipient hematopoietic system (Kollet *et al.*, 2000). A 12 weeks period of repopulation is chosen by most researchers to define enriched cells as LT-HSCs, however a longer period of 8 months was considered the best choice to distinguish between transient and long term reconstituting HSCs (Glimm *et al.*, 2001; Notta *et al.*, 2011).

4.1.2 HSC transplantation (HSCT)

HSCs have been studied for more than 50 years, and this vast experience allowed scientists to develop sufficient understanding to use these cells in clinical therapies with increasing background knowledge. The transplantation of HSCs has evolved from a highly experimental procedure to a standard therapy (Gratwohl, Baldomero *et al.*, 2010). HSCT is done *via* intravenous infusion of autologous or allogeneic HSCs in order to restore the hematopoietic functions of a patient whose immune system is damaged or defective. More than 25.000 HSCTs are performed each year. HSCT has become the standard care for many patients with several malignant and non-malignant hematologic and other diseases (Ljungman *et al.*, 2006). Currently, most HSC transplant samples are isolated from peripheral blood (PB) after mobilization or from bone marrow (BM) aspirates of healthy donors. However, cord blood (CB)-derived HSCs are a promising alternative source for HSCT (Ballen *et al.*, 2013).

4.1.3 Sources of HSCs for transplantation

The sources of HSCs for autologous or allogeneic transplantation are BM, PB or CB. Adult humans have on average 2,6 kg of BM, the internal tissue of large bones. For transplantation, BM is harvested from the posterior iliac crests of donors and can be used directly for transplantation (Hatzimichael *et al.*, 2010). For a stable long-term engraftment, 2×10^8 nucleated BM cells per kg of patient's body are used, although even 1×10^8 /kg cells can be sufficient (Bahceci *et al.*, 2000). PB stem cells (PBSC) are also a widely used source for allogeneic transplantation due to the fact that they engraft more quickly than BM-derived HSCs (Lin *et al.*, 2011). PBSCs are obtained from the donor PB by apheresis, following treatment with granulocyte-colony stimulation factor to mobilize HSCs to the peripheral blood (Bensinger *et al.*, 1993). BM HSC and PBSC transplantation have however a high risk of graft-versus-host disease (GvHD), the HSCs from both these sources are difficult to obtain, and have a considerable risk of viral transmission. Moreover, for allogeneic HSCT, the possibility of receiving a transplant may be limited due to the low frequency of suitable human leukocyte antigen (HLA) donors. The discovery of CB HSCs as a source for transplantation has increased the chances of finding allogeneic donors for both pediatric and adult patients.

4.1.4 Umbilical cord blood as source of HSCs

Since the first umbilical cord blood transplantation (UCBT) was performed successfully in France in 1988 (Gluckman *et al.*, 1989) more than 30.000 UCBT have been done worldwide and more than 600.000 CB units have been stored for transplantation (Stanevsky *et al.*, 2009). CB as a source of HSCs has been increasingly used in the last two decades because of its rapid availability, banking features, absence of risk for mothers and newborns during CB collection, and reduced probability of transmitting infections from donor to recipient (Sideri *et al.*, 2011). Furthermore, UCBT showed increased chance of HLA matching between donor and patient; this is due to the higher flexibility in case of mismatches compared to BM or PBSC transplants, with a tolerance of 1-2 HLA mismatches out of 6 (Chao *et al.*, 2004). This characteristic is of primary importance as it holds the potential of finding donors for patients with rare HLA types or for ethnic minority populations. Moreover, UCBT showed a diminished incidence of GvHD in comparison to BM transplantation (Bradley *et al.*, 2005), because the new-born immune cells possess lower numbers and a mostly naive repertoire of

CB-derived T cells (Nitsche *et al.*, 2007; Garderet *et al.*, 1998). Recent studies have demonstrated that CB possesses a high number of immunosuppressive regulatory T cells (Godfrey *et al.*, 2005). Also, CB has a higher enrichment of HSCs compared to BM and PB (Wang *et al.*, 1997), and they proliferate more rapidly most likely due to longer telomere lengths of CB-derived HSCs (Gammaitoni *et al.*, 2004; Schuller *et al.*, 2007). CB units can be cryopreserved and stored for years without loss of cell viability (Broxmeyer *et al.*, 2011), this is why public CB banking is beneficial on a worldwide scale for a rapid availability of HSCs for transplantation. CB graft that contains $\geq 2 \times 10^7$ nucleated cells per kg, $\geq 1.7 \times 10^5$ CD34⁺ cells per kg of recipients body weight and has \leq two HLA disparities is acceptable for transplantation into adult recipients (Wagner *et al.*, 2002; Gluckman *et al.*, 2004; Kamani *et al.*, 2008). Therefore, for patients weighing more than 35 – 40 kg, obtaining enough cells from a single CB unit is challenging.

The above-discussed advantages are the primary reason why more than 30.000 UCBT were performed worldwide. However there are known disadvantages in using CB as source of HSC transplantation. Despite optimization of isolation and processing techniques, the low number of cells collected per CB unit, the longer time of engraftment in adult donors of neutrophils and platelets compared to BM or PBSCs, together with the inability to robustly expand CB-HSCs render insufficient HSC numbers a major constraint in many settings of UCBT (Rocha *et al.*, 2010; Laughlin *et al.*, 2004). Since engraftment failure and prolonged time to engraft due to low cell dose is the main limitation of UCBT, several approaches have been developed to overcome this obstacle. A promising strategy to overcome the low cell content of single CB units is co-transplantation of two units (Sideri *et al.*, 2011). In this approach, 2 partially HLA-matched CB units from unrelated donors are transplanted simultaneously (Barker *et al.*, 2003; Barker *et al.*, 2005). In the last decade the number of adult patients receiving double UCBT has increased more than the number of adults receiving single UCBT (Rocha *et al.*, 2010). For co-transplantation of two CB units, the CB grafts are chosen firstly based on the CD34⁺ cell dose and secondly on the degree of HLA disparity (Wagner *et al.*, 2002). However, combining two CB units raised questions regarding higher chances of GvHD, lack of engraftment due to the immune reactivity between the two units, and the graft-*versus*-graft effect (Tarnani *et al.*, 2008; Liao *et al.*, 2011). Therefore, besides the double CB transplantation strategy, UCBT is an important object of study to enhance its clinical efficacy *via* different approaches which include addition of mesenchymal stem cells, direct intra-bone injection, modulation of CD26 expression to improve the homing potential, and *ex vivo* expansion of HSCs isolated from CB (Delaney *et al.*, 2010), which is the focus of this study.

4.1.5 Expansion strategies

Despite the efforts of many scientists over the past 30 years focusing on finding optimal expansion conditions for HSCs, the efficient increase of HSCs numbers *in vitro* remains challenging (Chou *et al.*, 2010). Numerous experimental strategies were reported that allow robust expansion of HSCs and include the use of combinations of recombinant cytokines, a multitude of cell-intrinsic and extrinsic self-renewal factors, addition of stromal cell cultures, 3D culture systems, transcription inhibitors and copper chelators (Dahlberg *et al.*, 2011; Walasek *et al.*, 2012; Mendez-Ferrer *et al.*, 2010; Araki *et al.*, 2006; Seet *et al.*, 2009; Schiedlmeier *et al.*, 2007). Early clinical trials are currently evaluating the use of Notch signaling pathway to expand CB-derived HSPCs. Recent publications indicate a 100-fold increase in CD34⁺ cell numbers when cultured in the presence of Notch ligand Delta1 (Fernandez-Sanchez *et al.*, 2011; Delaney *et al.*, 2010), and showed improved engrafting potential in the myeloid compartment when tested in a Phase I trial (Delaney *et al.*, 2010). Under clinical evaluation are also co-culture systems expanding CB-derived HSPCs together with components of the stem cell niche (mesenchymal stromal cells) that reported a 40-fold expansion of CD34⁺ cells, neutrophil engraftment in 97% and platelet engraftment in 81% of patients (de Lima *et al.*, Blood. 2010; 116 Abstract 362). A tetraethylenepentamine (TEPA)-based expansion approach was reported to lead to a 159-fold increase in CD34⁺ cells after 7 days of expansion (Peled *et al.*, 2004), and CB-derived HSPCs expanded in the presence of the copper chelator TEPA resulted in 90% engraftment in patients with advanced hematological malignancies in a Phase I/II trial (de Lima *et al.*, 2008). A brief *ex vivo* incubation (1-2 hours) of CB units with prostaglandin E2 (PGE2) prior infusion is currently being tested in a clinical trial as it was reported that this incubation significantly increased the numbers of repopulating HSCs (Goessling *et al.*, 2009). In addition to this, a report by Boitano *et al.* identified an aryl hydrocarbon receptor antagonist named Stem-Regenin1 capable of robustly enhance HSCs expansion (Boitano *et al.*, 2010) in a pre-clinical model. Other studies report that the overexpression of the homeoprotein homeobox B4 (HOXB4) promotes HSCs expansion (Sauvageau *et al.*, 1995; Haddad *et al.*, 2008).

4.1.6 Cytokine-based *ex vivo* expansion

To establish optimum growth factor combinations for the expansion of isolated CB HSPCs different combinations and concentrations of cytokine cocktails are currently the topic of research (Lam *et al.*, 2001; Kelly *et al.*, 2009). Transcriptome studies of HSCs did not yet further improve the concept of HSC expansion (Ivanova *et al.*, 2002; McKinney-Freeman *et al.*, 2012), however it has been reported that the presence of stimulatory cytokines that act at early stages of hematopoiesis i.e. stem cell factor (SCF) and thrombopoietin (TPO) are essential for expansion of primitive hematopoietic cells (Piacibello *et al.*, 1997). These hematopoietic factors are present in most common combinations of cytokine cocktails together with fetal liver tyrosine kinase-3 ligand (FL), interleukin-6 (IL-6) and interleukin-3 (IL-3) (Kelly *et al.*, 2009). Fibroblast growth factor-1 (FGF-1) and insulin-like growth factor (IGF2) have also been reported as promising growth factors in the context of HSCs expansion (Yeoh *et al.*, 2006; Zhang *et al.*, 2004). This was supported by the discovery that all fetal liver and BM HSCs express receptors of IGF2 (Zhang *et al.*, 2004). Two years after that Zhang *et al.* reported that using a combination of SCF, TPO, IGF-2 and FGF-1 supplemented with Angiopoietin-like proteins (Angptls), a group of secreted glycoproteins, for 10 days resulted in up to 30-fold expansion of murine LT-HSCs (Zhang *et al.*, 2006). Furthermore, the introduction of Insulin-like growth factor-binding protein 2 (IGFBP2) and Angiopoietin-like 5 (Angptl5) as additional proteins increased 20-fold the number of human SCID-repopulating cells (SRCs) (Zhang *et al.*, 2008).

4.2 Epigenetics

In 1942 Conrad Waddington conceived the term epigenetics and described it as “the branch of biology which studies the causal interactions between genes and their products which brings the phenotype into being” (Waddington, 1942). Some years later, he sketched his model (Figure 2) into a simple visualization scheme with a downhill rolling marble representing the differentiation process and fate decisions. As a stem cell moves down, its

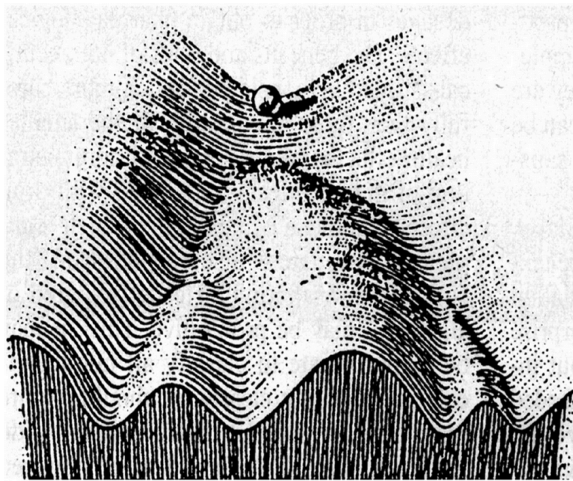


Figure 2: Waddington's epigenetic landscape.

The marble represents a stem cell rolling through developmental processes. Its fate depends on the path taken by the marble as it rolls down the valleys. Sketch, C.A. Waddington, 1957.

genetic information is not lost but becomes differentially expressed, and the potential of the cell becomes restricted. This model got support by John Gurdon who in 1958 discovered that by cell nuclear transplantation a mature somatic cell nucleus retains all the genetic information necessary to become any other cell of an organism (Gurdon *et al.*, 1958).

Today epigenetics is defined as the study of heritable changes in a gene function that do not entail a change in DNA sequence. In an eukaryotic cell, DNA is compact and folded by histone and nonhistone proteins into chromatin. All tissue-specific somatic cells possess the same genetic information but they exhibit different cell-type-specific gene expression patterns. Thereby *via* activating or silencing transcription distinct cell types use the same DNA sequence differently. Chromatin modifications, chemical modifications of DNA and histones, are the principal epigenetic mechanisms by which specific gene expression patterns are established and maintained (Dupont *et al.*, 2009). Also, non-coding RNAs, chromatin compactation and transcription factors define gene expression programs on the epigenetic level (Bonifer *et al.*, 2008). The gene expression patterns will be maintained beyond cell division (Egger *et al.*, 2004). Several histone modifications occur to transiently adjust chromatin density and tighten or loosen chromatin to forbid or to allow accessibility for chromatin-associated proteins. The combination of different histone modifications can be

regarded as the histone code that extends the information potential of the genetic code (Jenuwein *et al.*, 2001). Chromatin can switch between two principal configurations; euchromatin, characterized by a low condensation of nucleosomes that is accessible to the transcriptional machinery, and heterochromatin in which the high compaction of nucleosomes leads to the inaccessibility of DNA preventing transcription (Probst *et al.*, 2009). The structure of chromatin carries out essential functions *via* the condensation and protection of DNA but also *via* the preservation of genetic information and the control of gene expression. The N-terminal tails of core histones are subject to post-translational and reversible epigenetic modifications including acetylation, methylation, ubiquitination, phosphorylation, SUMOylation, citrullination or ADP-ribosylation. The importance of histone modifications is demonstrated by the fact that epigenetic mechanisms are essential for development and that epigenetic misregulation can lead to diseases including cancer (Rountree *et al.*, 2001).

4.2.1 Bivalent domains

The methylation of specific lysine and arginine residues at the N-terminal tails of histones is found in certain transcriptional regulatory regions of the genome. Such modifications have prominent roles in epigenetic regulation. Trithorax group (TrxG) proteins and Polycomb group (PcG) proteins are two systems with chromatin-modifying activities that are evolutionarily conserved and sustain gene activation and repression, respectively (Schuettengruber *et al.*, 2007). Both TrxG and PcG genes encode components of multiprotein complexes that regulate higher-order chromatin structure and accessibility of chromatin to various factors. Both influence gene expression by adding specific modifications to histone tails. A subset of TrxG proteins, SET1A, SET1B or MLL, catalyze the trimethylation of histone H3 lysine 4 (H3K4me³) that marks transcriptionally active regions (Shilatifard, 2012). In contrast, methylation of H3K27 is catalyzed by PRC2 component EZH2 or its homolog EZH1 (Shen *et al.*, 2008). H3K27me³ marks silenced chromatin (Margueron *et al.*, 2011). The coexistence of H3K27me³ and H3K4me³, also known as bivalent domains, maintains genes in a permissive chromatin conformation. Thus, developmental promoters have ready access to both transcriptional activation and inhibition in response to microenvironmental signals (Strahl *et al.*, 2000; Bernstein *et al.*, 2006; Jorgensen *et al.*, 2006).

4.2.2 Epigenetic regulation of hematopoiesis

Lineage-specific transcription factors and chromatin-associated factors direct the generation of all mature blood cells (Orkin *et al.*, 2008). Across all hematopoietic differentiation stages, transcriptional and epigenetic circuits work in close relationship for the maintenance of self-renewal and differentiation of HSCs, by a network that integrates and coordinates extra- and intracellular signals (Novershtern *et al.*, 2011). Epigenetic alterations result in the silencing of lineage-specific genes throughout hematopoietic differentiation. This is achieved *via* directly shaping and restricting the lineage potential of HSCs by controlling chromatin compaction and accessibility (Weishaupt *et al.*, 2010; Novershtern *et al.*, 2011). Particularly, the evolutionary conserved PcG and TrxG proteins have previously been identified as regulators of HSC functions (Huang *et al.*, 2013; Xie *et al.*, 2014). The major complexes formed by PcG proteins in mammals are the Polycomb Repressive Complex (PRC) 1 and 2. PRC2 is responsible for the *de novo* establishment of the repressive H3K27me³ mark (Sauvageau *et al.*, 2010). The H3K27me³ mark functions as a docking site to recruit the canonical PRC1, which maintains gene repression *via* ubiquitination of H2AK119 (Wang *et al.*, 2004). Among PRC1 proteins, the role of Bmi1 is crucial for PRC mediated silencing. Park *et al.* showed that the absence of Bmi1 reduced the long-term, but not short-term, repopulation capacity of HSCs (Park *et al.*, 2003). It has also been shown that overexpression of Bmi1 or EZH2, a subunit of PRC2, augments HSC self-renewal and prevents HSCs exhaustion (Iwama *et al.*, 2004; Kamminga *et al.*, 2006). However, EZH2 overexpression leads to a significant increase in HSCs and to abnormal myeloid expansion in BM, leading to the development of severe myeloproliferative disease (Herrera-Merchan *et al.*, 2012). EZH2 mutation was reported to cause deficiencies in early B cell development (Su *et al.*, 2002; Mochizuki-Kashio *et al.*, 2011). In addition, the deletion of the PRC2 component Eed resulted in HSC exhaustion (Xie *et al.*, 2014). Thus, there are different roles of PRC1 and PRC2 in the regulation of HSCs' cell status. DNA methylation is another important epigenetic modification, and some of the members of the DNA methyltransferase (DNMT) enzymes have pivotal roles in hematopoiesis. DNMT1 is essential for hematopoietic development. DNMT1-deficient HSCs showed reduced self-renewal and reduced myelo/erythroid lineage commitment (Trowbridge *et al.*, 2009). The loss of DNMT3A and DNMT3B at the same time results in an impairment of HSCs self-renewal (Tadokoro *et al.*, 2007). Moreover, loss-of-function mutations of the DNA demethylase TET2 are frequent in myeloid malignancies and TET2 is required for normal blood development. TET2-knockout mice showed expansion of HSCs with decreased differentiation potential and

developed leukemia at an early age (Moran-Crusio *et al.*, 2011). The crosstalk between DNA methylation and histone modifications during hematopoiesis is an active area of study. Also bivalent domains have an essential role in the regulation of hematopoietic genes. Many HSC- and HSPC-specific genes are also bivalently marked in ESCs, but lose the repressive H3K27me³ mark in early blood cells (Adli *et al.*, 2010). Remodelling of the bivalent landscape accompanies the differentiation of HSCs (Cui *et al.*, 2009; Weishaupt *et al.*, 2010; Abraham *et al.*, 2013). Epigenetics coordinates HSCs' function and differentiation, as supported by the notion that combinatorial modification patterns guarantee the cooperative regulation of transcription. This was supported by Cui *et al.* who mapped the epigenetic landscapes of HSCs and erythrocyte precursors (Cui *et al.*, 2009). Chung *et al.* compared H3 and H4 global acetylation levels of CD34⁺ and CD34⁻ cells and showed that HSCs and HSPCs have higher levels of acetylation than differentiated cells. Moreover they found that acetylation turnover was higher in immature cells pointing to a more dynamic and open chromatin in undifferentiated hematopoietic cells (Chung *et al.*, 2009). The study of global patterns of chromatin modifications will further help in understanding the mechanisms behind the maintenance and differentiation of HSCs. While high-resolution and genome-wide histone modification maps of fresh HSCs were described (Cui *et al.*, 2009; Adli *et al.*, 2010; Weishaupt *et al.*, 2010), the study of how *ex vivo* culture influence chromatin modifications of HSCs is still at an early stage. It was reported that, upon culture, human HPSCs acquired DNA-hypermethylation at specific sites in the genome (Yamagata *et al.*, 2012; Weidner *et al.*, 2013). The fundamental role of epigenetics in hematopoiesis was strengthened from the discovery of the involvement of chromatin modifiers in several blood malignancies (Neff *et al.*, 2013; Butler *et al.*, 2013; The Cancer Genome Atlas Research Network, 2013). The knowledge of chromatin remodeling during hematopoietic development is increasingly being translated into practice as epigenetic strategies are considered for HSC expansion and as treatment option for hematopoietic malignancies (Neff *et al.*, 2013; Obier *et al.*, 2010; Jones 2014; Mahmud *et al.*, 2014).

4.2.3 EZH2 in hematopoiesis

Over the last years, it was noticed that EZH2 is overexpressed in a variety of cancers, and that its overexpression is associated with aggressive tumor development and progression (Chen *et al.*, 2012; Bracken *et al.*, 2003). Therefore, the role of EZH2 in normal and malignant hematopoiesis has been an object of numerous studies. EZH2 is the methyltransferase component of PRC2, that is composed of three core components: EZH2, EED, and SUZ12. EZH2 was reported to be essential for cell proliferation (Bracken *et al.*, 2003). EZH2 expression is controlled by a complex network of mechanisms, and its dysregulation has been associated with various cancers. For instance, while EZH2 loss-of-function has been reported for myeloid leukemias, gain-of-function mutations have been found in lymphoid malignancies (Butler & Dent, 2013). Thus, depending on the cellular context and gene dosage, EZH2 can have a role either oncogenic in one setting or tumor-suppressiv in another, thereby underlining the complexity of epigenetic regulation. Moreover, EZH2 is capable of stabilizing chromatin structure and maintaining HSCs' self-renewal by silencing pro-differentiation genes and its ectopic expression confers growth advantages and facilitate the progression through the cell cycle (Kamminga *et al.*, 2006; Bracken *et al.*, 2003). These findings demonstrate the role of EZH2 in tumor progression and stem cell maintenance and this makes EZH2 an attractive therapeutic target. Several studies used the carbocyclic adenosine analog 3-deazaneplanocin (DZNep), known to inhibit methylation and to induce EZH2 degradation, and showed that it suppresses cancer growth and tumor formation (Chang *et al.*, 2012). However, the effect of DZNep is rather global upon histone methylation and not EZH2-specific (Miranda *et al.*, 2009). Numerous novel and selective small-molecule EZH2 inhibitors are in development, such as GSK126, GSK343, EPZ005687, EPZ-6438 and EI1 (Helin *et al.*, 2013). For instance, the use of GSK126 resulted in complete tumor growth inhibition and increased survival when assessed in xenograft models (McCabe *et al.*, 2012). The safe use of EZH2 inhibitors is an object of numerous studies, but several prolonged animal studies have shown their high tolerance which has lead to similar molecules such as EPZ-6438 to enter phase 1/2 clinical trial and several others will follow shortly (Knutson *et al.*, 2013). Combining the knowledge on the role of EZH2 in normal and malignant hematopoiesis and the development of novel selective epigenetic drugs will lead to targeted and lower toxicity therapies (Helin *et al.*, 2013).

4.3 Aim and experimental strategy

CB is a valuable source of HSCs for transplantation as a therapy for hematopoietic disorders. However due to the limited amount of CB-HSC available within a single graft CB-HSC transplantation is mainly restricted to pediatric recipients. During the last decades several combinations of cytokine cocktails have been tested for the *in vitro* expansion of human CB-CD34⁺ cells, a cell population that includes hematopoietic stem and progenitor cells (HSPCs). Zhang *et al.* in 2008 reported that IGFBP2 in combination with Angptl5 (STFIA cocktail) are powerful growth factors that support CB-CD34⁺ expansion (Zhang *et al.*, 2008). To prove the hypothesis that the epigenome of HSPCs defines their self-renewal and differentiation capacities, I sought to determine whether and how the expansion of CB-CD34⁺ cells under STFIA cocktail culture condition alters histone modifications genome-wide and remodels global and local chromatin states. This study firstly compared side by side the abilities of STF and STFIA cocktails to expand human CB-CD34⁺ cells *ex vivo* and to generate engraftment in NSG mice *in vivo*, then it analysed global and local histone modification changes upon CB-CD34⁺ cell expansion. Finally, it identified the PRC2 protein EZH2 as being involved in the loss of engrafting potential caused by CB-CD34⁺ expansion. The experimental design is shown in Figure 3: after expansion, CB-CD34⁺ cells were analysed for their stem and progenitor cell activity *in vitro* and *in vivo*, gene expression, and H3K4me³ and H3K27me³ histone marks distributions.

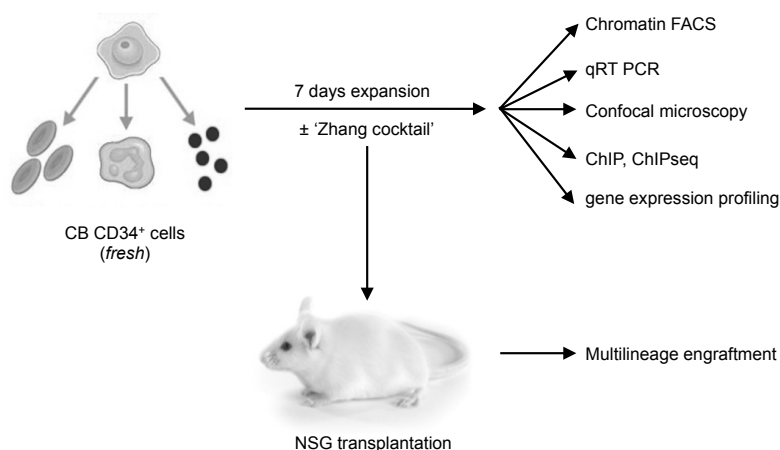


Figure 3: Experimental strategy. Human CB-CD34⁺ cells were isolated *via* MACS technology, expanded under STF or STFIA conditions and analysed *in vitro* and *in vivo* by primary and secondary transplantations into NOD.Cg-Prkdc^{scid} Il2rg^{tm1Wjl}/SzJ mice (NSG) mice. In addition, expanded cells were checked for hematopoietic activity, gene expression and chromatin changes.

5 RESULTS

5.1 Morphological and immunophenotypic changes upon expansion of human CB-CD34⁺ cells

Human CB-CD34⁺ cells were freshly isolated from a single CB unit per experiment and cultured in parallel for 7 days under two different cytokine cocktail conditions. The cytokine cocktails used were STFIA (see section 7.1.1), as it was shown to stimulate the *ex vivo* expansion of hCB-HSCs (Zhang *et al.*, 2008), and STF representing a standard cocktail widely used for HSC/HSPCs expansion (Piacibello *et al.*, 1997; Yeoh *et al.*, 2006; Zhang *et al.*, 2004). First, I monitored hematopoietic cell morphology and proliferation for a time course of 7 days of culture (Fig. 4A). Total nuclear cell (TNC) numbers were determined at the indicated time points by dividing the total number of cells in culture by the number of input cells at day 0. The TNCs were not significantly different between STF- and STFIA-expanded cells, with 17,5- and 18-fold increases, respectively. Morphologically, there were no visible differences between STF- and STFIA-cultured cells. Upon culture, freshly isolated CB-CD34⁺ cells under both expansion conditions slightly increased in size and developed uropods as indicated in Figure 4A, typical of migratory polarized cells (Giebel *et al.*, 2004). Next, the expression of several surface markers was analysed in CB-CD34⁺ cells expanded for 7 days under STF or STFIA conditions in comparison with fresh CB-CD34⁻ and CB-CD34⁺ cells. As CB-CD34⁺ cells contain a mixture of progenitors, lineage-committed and mature cells (Wisniewski *et al.*, 2011), it is of primary importance to monitor the phenotypical changes of CB-CD34⁺ cells upon expansion. Therefore, a selection of surface markers uniquely expressed on the surface of HSPCs and that make them distinguishable from other cell types was used. On the basis of the selected markers, Figure 4B shows the typical primitive immunophenotype of fresh CB-CD34⁺ cells compared to fresh CB-CD34⁻ cells (see also Table 1). After 7 days of expansion under both STF and STFIA conditions the cells maintained a primitive immunophenotype comparable to fresh cells: primitive markers such as CD34 and CD133 were still highly expressed (see Fig. 4C). Table 1 summarizes the average percentage of 3 independent

immunophenotypic analyses on fresh and expanded CB cells. Upon expansion the cells show high expression of CD34 and CD133, and low expression of CD38 and CD90 surface markers both of which are lowly expressed in HSPCs.

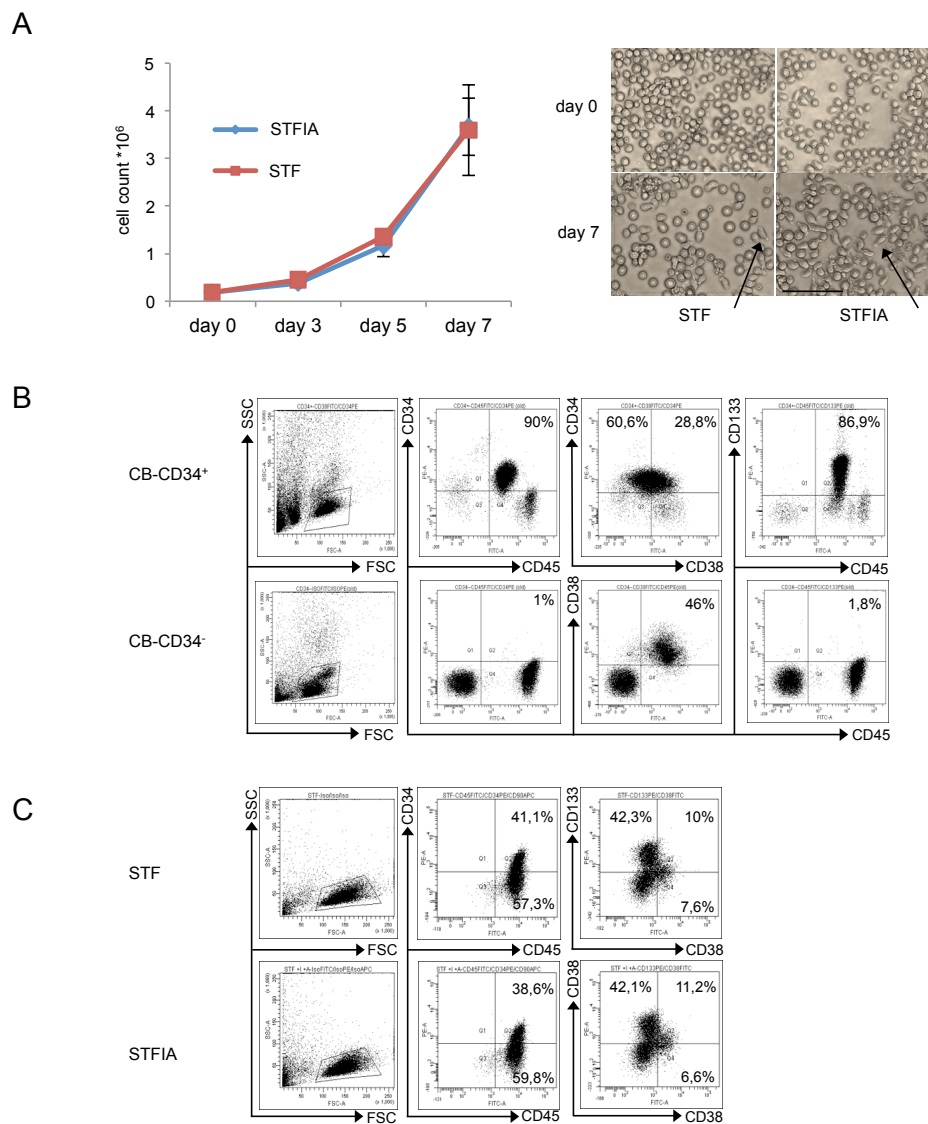


Figure 4: Cell proliferation, morphology and immunophenotype of fresh and expanded CB-CD34⁺ cells.

A) $0,2 \times 10^6$ human CB-CD34⁺ cells were cultured for 7 days in either serum-free STF medium (STF) or STF medium containing 500 $\mu\text{g}/\text{ml}$ Angiopoietin-like 5 and 100 $\mu\text{g}/\text{ml}$ IGFBP2 (STFIA). Total cells were counted at the indicated time points (left panel). Shown are phase-contrast images of fresh CB-CD34⁺ and 7 days expanded CB-CD34⁺ cells under STF or STFIA conditions. The typical morphological cell polarity is indicated. Scale bar: 50 μm (right panel). **B)** Immunophenotype analyses of CB-CD34⁻ (CD34⁻) and CB-CD34⁺ (CD34⁺) cells. The purity of the CB-CD34⁺ positive selection was analysed *via* flow cytometry using antibodies specific for CD34 surface marker together with CD133, CD38 and CD45 antibodies. **C)** Immunophenotype analyses of CB-CD34⁺ cells expanded for 7 days under either STF or STFIA conditions. Cells were analysed for CD45 expression and for markers specific for hematopoietic progenitor cells. Percentages of positive cells are indicated.

Table 1: Immunophenotype of fresh CB-CD34⁻ and CB-CD34⁺ cells, and CB-CD34⁺ cells expanded using different cytokine cocktails. Cells were sorted by MACS technology and analysed *via* flow cytometry, n=3.

	fresh sorted CB-CD34 ⁻	fresh sorted CB-CD34 ⁺	STF-expanded CB-CD34 ⁺	STFIA-expanded CB-CD34 ⁺
CD34	1% ± 0,5	92% ± 4,8	41% ± 3,4	39% ± 9,5
CD133	1,2% ± 0,3	86,9% ± 5	52,3% ± 10,1	53,2% ± 5,6
CD38	46,8% ± 7,3	33% ± 10,6	17,6% ± 9,3	17,8% ± 10,2
CD90	0% ± 0	2% ± 3	1% ± 0	2% ± 1
CD45	58% ± 20,2	98% ± 5,2	98,4% ± 7,5	98,4% ± 17,7

5.2 NSG transplantation of expanded CB-CD34⁺ cells with different cytokine combinations

Primary and secondary transplantation experiments of fresh and expanded CB-CD34⁺ cells into NSG mice were performed to test whether CB-CD34⁺ cells expanded with different cytokine combinations were capable of engrafting the entire hematopoietic system of a murine transplant recipient. For primary transplantation, $0,5 \times 10^5$ freshly isolated CB-CD34⁺ cells or their progeny after 7 days of expansion under STF- or STFIA-conditions were intravenously injected into sublethally irradiated NSG mice together with $0,2 \times 10^6$ NSG splenocytes (Fig. 5A). For secondary transplantation, the BM of one primary was injected into two secondary NSG recipients. Engraftment was assessed eight and sixteen weeks after transplantation by measuring the percentage of human CD45⁺ cells in BM, SP and PB of recipient mice. As shown in Figure 3A, in all mice human cells had engrafted, but recipients showed inter-experimental variations. Human chimerism in BM, SP and PB was higher among STFIA- compared to STF-expanded grafts. Chimerism achieved by injecting fresh CB-CD34⁺ grafts was maintained when CB-CD34⁺ cells were expanded under STFIA but not when they were expanded under STF condition. Eight weeks after primary transplantation, BM chimerism was $52,3 \pm 3,4\%$ with fresh CB-CD34⁺ grafts, $36,1 \pm 22,2\%$ with STFIA-expanded grafts and $10,9 \pm 13,8\%$ with STF-expanded grafts. Eight weeks after secondary transplantation, BM chimerism was $8,8 \pm 5\%$ with fresh CB-CD34⁺ grafts, $9,0 \pm 3,7\%$ with STFIA-expanded grafts and $3,5 \pm 1,6\%$ with STF-expanded grafts. Human chimerism in SP and PB followed similar trends, being higher in STFIA-expanded than in STF-expanded grafts. Multilineage

engraftment was also assessed in mouse BM and SP by CD19- (B lymphocytes surface marker), CD14- (monocytes and macrophages surface marker) and CD3-specific (T-cells surface marker) flow cytometry (Fig. 5B). Multilineage engraftment analyses revealed increased percentages of lymphocyte types (CD19, CD3 stainings) in STFIA-grafts compared to STF-grafts. In summary, the functional characterization of CB-CD34⁺ cells cultured under different cytokine cocktail conditions confirmed the increased capability of multilineage engraftment in primary and secondary NSG recipients in STFIA- *versus* STF-cultured CB-CD34⁺ cells as previously reported (Zhang *et al.*, 2008).

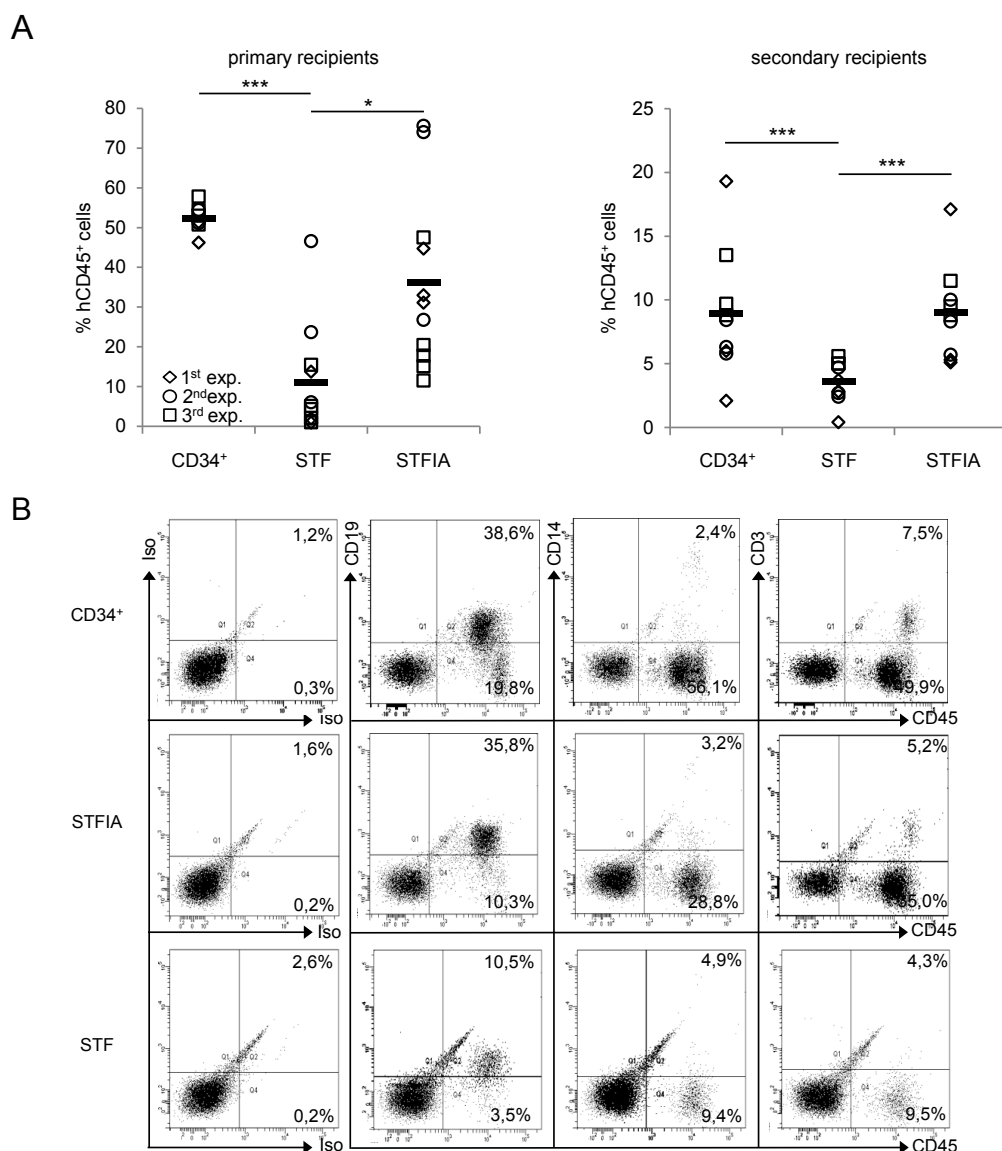
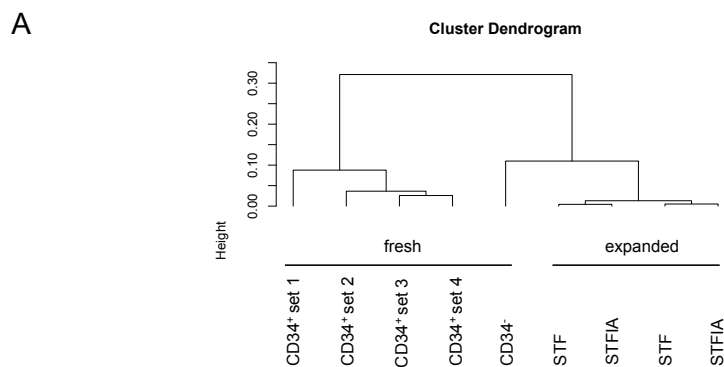


Figure 5: A cocktail of STFIA maintains in vivo repopulation capacity of CB-CD34⁺ cells. A) Shown are percentages of human chimerism by measuring the percentage of human CD45⁺ cells *via* flow cytometry in the BM of NSG transplant recipients. After 7 days of culture the progeny of 2x10⁵ CB-CD34⁺ cells expanded under STF- or STFIA-cultures were equally split and injected into 4 recipients. Recipients injected with 0,5x10⁵ fresh CB-CD34⁺ cells are shown as controls. Each symbol represents the engraftment of a single recipient 8 weeks after transplantation (left). Shown are the percentages of human chimerism in the bone marrow of mice that

received bone marrow cells of primary recipients. The bone marrow of one primary was injected into two secondary recipients. Recipients were analysed 8 weeks post transplant (right). Student t-test, *** $p < 0,001$, * $p < 0,05$. $n=3$. **B)** Representative analysis of human chimerism in the spleen of primary recipients that were injected with either fresh CB-CD34⁺ or STF- or STFIA-expanded CB-CD34⁺ cells. Splenocytes of animals were analysed *via* flow cytometry 8 weeks post transplantation using antibodies specific for human hematopoietic cells. Percentages of positive cells are indicated, $n=3$.

5.3 Expansion of CB-CD34⁺ cells is accompanied by marginal changes of gene expression but significant alterations of global histone modification

As compared to the STF cocktail, the STFIA cocktail maintained *in vivo* repopulation capacity of CB-CD34⁺ cells. In collaboration with the group of Professor Zenke (RWTH, Aachen) we assessed global gene expression changes upon CB-CD34⁺ cell expansion *via* microarray analysis. Hierarchical clustering of gene expression changes was performed using Pearson correlation coefficient and was represented by dendrogram and heatmap. Due to the low cell numbers of fresh CB-CD34⁺ cells, 4 published gene expression datasets of isolated CD34⁺ cells were used (GSM999015, GSM999018, GSM999021, GSM1139830). As shown in Figure 6A, two independent experiments were performed and in both experiments global gene expression analyses of STF- *versus* STFIA-expanded CB-CD34⁺ cells revealed only minor transcriptomic changes, while gene expression in fresh compared to expanded CB-CD34⁺ cells differed. In two experiments comparing the gene expression of STF- *versus* STFIA-expanded cells, we found fewer than 200 probes that were differentially expressed. Heatmaps of differentially expressed genes in fresh and expanded cells demonstrated the consistency of gene expression levels in the two independent experiments (Fig. 6B).



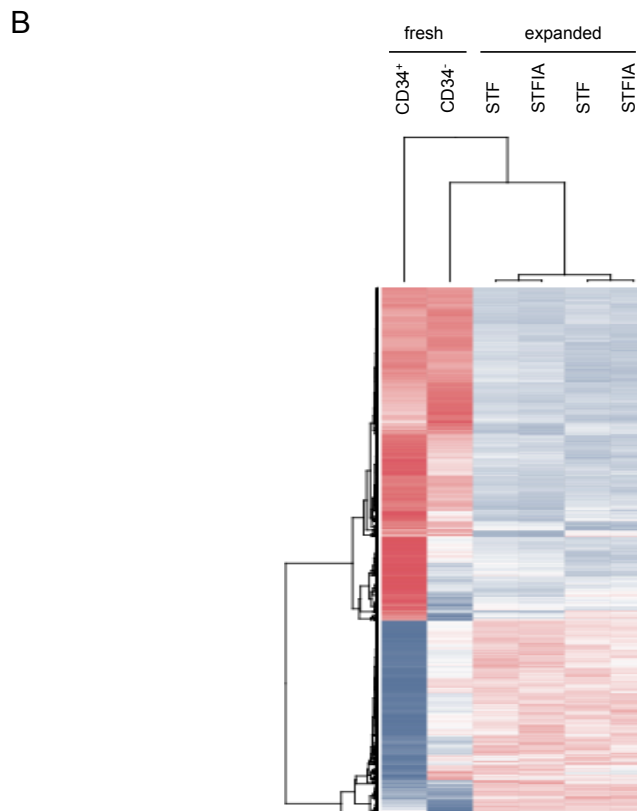


Figure 6: Hierarchical clustering of gene expression data of fresh and expanded CB-CD34⁺ cells. **A)** Dendrogram of unsupervised hierarchical clustering analysis of global gene expression profiles of fresh and expanded CB-CD34⁺ datasets showing the relatedness in gene expression. For the fresh CB-CD34⁺ sample, 4 published datasets were used (GSM999015, GSM999018, GSM999021, GSM1139830). **B)** Heatmaps of differentially expressed genes between fresh and expanded cells. In this representation, samples that share similar expression profiles have closer Euclidean distances to common branch points and are grouped. Gene expression levels are color-coded (blue, low expression; red, high expression).

To assess culture-induced global epigenetic changes between fresh and expanded cells I used intranuclear flow cytometry, Western blot and immunofluorescence analysis. Figure 7A shows a representative intranuclear flow cytometry analysis. In the example, STFIA-expanded CB-CD34⁺ cells were stained with CD34 and CD45 surface markers together with intranuclear stainings specific for H3K4me³ and H3K27me³. With this analysis it is possible to analyse cell populations with distinct stainings and FSC/SSC characteristics. Measuring of global H3 levels was done as internal control as it can be assumed that global H3 levels should be identical in cells with the same DNA content. Four independent intranuclear flow cytometry analysis experiments revealed higher levels of the histone modifications H3K4me³, associated with transcriptional activation, and H3K27me³, linked with repression, in fresh CB-CD34⁺ compared to CB-CD34⁻ cells (Fig. 7B). Following the analysis of global H3K4me³ and H3K27me³ levels by chromatin flow cytometry, Western blot analysis was used to study global

levels of the two modifications of interest so as to clarify and prove the previous results. Immunoblot detection of H3 was used as a loading control (Fig. 7C). Upon culture of CB-CD34⁺ cells I noticed that global H3K27me³ but less H3K4me³ levels changed and that STFIA-cultured cells carried less H3K27me³ than fresh CB-CD34⁺ or STF-cultured CB-CD34⁺ cells. Immunostainings of fresh CB-CD34⁻ and CB-CD34⁺ cells and of CB-CD34⁺ cells expanded under STF or STFIA conditions confirmed the results obtained by Western blot and chromatin FACS analyses (Fig. 7D). Confocal microscopy also showed elevated levels of H3K4me³ and H3K27me³ in freshly isolated CB-CD34⁺ compared to CB-CD34⁻ cells. However, confocal microscopy did not detect altered H3K27me³ levels between the two expansion conditions.

CD133 is another useful surface marker for HSC isolation (Shmelkov *et al.*, 2005), and it was shown that transplanted CD133⁺/CD34⁻ cells can differentiate into CD133⁺/CD34⁺ cells (Bhatia *et al.*, 2001). As intranuclear flow cytometry allows the analysis of subpopulations within a mixed population, I choose this method to further analyse within the CD133⁺ subpopulation two other relevant histone modifications: the repressive H3K9me³ and the active H3K79me³ marks. I observed that the CD133⁺/CD34⁺ population compared to the CD133⁺/CD34⁻ population of cells both selected from the pool of STF-cultured cells, had higher H3K27me³ levels (Fig. 8). Following STFIA expansion, H3K27me³ levels decreased in the CD133⁺/CD34⁺ population compared to the CD133⁺/CD34⁻ population. Global levels of H3K79me³ and of H3K9me³ marks did not differ between CD133⁺/CD34⁺ and CD133⁺/CD34⁻ cells in both expansion conditions.

In conclusion, despite high similarities in gene expression between the two different culture conditions, just the STFIA-cultured cells showed elevated repopulation potential. Surprisingly I found that the expansion of CB-CD34⁺ cells is accompanied by global histone modification changes that are mainly regarding H3K27me³. Together this shows that global changes of H3K27me³ but less of H3K4me³ levels accompany STFIA culture-associated preservation of engraftment potential, while gene expression is not altered.

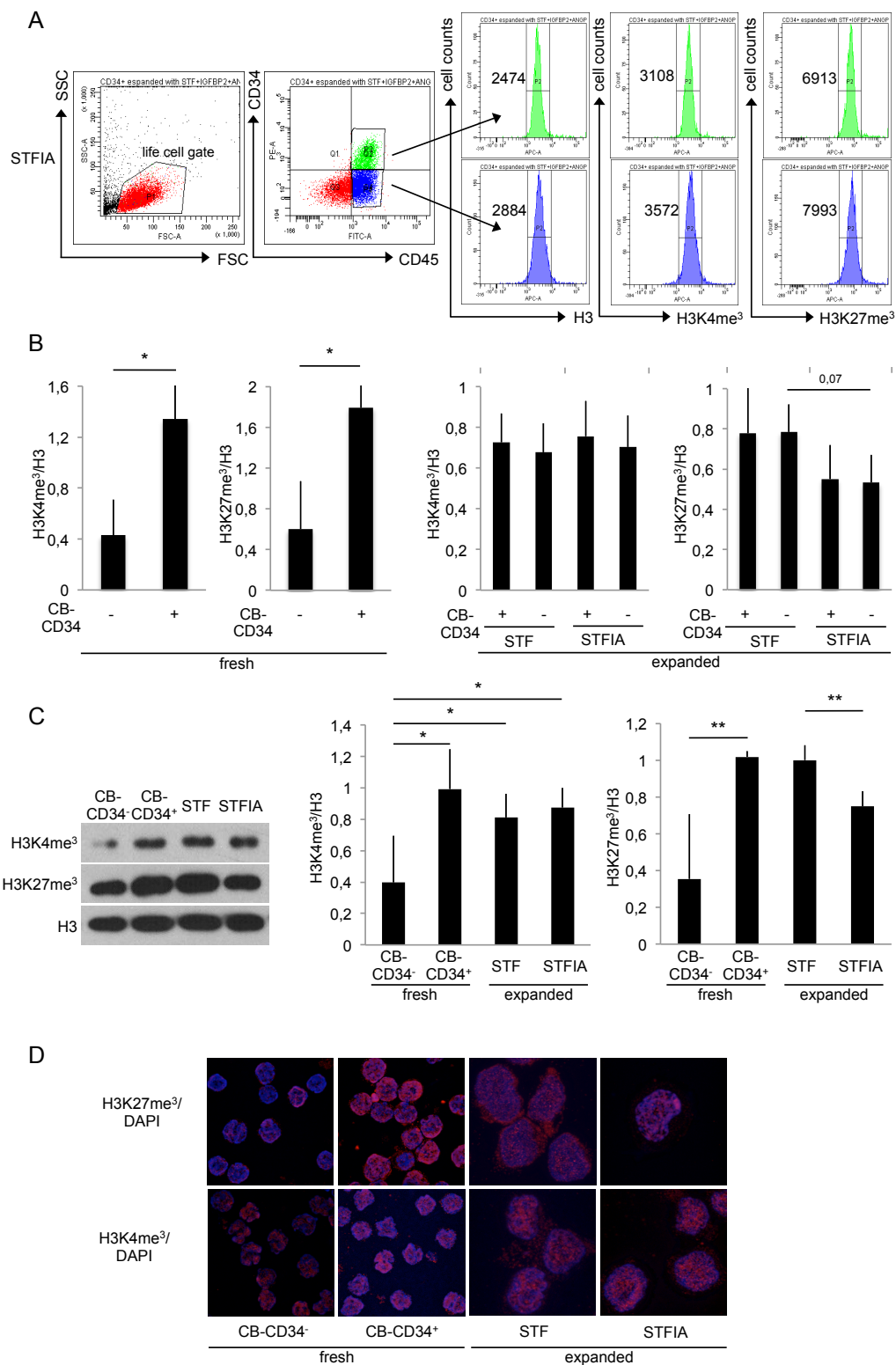


Figure 7: Global H3K27me³ and H3K4me³ levels in fresh and expanded CB-CD34⁺ cells. A) Intranuclear flow cytometry allows the detection and analysis of different cell populations within the same sample. A representative analysis is shown: CB-CD34⁺ cells expanded for 7 days with STFIA cytokine cocktail were stained for the surface markers CD45 and CD34 together with antibodies specific for H3, H3K4me³ and H3K27me³. **B)** Summary of H3-normalized values of global H3K4me³ and H3K27me³ fluorescence levels of fresh CB-CD34⁻ and CB-CD34⁺ cells, and of CB-CD34⁺ cells expanded for 7 days with either STF or STFIA cocktails analysed *via* intranuclear flow cytometry, * $p < 0,05$, $n=4$. **C)** Representative image from one of four independent experiments of H3K4me³- and H3K27me³-specific Western blot analysing fresh CB-CD34⁻ and CB-CD34⁺ cells,

and CB-CD34⁺ cells expanded for 7 days with either STF or STFIA cocktails (left). H3K4me³- and H3K27me³-specific signal intensities of bands were quantified, and normalized against H3- specific signal intensities (middle, right). Student t-test, ** p< 0,01, * p< 0,05. n=4. **D)** Representative confocal images of fluorescence intensity of H3K4me³ or H3K27me³ in fresh CB-CD34⁺ and CB-CD34⁺ cells, and of CB-CD34⁺ cells expanded for 7 days with either STF or STFIA. Nuclei were co-stained with DAPI. Scale bars: 100 μ m.

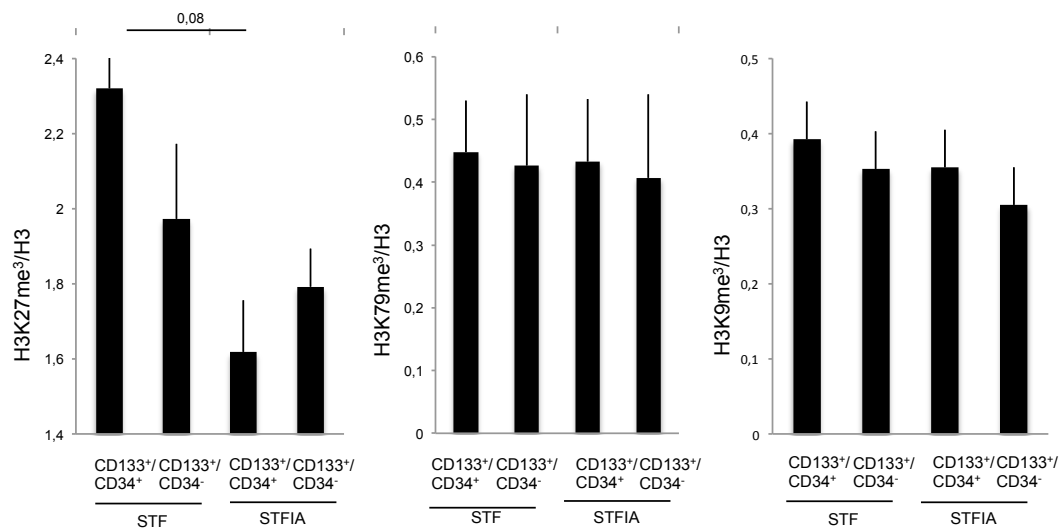


Figure 8: Intranuclear flow cytometry specific for H3K79me³, H3K27me³ and H3K9me³ histone modifications. Global changes of H3K79, H3K27 and H3K9 trimethylation levels were analysed in CD133⁺/CD34⁺ or in CD133⁺/CD34⁻ cell populations. Prior analysis, CB-CD34⁺ cells were expanded for 7 days under STF- or STFIA-condition. H3K79, H3K27 or H3K9 trimethylation levels were normalized against H3 fluorescence signals. n=3.

5.4 Remodelling of H3K4me³ and H3K27me³ marks upon culture of CB-CD34⁺ cells

The use of chromatin immunoprecipitation and next generation sequencing (ChIP-seq) was chosen to better define the differences between epigenotypes of fresh and expanded cells, as well as between epigenotypes of STF- and STFIA-expanded cells. To characterize the impact of *in vitro* expansion on chromatin signatures, in collaboration with Dr. Rainer Claus and Professor Christoph Plass (DKFZ, Heidelberg) we performed H3K4me³- and H3K27me³-specific ChIP-seq analyses and mapped the histone modification enrichments on a genome-wide level. To this end, I established a reproducible protocol for chromatin preparation that was optimized for low cell numbers (Dahl *et al.*, 2009). Typically 80.000 cells were used, and four paralleled chromatin IP samples were pooled per antibody for one ChIP-seq analysis. Raw data processing and quality control revealed high replicate correlations between individual samples according to ENCODE ChIP-seq guidelines (Fig. 9) (Landt *et al.*, 2014). Pearson's correlation coefficients between the replicates were all between 0,96 and 0,73. Considering the high replicate correlation coefficients between the individual experiments, replicates were merged for subsequent analyses. First, we performed unsupervised hierarchical clustering of complete data sets comprising the entire genome partitioned into 500 bp windows to assess similarities between individual samples. The clustering was done using Ward's minimum variance method. Regarding the H3K4me³ histone modification clustering analysis of the datasets, the samples revealed a closer relationship between STF- and STFIA-cultured cell datasets than to the two fresh cell datasets (Fig. 10A). In contrast, for H3K27me³ hierarchical clustering showed that samples of the two expanded cells and fresh CB-CD34⁺ cells grouped together while the CB-CD34⁻ sample separated.

We then looked at the total reads found around the TSSs and within the gene bodies of the different samples. As expected, H3K4me³ was highly enriched at the promoters and showed the typical bimodal distribution with a nucleosome gap at the TSSs. We observed that H3K4me³ meta-profiles on all TSSs and gene bodies were maintained during expansion of CB-CD34⁺ cells, independently of cocktail composition, while the ChIP-seq read density was slightly higher in fresh CB-CD34⁻ cells (Fig. 10B). A closer look at the distribution of H3K27me³ reads revealed that upon expansion of CB-CD34⁺ cells, H3K27me³ levels at TSSs and within gene bodies slightly decreased independently of the cytokine cocktail.

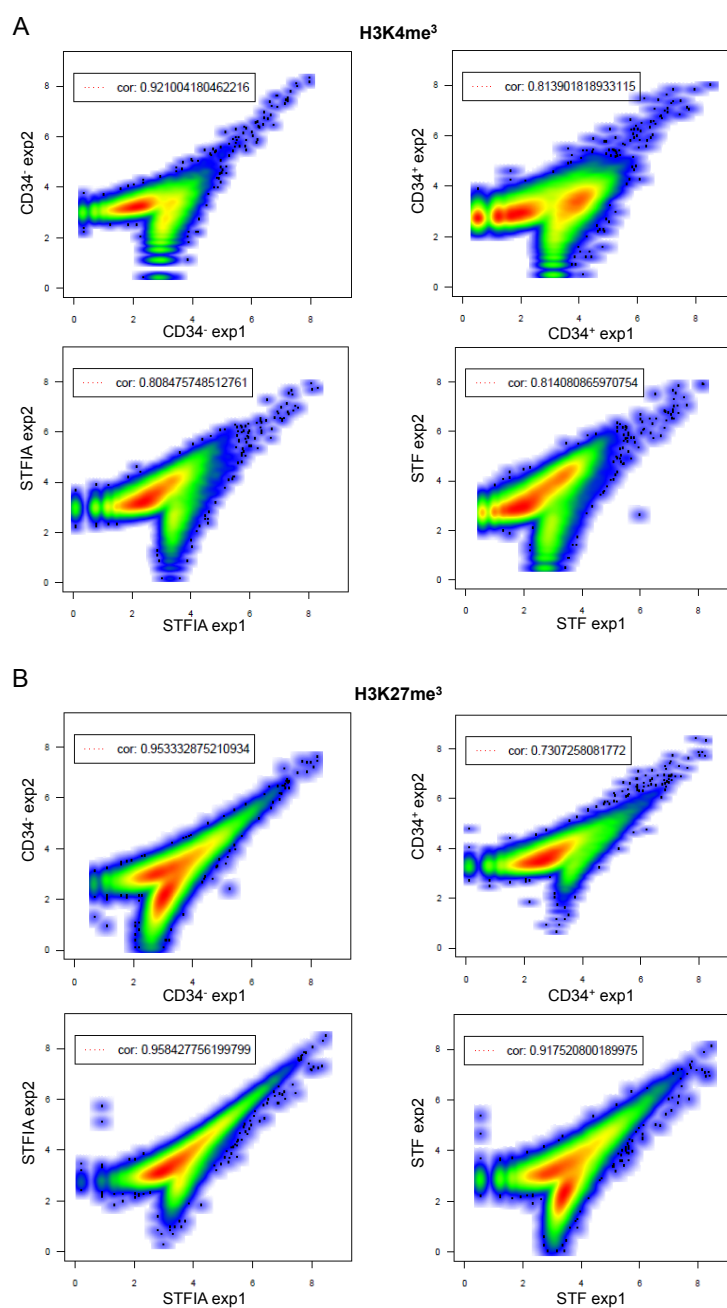


Figure 9: ChIP-seq raw data quality control. Reproducibility analysis of two ChIP-seq replicates is shown. Two independent ChIP-seq experiments per biological condition were processed and compared before merging. Correlations of sequencing tag counts between replicates in peak regions were plotted (using logarithmic scale) and calculated using Pearson's correlation coefficient. The correlation coefficients showing high reproducibility are indicated.

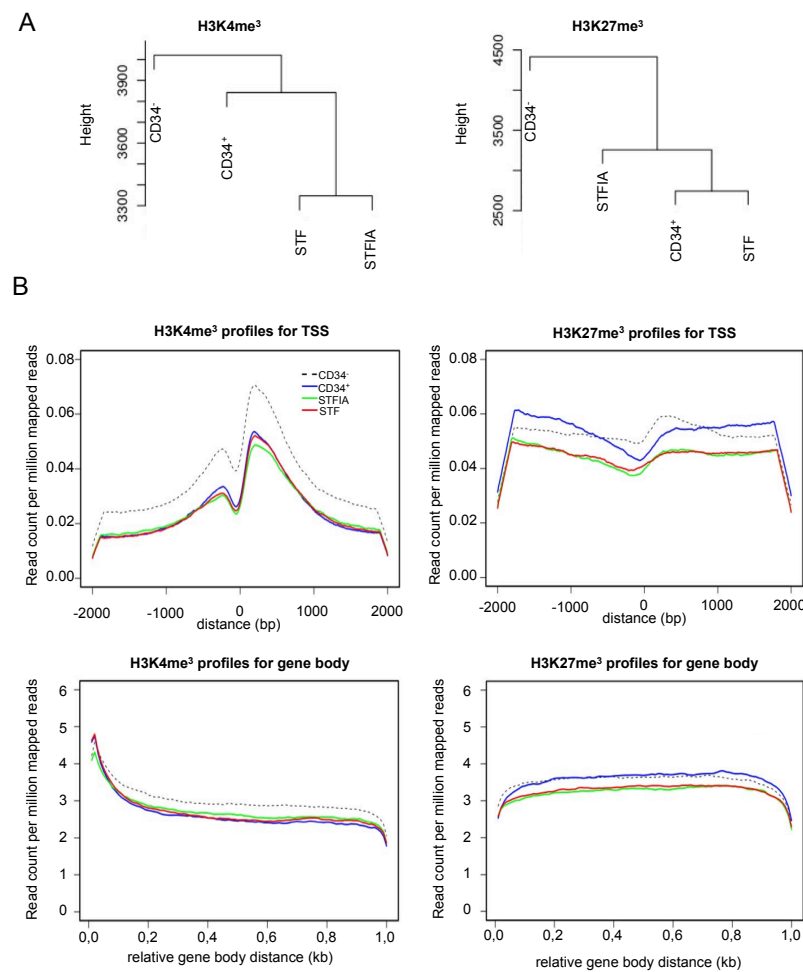


Figure 10: Hierarchical clustering and chromatin profiles of H3K4me³ and H3K27me³ in fresh and expanded CB-CD34⁺ cells. **A)** Unsupervised hierarchical cluster analysis of H3K4me³ and H3K27me³ data sets of fresh CB-CD34⁻ and CB-CD34⁺ cells, and of CB-CD34⁺ cells expanded for 7 days with either STF or STFIA cocktails. Data sets of two independent experiments per sample were merged. The entire sequenced genome was partitioned in 500 bp bins. **B)** H3K4me³ and H3K27me³ profiles around the TSSs and within gene body regions in fresh CB-CD34⁻, CB-CD34⁺, and in 7 days STF- or in STFIA-expanded CB-CD34⁺ cells. Y axes display read density per 10⁶ reads. Gene body distances are displayed as percentage of variable gene body size.

We then used peak detection to identify regions of significant H3K4me³ and H3K27me³ histone mark enrichment. Examination of peak signals revealed that considerably larger portions of the genome were enriched with H3K27me³ compared to H3K4me³ marks in all four samples, as expected (Fig. 11A). The genome fraction covered by significant H3K4me³ enrichment was the double in STFIA- and STF-cultured CB-CD34⁺ as compared to fresh CB-CD34⁺ or CB-CD34⁻ cells. In contrast, the genome fraction covered by H3K27me³ peaks was increased upon STFIA- but not STF-culturing. Peak counts of H3K27me³-marked regions in STF cells were reduced compared to other samples. This result was unexpected, considering

that we found globally higher levels of H3K27me³ in cells expanded under STF condition. Therefore we decided to have a closer look at the nature of the detected peaks, with a focus on the genome-wide distribution and the horizontal expansion of the enriched regions. The analysis of the size of H3K4me³- and H3K27me³-enriched regions (referred to as islands) was assessed to examine how the histone modification domains were shaped across the four samples. We observed that H3K4me³ islands in fresh CB-CD34⁻ and CB-CD34⁺ cells were similarly sized, while upon expansion the size distribution of H3K4me³ peaks changed. STF and STFIA culture seemed to increase the size of H3K4me³ islands (Fig. 11B). It is reported that H3K27me³ occupies broad domains in comparison to other histone modifications (Pauler *et al.*, 2009; Pinello *et al.*, 2014): as expected we noticed that H3K27me³ peaks were wider than H3K4me³ peaks in all samples (Fig. 11B). Furthermore, the reduced peak counts of H3K27me³-marked regions in STF-cultured cells was explained by the discovery that H3K27me³-enriched regions were considerably broadened in STF-cultured cells, similar to fresh CB-CD34⁻ cells. Our data revealed that the distribution of H3K4me³- and H3K27me³-enriched regions varied among the different samples. Genome-wide analysis of H3K4me³ peak distribution over functional genomic elements revealed that between 15% and 20% of total H3K4me³ peaks were found at promoters, around 40% in introns and around 20% in intergenic regions. In contrast, H3K27me³ was widely deposited in introns and intergenic regions with respectively 30% and 60% of total H3K27me³ peaks (Fig. 11C). It is known that intergenic regions contain important elements like promoters and enhancers and that H3K27me³ as compared to H3K4me³ is widely spread within gene bodies (Pauler *et al.*, 2009; Pinello *et al.*, 2014). Our results confirmed these notions as the majority of H3K27me³ peaks were found in intergenic regions. Upon expansion of CB-CD34⁺ cells, promoters lost and introns gained H3K4me³. The expansion of CB-CD34⁺ cells had no visible qualitative or quantitative impact on H3K27me³ marking at the analysed elements.

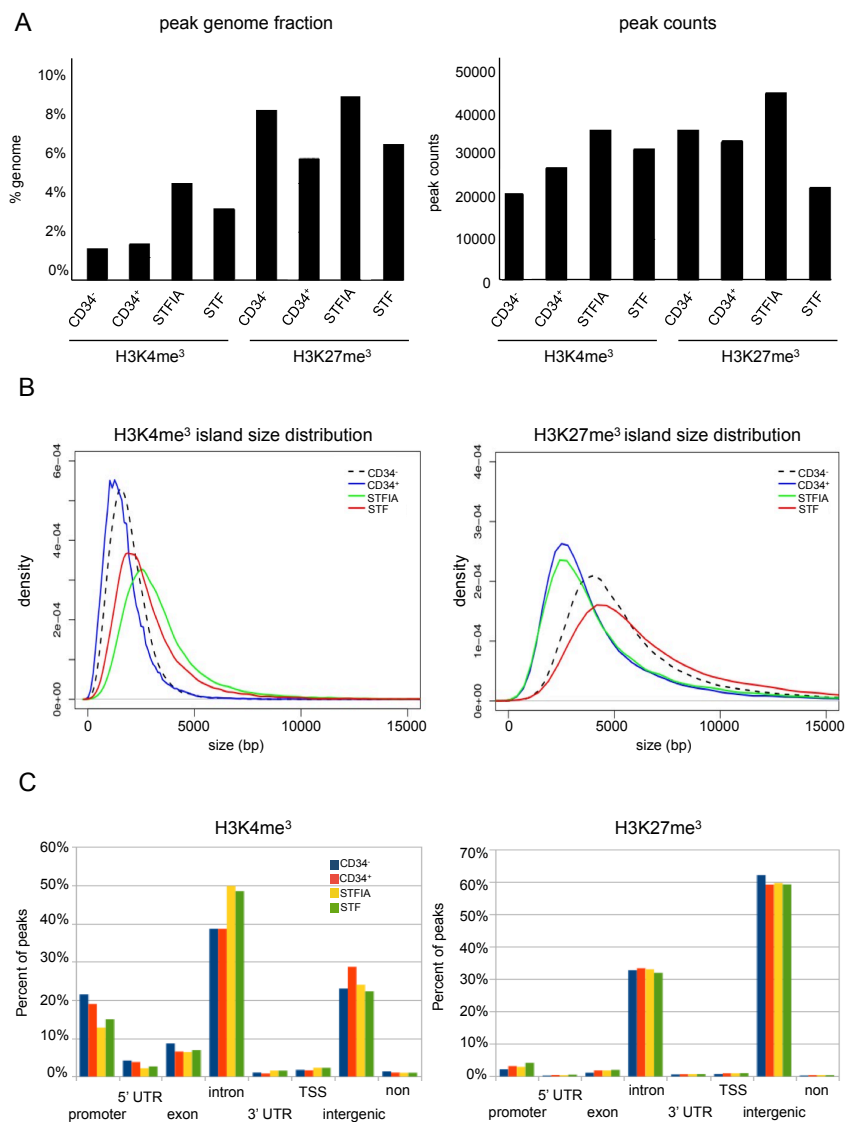


Figure 11: Peak counts and genome-wide distribution of H3K4me³- and H3K27me³-marked regions in fresh and expanded CB-CD34⁺ cells. **A)** Shown are the absolute numbers of H3K4me³ or H3K27me³ peaks after peak calling using SICER in the different datasets (right panel). Percentages of genome covered by significantly enriched regions (peaks) are displayed for H3K4me³ and H3K27me³ histone marks for fresh and expanded cells (left panel). **B)** Shown are the distributions of the sizes of H3K4me³- and H3K27me³- enriched regions in fresh CB-CD34⁻ and CB-CD34⁺ cells, and in CB-CD34⁺ cells expanded for 7 days with either STF or STFIA cocktails using kernel density graphs. **C)** Total numbers of H3K4me³- and H3K27me³- enriched regions in promoters, 5'UTRs, exons, introns, 3'UTRs, TSSs, intergenic and non-intergenic regions were identified. The graph shows the percentage of peaks per each defined region.

Previously, Cui *et al.* reported broad changes of H3K4me³ and H3K27me³ patterns in homeobox (Hox) gene clusters during CB-HSCs differentiation (Cui *et al.*, 2009). Thus, we continued the analysis of dynamic changes of H3K4me³ and H3K27me³ chromatin modifications by looking at whether culture of CB-CD34⁺ cells was paralleled by changes in H3K4me³ and H3K27me³ marking in the HoxA and HoxB loci. Along with Cui *et al.* data, we

found differences in H3K4me³ and H3K27me³ deposition at the HoxA and HoxB loci between fresh CB-CD34⁺ and CB-CD34⁻ cells but little changes between the two culture conditions. Overall the H3K27me³-specific profiles between the samples differed more than the H3K4me³-specific profiles. The CB-CD34⁺ expanded cells showed similar enrichment profiles like fresh CB-CD34⁺ cells in both HoxA and HoxB loci, with only few differences (i.e. in HoxA5 - A9 regions) of new H3K27me³-marked regions found upon culture. The center region of the HoxA locus comprising A5 – A9 was marked by higher H3K27 trimethylation in CB-CD34⁻ than in fresh or expanded CB-CD34⁺ cells. The H3K4me³ distribution in this area was not changed between the different samples. The distinct epigenetic profiles found in CB-CD34⁻ sample were associated with the silencing of HoxA6 and HoxA9 transcripts in CB-CD34⁻ cells, while their expression in fresh and expanded CB-CD34⁺ was higher (Fig. 12B). The majority of the HoxB genomic locus comprising B1 – B6 was characterized by higher H3K27me³ levels in CB-CD34⁻ than in fresh or expanded CB-CD34⁺ cells. The H3K4me³-specific profiles were similar between the four samples. The H3K27me³ distributions in this genome area were consistent with higher expression levels of HoxB4 in fresh and expanded CB-CD34⁺ but less expression in CB-CD34⁻ cells (Fig. 12B). The analysis of HoxA and HoxB clusters indicated a correlation between epigenetic modifications and gene expression, so we analysed the expression profiles and the chromatin status of a set of selected genes by qRT-PCR.

ChIP primers specific for promoter regions of developmental regulators of HSPC-specific genes were employed for the study of bivalent chromatin markers remodelling upon culture of CB-CD34⁺ cells (Fig. 13). As the CD34 gene itself is highly transcribed in CB-CD34⁺ but not in CB-CD34⁻ cells we first assessed H3K4me³ and H3K27me³ enrichment at the CD34 promoter. The distribution of H3K27me³ was consistent with the transcriptional state of the CD34 locus: both ChIP-seq and ChIP-PCR analyses revealed higher H3K27me³ levels in CB-CD34⁻ than in fresh or expanded CB-CD34⁺ cells. The H3K4me³ pattern was similar between the different samples (Fig. 13, top panel).

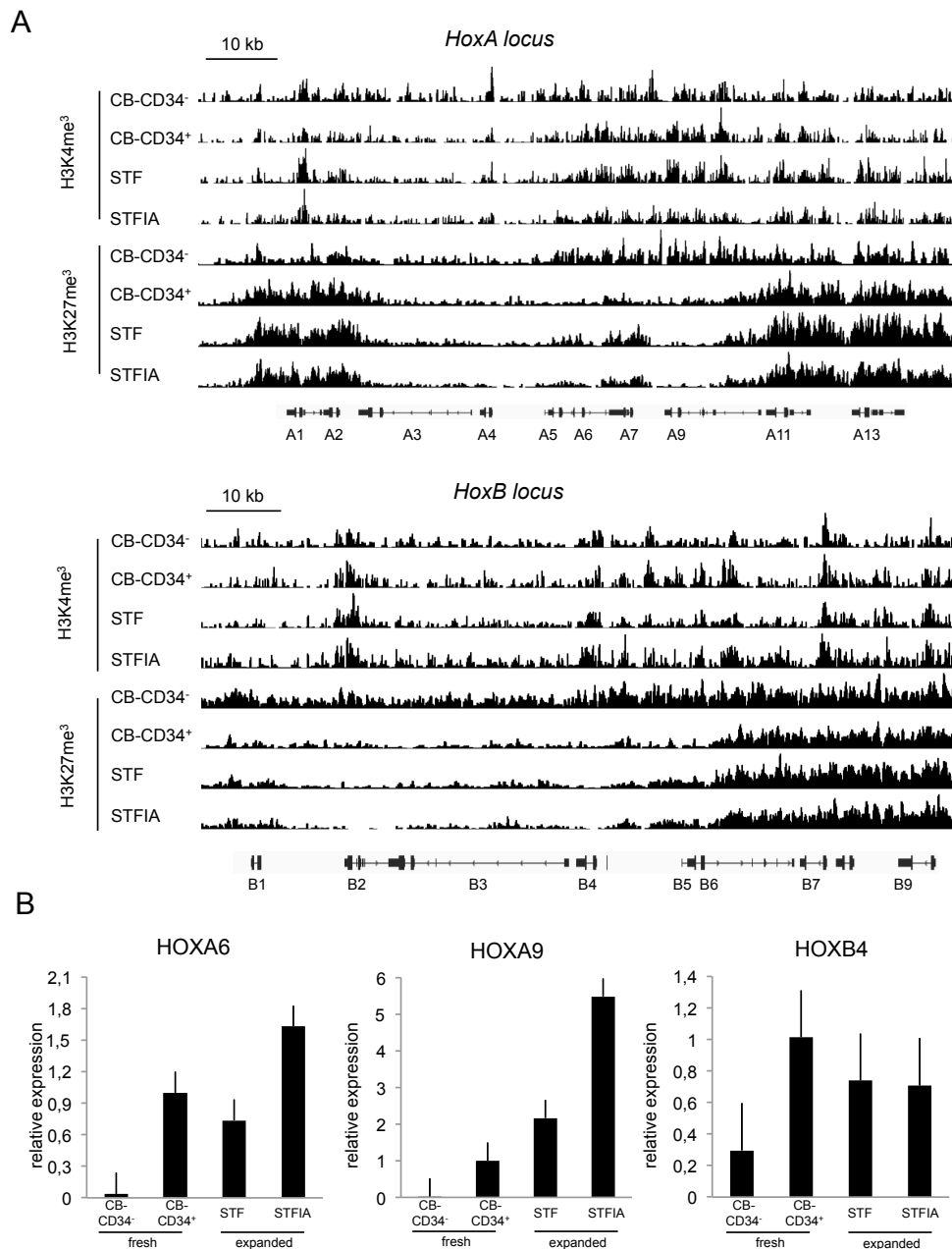


Figure 12: Culture-induced histone modification changes in the *HoxA* and *HoxB* loci.

A) Histone modification profiles of H3K4me³ and H3K27me³ in the *HoxA* and *HoxB* loci in fresh CB-CD34⁻ and CB-CD34⁺ cells, and in CB-CD34⁺ cells expanded for 7 days with either STF or STFIA cocktails. Data are displayed using the Integrative Genomics Viewer software. The positions of *HoxA* and *HoxB* genes are indicated below the panels. On the y-axis the number of reads per 200 bp windows are displayed. The position of introns, exons and the direction of transcription are shown. **B)** Shown are RT-PCR analyses of *HoxA6*, *A9* and *B4* loci in fresh CB-CD34⁻ and CB-CD34⁺ cells and in STF- or STFIA-expanded CB-CD34⁺ cells.

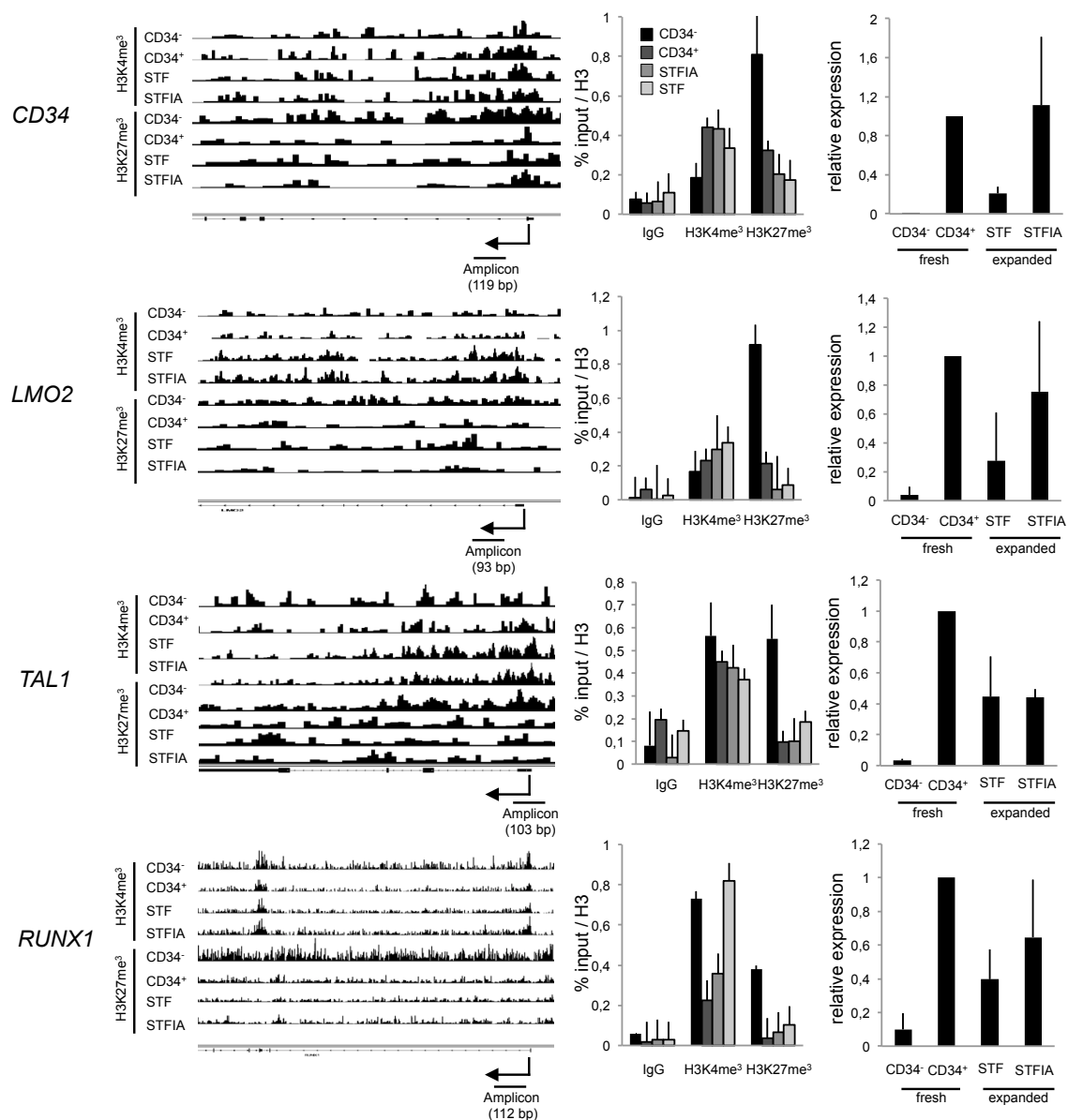


Figure 13: Correlation between local distribution of H3K4me³ and H3K27me³ and gene expression.

ChIP-seq profiles, ChIP-PCR and RT-PCR analyses of selected genes in fresh CB-CD34⁻ and CB-CD34⁺ cells and in STF- and STFIA-expanded cells. The TSS and the amplicon size and location are indicated, n=3.

The same correlation between gene expression and histone modification patterns was found in LMO2, TAL1 and RUNX1 loci, where higher H3K27me³ levels were found in CB-CD34⁻ cells with subsequent silencing of the analysed genes in the fresh CB-CD34⁻ population in comparison to fresh CB-CD34⁺ cells and CB-CD34⁺ cells expanded with either STF or STFIA cocktails. ChIP-PCR analyses were employed for validating the ChIP-seq profiling of the selected loci.

In addition, we analysed the correlation of H3K4me³ and H3K27me³ marks and gene expression. We looked at the chromatin profiles around the TSSs of fresh CB-CD34⁺ and CB-CD34⁺ cells, and of expanded CB-CD34⁺ cells of the 2000 highest and 2000 lowest expressed genes in fresh CB-CD34⁺ cells (Fig. 14). The promoters of the 2000 highest expressed genes were mainly enriched in H3K4me³: we observed in all four samples the typical distribution of H3K4me³ with a nucleosomes-free region at the TSS and almost complete lack of H3K27me³. For the genes highest expressed in CB-CD34⁺ cells, STFIA-expanded CB-CD34⁺ cells had a chromatin environment at the TSSs identical to fresh CB-CD34⁺ cells, whereas STF-expanded CB-CD34⁺ cells and CB-CD34⁺ cells showed higher and lower H3K4me³ tag density, respectively (Fig. 14A). In line with the gene expression profiles, the TSSs of the lowest expressed genes showed very low enrichment in H3K4me³ and more repressive H3K27me³ marks in all 4 samples (Fig. 14B).

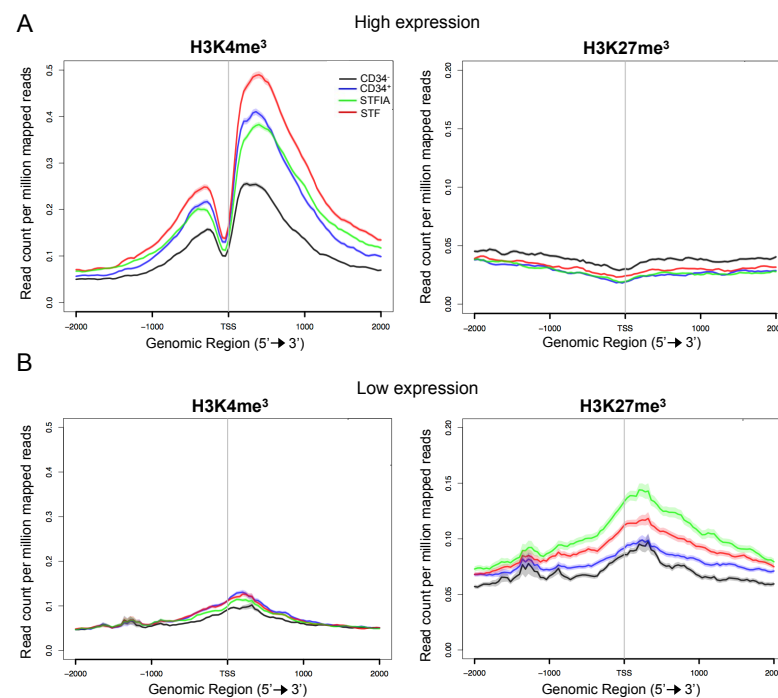


Figure 14: Comparison of H3K4me³ and H3K27me³ profiles around the TSSs of high and low expressed genes. A) H3K4me³ and H3K27me³ profiles around the TSSs of the 2000 highest expressed genes in fresh CB-CD34⁺ cells of fresh CB-CD34⁺ and CB-CD34⁺ cells, and of CB-CD34⁺ cells expanded for 7 days with either STF or STFIA cocktails. **B)** H3K4me³ and H3K27me³ profiles around the TSSs of the 2000 lowest expressed genes in fresh CB-CD34⁺ cells.

To further investigate the remodelling of H3K4me³ and H3K27me³ upon CB-CD34⁺ cell expansion, we analysed the sets of genes having the promoters enriched in H3K4- and/or H3K27- trimethylation. Figure 15A shows the overlap of genes with the promoters enriched in either H3K4me³ or H3K27me³ marks. We observed that culture conditions changed the set of enriched promoters giving a unique signature to each of the three samples containing CB-HSPCs. One third of the promoters were exclusively enriched with either H3K4me³ or H3K27me³ depending on the analysed sample. To gain insight into the categories of genes with enriched promoters in fresh and expanded CB-CD34⁺ cells, we performed Gene Ontology (GO) analysis. GO-analysis of H3K4me³-enriched promoters indicated the genes were enriched in functional categories of ‘transcriptional regulation’ and ‘metabolic processes’ in fresh and STFIA-expanded CB-CD34⁺ cells, while STF-expanded cells associated with ‘signaling’ and ‘cell death’ (Fig. 15B, C). The H3K27me³-enriched promoters were associated with the GO-terms ‘signal transduction’ and ‘differentiation’ in all three samples.

For relating changes of chromatin modifications and mRNA expression data, we ranked 26.000 transcripts represented on the Affymetrix expression arrays according to the fold-change of sequencing reads (of H3K4me³/H3K27me³ ChIP) in their promoter regions (-1000 bp to +500 bp around transcriptional start site) and asked for enrichment of either up- or downregulated genes. First we compared STF *versus* STFIA culture conditions (Fig. 16A, B). Although we observed more H3K4me³ loss than gain, H3K4me³ changes appeared to be more balanced with similar extent of lost and gained areas between the two samples. Looking at H3K27me³ changes we noticed a higher extent of remodelling compared to H3K4me³ histone modification (as shown by the enlarged saturated red and blue areas). The fold-changes of H3K27me³ and H3K4me³ between STFIA- and STF-cultured samples were also sorted by amplitude and plotted as line plots: Figure 16B shows the greater extent of H3K27me³ changes compared to H3K4me³. The analysis of the correlation between histone modification changes on promoters and gene expression indicated a higher remodelling of H3K27me³-enriched promoters compared to H3K4me³ promoters without transcriptomic changes.

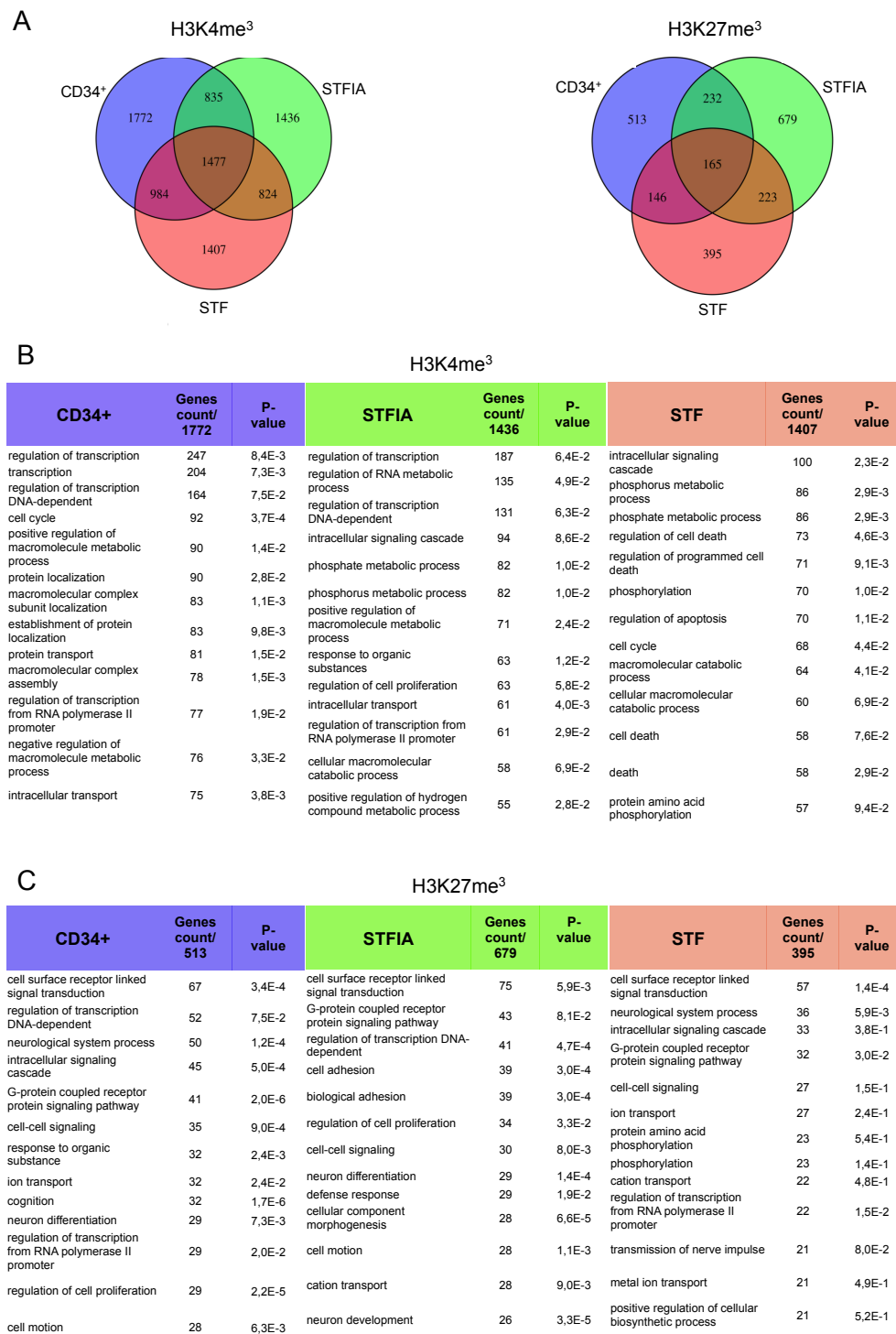


Figure 15: Promoter methylation states and GO analysis of genes with H3K4me³- and H3K27me³-enriched promoters. **A)** Venn diagram of the genes with the promoters enriched in either H3K4me³ or H3K27me³ marks in fresh CB-CD34⁻ and CB-CD34⁺ cells, and in CB-CD34⁺ cells expanded for 7 days with either STF or STFIA cocktails. **B)** Functional annotation analysis of the genes with either H3K4me³ or H3K27me³ enriched promoters in fresh and expanded CB-CD34⁺ cells using gene ontology analysis with Database for Annotation, Visualization and Integrated Discovery (DAVID). Gene counts and p-values are indicated.

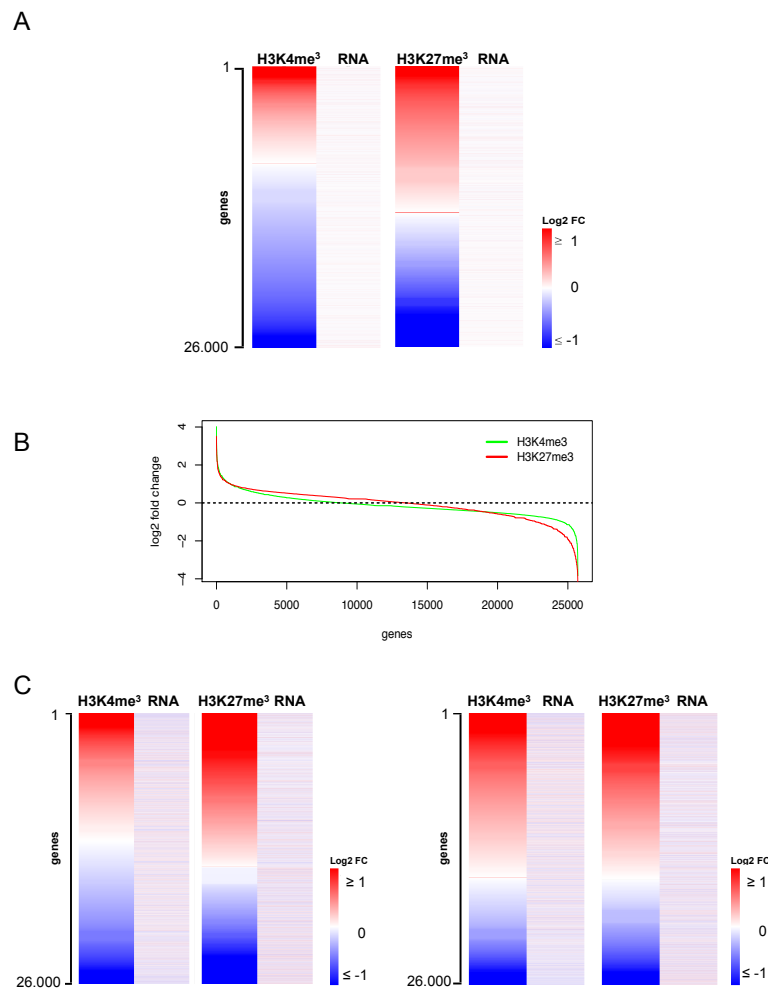


Figure 16: Correlation changes in gene expression and histone modification on promoters. A) Approximately 26.000 transcripts of STFIA- and STF-cultured CB-CD34⁺ cells were sorted according to the log₂-fold change (STFIA *versus* STF) of either H3K4me³ or H3K27me³ enrichment in their promoter regions (defined as -1000 bp to +500 bp around the TSS). Log₂-fold changes ranged from -3,84 to 4,02 for H3K4me³ and -4,19 to 3,51 for H3K27me³ and were displayed by color coding (shades of red = positive log₂-fold changes, grey = no change/0, blue = negative log₂-fold changes). The same representation was chosen for the log₂-fold changed mRNA expression values for the respective transcripts taken from the Affymetric expression arrays (lane labelled 'RNA'). **B)** Log₂-fold changes of H3K27me³ and H3K4me³ between STFIA- and STF-cultured samples were sorted by amplitude and plotted. The area below the curve indicates the relative extent of changes of either histone modification. **C)** Approximately 26.000 transcripts of fresh CB-CD34⁺ cells and of STFIA- or STF-cultured CB-CD34⁺ cells were ranked according to log₂-fold changes of either H3K4me³ or H3K27me³ enrichment in their promoter regions. Shown are (left) STFIA-cultured CB-CD34⁺ *versus* fresh CB-CD34⁺ and (right) STF-cultured CB-CD34⁺ *versus* fresh CB-CD34⁺ promoter regions. Log₂-fold changes (STFIA-cultured CB-CD34⁺ *versus* fresh CB-CD34⁺ (H3K4me³ ranged from (-3,83) to (4,51); H3K27me³ from (-4,45) to (4,81)); STF-cultured CB-CD34⁺ *versus* fresh CB-CD34⁺ (H3K4me³ ranged from (-3,83) to (4,19); H3K27me³ from (-4,32) to (4,55)) were displayed by color coding (shades of red = positive log₂-fold changes, grey = no change/0, blue = negative log₂-fold changes). The same representation was chosen for the log₂-fold changed mRNA expression for the respective transcripts (lanes labeled 'RNA').

In contrast, in STFIA-expanded CB-CD34⁺ cells H3K4me³ changes appeared to be more balanced whereas upon STF-culture there was mostly a gain of H3K4me³ when the two expansion conditions were compared to fresh CB-CD34⁺ cells. Under both culture conditions, gain of H3K27me³ at promoter regions was more frequent than loss when compared to fresh CB-CD34⁺ cells (Fig. 16C). We did not find any correlation between H3K4me³ or H3K27me³ changes and gene expression when the CB-CD34⁺ expanded cells were compared to fresh CB-CD34⁺ cells.

Promoters with a bivalent chromatin signature are assumed to be poised key genes important for development and differentiation (Voigt *et al.*, 2013). Therefore we looked at the genes showing enrichment of both bivalent marks in fresh CB-CD34⁻ and CB-CD34⁺ cells and in CB-CD34⁺ cells expanded under STF or STFIA conditions. The promoters with both H3K4me³ and H3K27me³ marks were twice the number in fresh CB-CD34⁺ and STF- or STFIA-cultured cells compared to CB-CD34⁻ cells (Fig. 17A). For understanding the bivalency reorganization upon expansion, we looked into the resolution of the 374 bivalent promoters found in fresh CB-CD34⁺ cells after expansion, and compared it with fresh CB-CD34⁻ cells (Fig. 17B). One third of the bivalent genes in fresh CB-CD34⁺ cells remained bivalent after expansion whereas only 47 genes were found to be bivalent in the CB-CD34⁻ population; one third of genes lost H3K27me³ mark and the remaining genes resulted to be not marked in all three samples. We therefore observed a cocktail-specific reorganization of the bivalency status.

To better understand the dynamics of bivalency resolution upon expansion we constructed maps of promoter bivalency status of fresh and cultured cells (Fig. 17C). Only about one third of the genes marked with both modifications in fresh CB-CD34⁺ cells maintained the bivalent mark upon STF or STFIA expansion. However we found newly established bivalent promoters in each of the samples. GO analysis revealed that genes grouping in categories of hematopoietic cell differentiation and development were occupied by bivalent marks in both fresh and expanded CB-CD34⁺ cells but not in the fresh CB-CD34⁻ sample (Fig. 18). GO analysis further revealed enrichment of genes belonging to blood vessel development and morphogenesis in the STFIA sample.

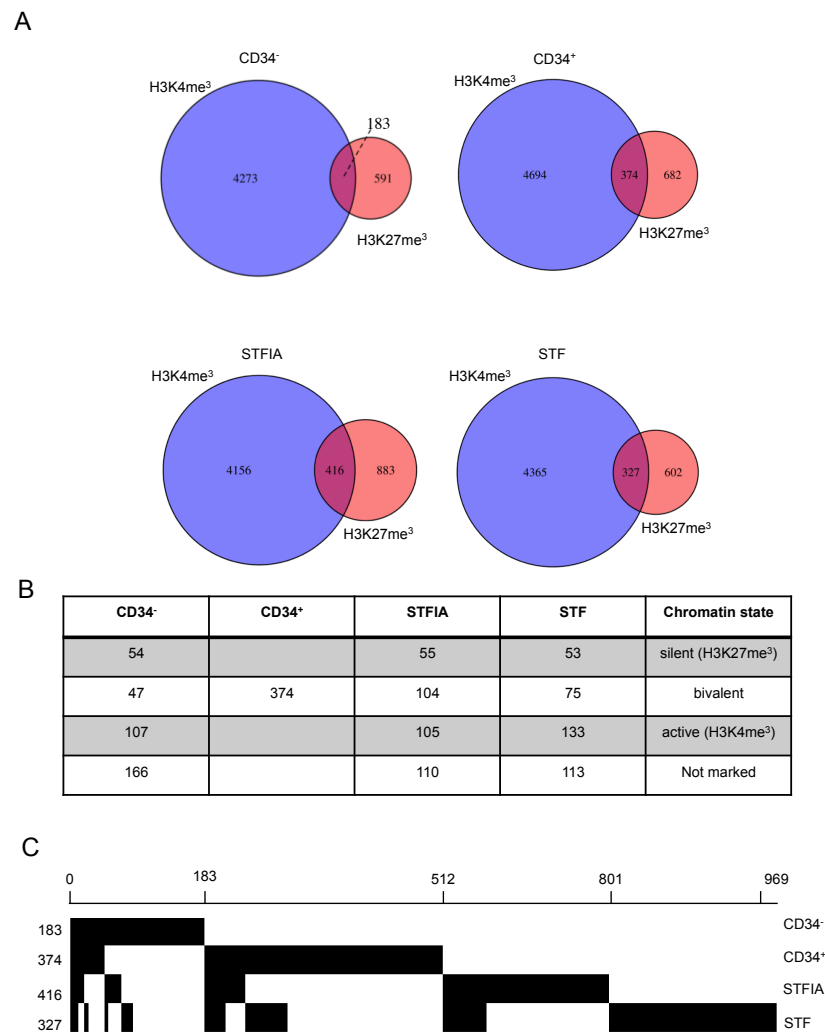


Figure 17: Bivalent promoter methylation profiles in fresh and expanded CB-CD34⁺ cells. A) Comparison of the number of promoters marked with H3K4me³ and H3K27me³ and numbers of H3K4me³ and H3K27me³ co-occupancy on promoters in fresh CB-CD34⁻ and CB-CD34⁺ cells, and in CB-CD34⁺ cells expanded for 7 days with either STF or STFIA cocktails. **B)** The table shows how the promoters of the genes bivalently marked in fresh CB-CD34⁺ cells are marked in fresh CB-CD34⁻ or in expanded CB-CD34⁺ cells. The number of genes possessing H3K4me³ but lacking H3K27me³, possessing H3K27me³ but lacking H3K4me³, and possessing neither H3K4me³ nor H3K27me³ in fresh CB-CD34⁻ or in expanded CB-CD34⁺ cells are indicated. **C)** H3K4me³ and H3K27me³ bivalent promoters resolution, formation and mutual exclusion in fresh and cultured cells. The columns represent genes recorded as bivalent in any of the 4 samples. Total number of bivalent genes per sample is indicated on the left (n=2).

CD34⁺	P-value	STFIA	P-value
cell-cell signaling	3,4E-9	blood vessel development	9,5E-6
developmental induction	2,3E-5	vasculature development	1,3E-5
cell-cell signaling involved in cell fate specification	2,3E-5	cell-cell signaling	1,9E-4
gland development	5,5E-5	regulation of cell development	2,6E-4
ion transport	6,3E-5	blood vessel morphogenesis	3,5E-4
induction of an organ	8,1E-5	muscle organ development	3,5E-4
behavior	9,6E-5	cell morphogenesis involved in differentiation	4,3E-4
neuron differentiation	2,8E-4	regulation of striated muscle tissue development	4,7E-4
tube development	3,1E-4	regulation of muscle development	5,3E-4
cell fate commitment	3,3E-4	axogenesis	5,4E-4
inorganic anion transport	4,0E-4	response to alkaloid	7,2E-4
positive regulation of locomotion	5,6E-4	response to hormone stimulus	1,1E-3
STF	P-value	CD34⁻	P-value
cell-cell signaling	1,2E-6	neuron differentiation	2,0E-4
regulation of axogenesis	5,0E-6	axon guidance	4,7E-4
metal ion transport	1,5E-5	cell projection organization	6,0E-4
ion transport	1,7E-6	cellular component morphogenesis	1,1E-3
potassium ion transport	1,8E-5	regulation of neuron differentiation	1,5E-3
regulation of cell morphogenesis involved in differentiation	4,7E-5	gland development	1,6E-3
regulation of cell morphogenesis	7,9E-5	cell morphogenesis involved in differentiation	1,9E-3
regulation of neuron differentiation	9,0E-5	axogenesis	2,1E-3
regulation of cell projection organization	1,3E-4	neuron projection development	2,6E-3
cation transport	1,9E-4	regulation of cell development	2,9E-3
cell surface receptor linked signal transduction	5,4E-4	cell morphogenesis involved in neuron differentiation	3,3E-3
regulation of cell development	7,7E-4	neuron projection morphogenesis	3,6E-3

Figure 18: Gene ontology enrichment analysis of bivalent promoters. Top 12 biological processes of bivalent promoters in fresh CB-CD34⁻ and CB-CD34⁺ and expanded CB-CD34⁺ cells using gene ontology analysis with Database for Annotation, Visualization and Integrated Discovery (DAVID). p-values are indicated.

5.5 Clonogenic potential of EZH2 inhibitor-treated CB-CD34⁺ cells

Analysing the chromatin organization and dynamics of fresh and expanded CB-CD34⁺ cells we observed a culture-associated chromatin remodelling and a genome-wide increase and redistribution especially of H3K27me³ mark. PRC2 is the complex with the histone methyltransferase activity that trimethylates histone H3 on lysine 27. Given that EZH2 is the protein ruling the enzymatic activity of PRC2 that catalyzes the H3K27me³ mark (Cao *et al.*, 2002), I firstly looked for EZH2 expression in fresh and expanded CB-derived cells. Three independent Western blot analyses revealed higher EZH2 protein levels in fresh CB-CD34⁺ compared to CB-CD34⁻ cells and elevated EZH2 levels in STF- compared to STFIA-cultured cells (Fig. 19A). I then analysed the gene expression of EZH2 and qRT-PCR analyses confirmed the higher expression of EZH2 in STF-expanded compared to STFIA-expanded cells (Fig. 19B). ChIP-PCR analyses of the *EZH2* locus revealed higher H3K4me³ promoter marking in fresh CB-CD34⁻ and in STF-expanded CB-CD34⁺ cells, but higher H3K27me³ levels only around the TSS of fresh CB-CD34⁻ cells (Fig. 19C). Therefore I hypothesized that employing selected EZH2 inhibitors might antagonize the elevated H3K27me³ levels of STF- *versus* STFIA-expanded cells. Fresh CB-CD34⁺ cells were expanded for 7 days under STF conditions and were treated with either GSK343 or GSK126 EZH2 inhibitors (Verma *et al.*, 2012; McCabe *et al.*, 2012). First we tested the efficiency of the EZH2 inhibitors treatment *via* chromatin flow cytometry: treatment of STF-expanded CB-CD34⁺ cells with both EZH2 inhibitors decreased global H3K27me³ levels to the levels of STFIA-expanded cells (Fig.19D). We then monitored CB-CD34⁺ cells expansion and viability upon 7 days of culture with or without EZH2 inhibitors treatment. The TNCs and the total dead cells counts were not significantly different between treated and untreated STF-cultured CB-CD34⁺ cells (Fig. 19E).

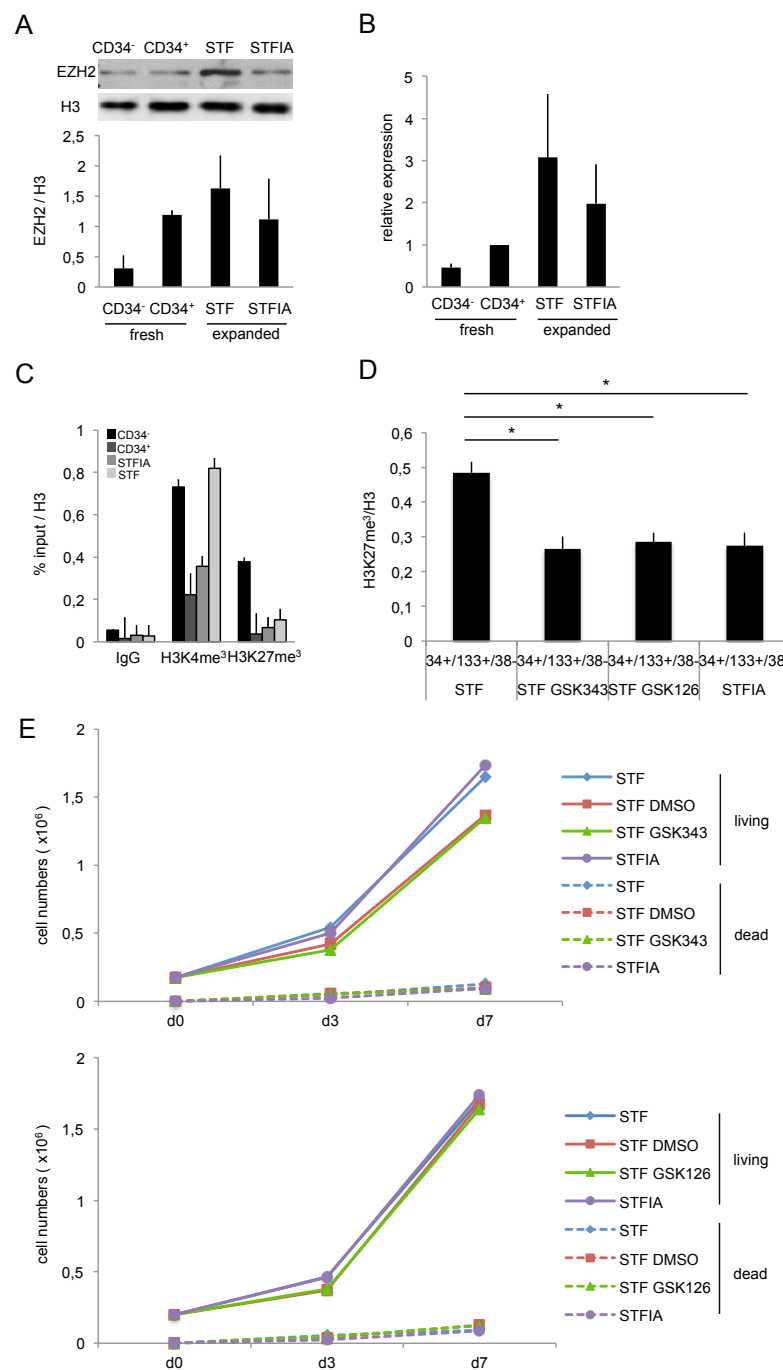


Figure 19: Treatment of CB-CD34⁺ cells with PRC2 inhibitors. **A)** Representative image from one of three independent EZH2-specific Western blot analyses of fresh CB-CD34⁻ and CB-CD34⁺ cells, and of CB-CD34⁺ cells expanded for 7 days with either STF or STFIA cocktails (upper panel). Relative signal intensities of bands were quantified and normalized against H3- specific signal intensities (lower panel), n=3. **B)** ChIP-PCR and RT-PCR analyses of the EZH2 (chr7:148,502,464-148,583,441) locus of fresh CB-CD34⁻ and CB-CD34⁺ cells and of 7 days STF- and STFIA-expanded cells. **C)** 0,15X10⁶ human CB-CD34⁺ cord blood cells were expanded for 7 days with either STF or STFIA cocktails +/- the EZH2 inhibitors GSK343 (1 mM) or GSK126 (1 mM) and total living and dead cells were counted at the indicated time. **D)** CB-CD34⁺ cells expanded for 7 days with either STF or STFIA cocktails +/- either GSK343 or GSK126 inhibitors. Intranuclear flow cytometry analysis specific for H3-normalized values of H3K27me³ global levels of gated CD34⁺/CD133⁺/CD38⁻ cells. Student t-test, ** p<0,01, n=3.

Clonogenic potential has been used as a measure for hematopoietic progenitor cells. Each colony formed represents the progeny of a single multipotent stem cell. We therefore determined the colony forming capacity of fresh CB-CD34⁺ cells and of CB-CD34⁺ cells expanded with either STF or STFIA cocktails +/- EZH2 inhibitors by a methylcellulose-based colony formation assay. After 14 days of culture in methylcellulose, plates were scored for the number of BFU-E (burst forming unit - erythroid) CFU-GEMM (colony forming unit-granulocyte, erythrocyte, macrophage, and megakaryocyte), and CFU-GM (colony forming unit- granulocyte, macrophage) under an inverted light microscope (Fig. 20A). Hematoxyline and eosin stainings demonstrated the presence of the corresponding hematopoietic cell types per colony forming category (Fig. 20B). All tested conditions supported CFU formation and CFUs were highest with STFIA-expanded cells. STFIA-expanded cells were able to significantly higher total numbers of CFUs in comparison to STF-expanded cells (reflecting their higher engraftment potential). However, the treatment of STF-expanded cells with EZH2 inhibitors did not significantly raise the CFUs formation to the levels recorded for STFIA-expanded cells (Fig. 20C).

5.6 EZH2 inhibition increases the engrafting potential of expanded CB-CD34⁺ cells

Despite a lack of differences in the progenitor cells capability to form CFUs after treatment of STF-expanded cells with EZH2 inhibitors, the impact of EZH2 inhibitor treatment on hematopoietic engraftment potential was assessed. The progeny of $0,5 \times 10^5$ CB-CD34⁺ STF-, STFIA-cultured or STF-plus inhibitor-cultured CB-CD34⁺ cells were harvested after 7 days of expansion and injected into irradiated NSG mice together with $0,2 \times 10^6$ NSG splenocytes. Engraftment was assessed four, eight and twelve weeks after transplantation by measuring the percentage of human CD45⁺ cells in the PB. I observed that treatment of STF-cultured CB-CD34⁺ cells with both EZH2 inhibitors significantly increased hematopoietic engraftment at four, eight and twelve weeks post transplantation to levels similar to STFIA-cultured CB-CD34⁺ cells (Fig. 21A). Multilineage hematopoietic engraftment potential of STF-treated *versus* STF-untreated CB-CD34⁺ cells was assessed in the BM and SP of the recipients eight weeks after transplantation by CD19, CD14 and CD3 stainings. The multilineage engraftment assay confirmed the increased capability of multilineage engraftment of STF-treated *versus* STF-untreated CB-CD34⁺ cells (Fig. 21B). To be pointed out, multilineage engraftment analyses

revealed increased percentages of lymphocyte types in STF-treated- compared to STF-untreated-grafts, as reported for STFIA-grafts.

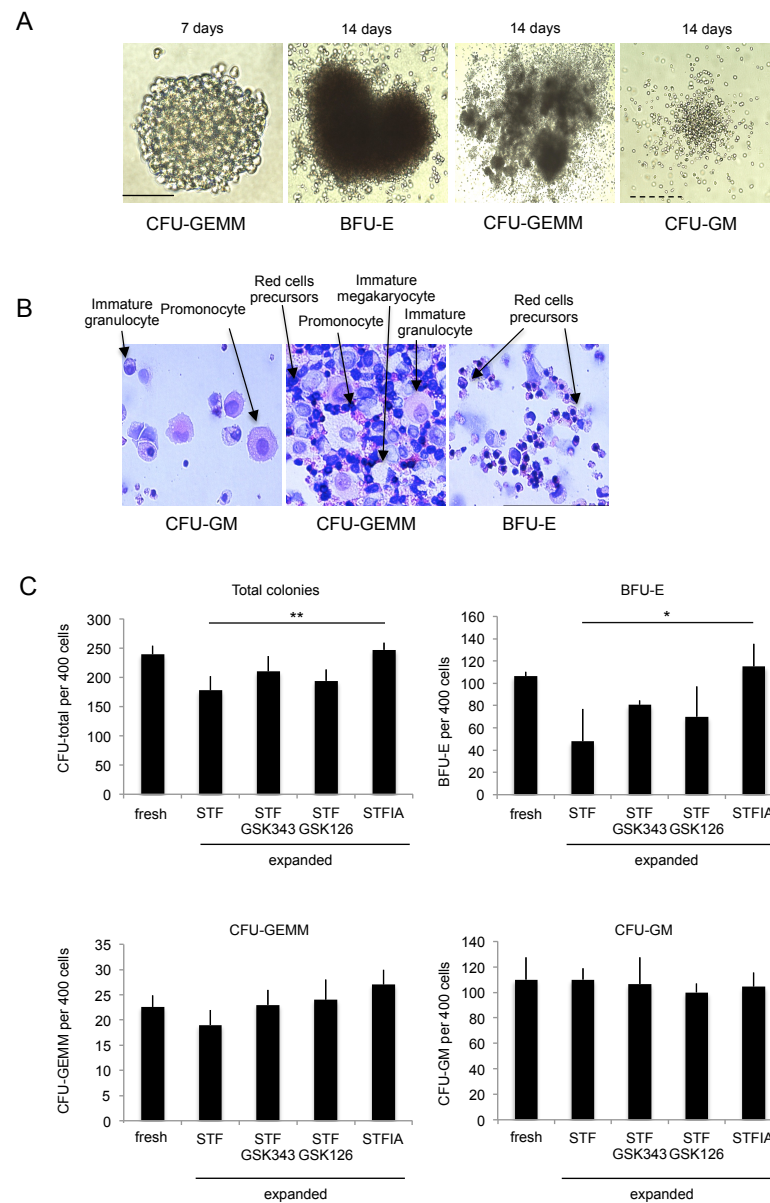


Figure 20: Only CB-CD34⁺ cells expanded with STFIA show improved colony-forming cell potential. A) After 7 days of expansion with either STF or STFIA cocktails +/- the EZH2 inhibitors GSK343 (1 mM) or GSK126 (1 mM), 400 cells were seeded into methylcellulose medium to evaluate the clonogenic potential under the different culture conditions. The clonogenic potential was assessed by plating 400 fresh CB-CD34⁺ cells/plate. The example shows phase-contrast images of typical morphologies of CFU-GM, BFU-E, or CFU-GEMM colonies after 7 and 14 days of culture into methylcellulose, scale bar = 50 μ m. **B)** Representative example of hematoxylin and eosin staining of BFU-E, CFU-GEMM and CFU-GM colonies after 14 days of culture in methylcellulose. The different hematopoietic cell types are indicated. **C)** Total CFU, BFU-E, CFU-GEMM and CFU-GM per 400 cells are shown. Results express mean \pm SD of two independent experiments performed in triplicate. Student t-test, * $p < 0,05$, ** $p < 0,01$, $n=2$.

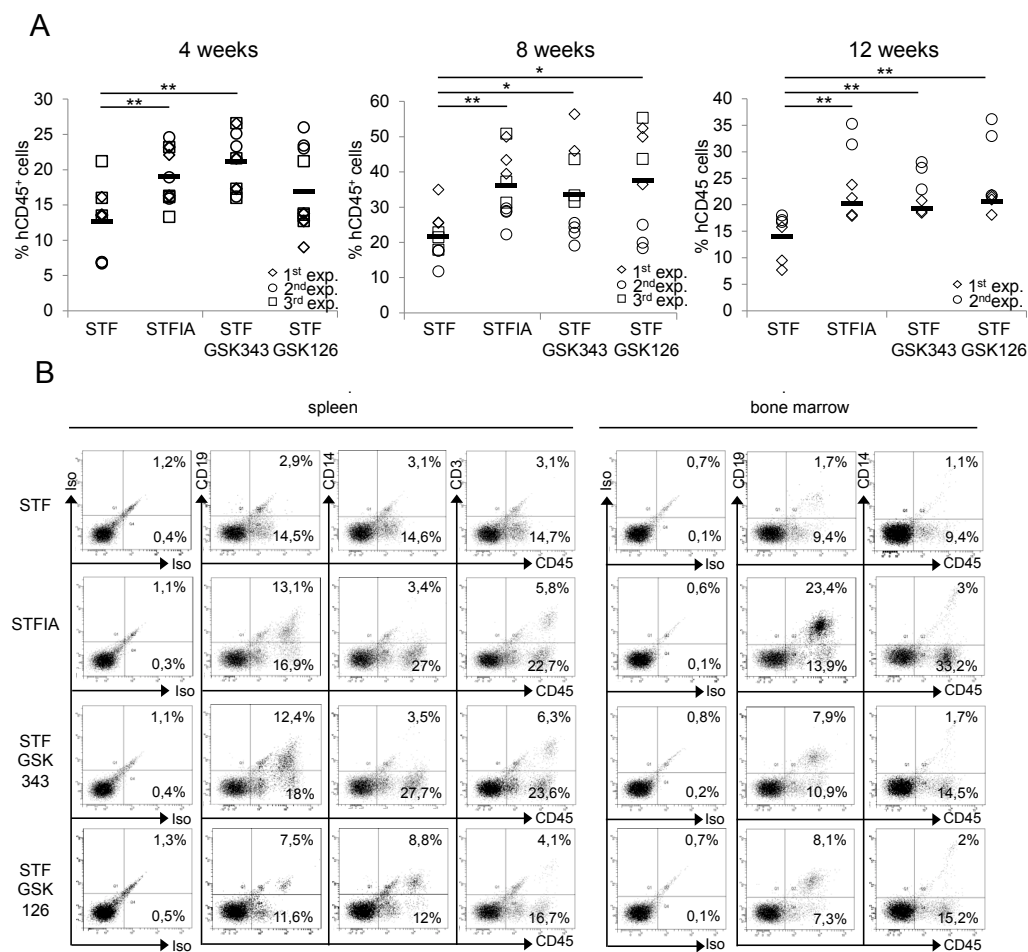


Figure 21: Multilineage engraftment analysis of CB-CD34⁺ cells treated with EZH2 inhibitors. A) The progeny of 2×10^5 CB-CD34⁺ cells expanded for 7 days with either STF or STFIA cocktails +/- either GSK343 or GSK126 inhibitors were equally split and injected into 4 recipients. Shown are percentages of human chimerism by measuring the percentage of human CD45⁺ cells *via* flow cytometry in the BM of NSG transplant recipients. Each symbol represents the engraftment of a single recipient analysed 4, 8 or 12 weeks post transplant. Student t-test, * $p < 0,05$, ** $p < 0,01$. **B)** Representative analysis of human chimerism in the SP and BM of transplant recipients of CB-CD34⁺ cells expanded with either STF or STFIA cocktails +/- either GSK 343 or GSK 126 inhibitors. Animals were analysed 8 weeks post transplantation using antibodies specific for human hematopoietic cells. Percentages of positive cells are indicated.

6 DISCUSSION

The work presented in this thesis contributes to a better understanding of chromatin changes upon *in vitro* expansion of human CB-HSPCs. I observed that short- and long-term engraftment in NSG mice when using a STFIA cytokine cocktail for expansion is superior to a STF cocktail only. I found that freshly isolated CB-CD34⁺ and CB-CD34⁻ cells have different global H3K4me³ and H3K27me³ levels and that the *ex vivo* environment remodels the epigenetic landscape of CB-CD34⁺ cells. I noticed that especially global H3K27me³ levels change depending on the expansion conditions. I also observed a higher degree of changes in the local distribution of H3K27me³- than of H3K4me³-marked regions. Furthermore, I detected higher EZH2 protein levels in STF- compared to STFIA-cultured CB-CD34⁺ cells and treatment with two different EZH2-specific inhibitors increased hematopoietic engraftment potential of cultured CB-CD34⁺ cells.

6.1 STFIA cocktail maintains the engrafting potential of CB-CD34⁺ cells

HSC expansion requires a complex combination of growth factors and cytokine cocktails that control the proliferative potential of HSCs (Devine *et al.*, 2003). The searching for optimized growth factor conditions for robust HSC expansion is of primary importance to establish trusted methods that maintain reliable HSCs potential during culture (Doulatov *et al.*, 2012). I here evaluated the expansion potential and culture-related chromatin remodeling of CB-CD34⁺ cells using 2 different cytokine cocktails: STFIA and STF. STFIA combines SCF, TPO, FGF-1 (i.e. the so-called STF cocktail) with Angptl5 and IGFBP2 and it was shown to highly expand HSCs (Zhang *et al.*, 2006; Drake *et al.*, 2011). Firstly I compared the morphology of expanded CB-CD34⁺ cells with fresh CB-CD34⁺ cells and I observed a higher degree of polarization in both culture conditions as compared to fresh CB-CD34⁺ cells. Polarization is the ability of CB-CD34⁺ cells to gain polarized shape upon *ex vivo* expansion (Giebel *et al.*, 2004) and it is correlated with migration potential (Alakel *et al.*, 2009). One

would have expected a higher degree of polarization in STFIA-expanded cells, as it is reported that IGFBP2 and IGFBP4 enhance the migration potential of human HSPCs (Bartling *et al.*, 2010). However, the concentration of IGFBP2 used by Bartling *et al.* that was stimulating cell migration was 500 µg/ml and 900 µg/ml, which corresponded to the amount of protein found in a healthy donor blood. This amount is 5 and 10 times higher than the concentration used in my study, so the amount of IGFBP2 used was too low to cause a higher degree of polarization of STFIA-cultured cells. When the cells were analysed *via* CFU assay, higher expansion of CFU-initiating cells was found using STFIA- in comparison to STF-conditions (Figure 20). The addition of Angptl5 and IGFBP2 significantly enhanced the CFU potential of CB-HSPCs as previously published (Zhang *et al.*, 2008). However, it was also confirmed that after 7 days of expansion with both expansion conditions less CFU-initiating cells were present in the cultures when compared to fresh CB-CD34⁺ cells (Walenda *et al.*, 2011). Similar to a previously published report I observed that after culture under both expansion conditions the progeny of 50.000 fresh CB-CD34⁺ cells was able to repopulate the hematopoietic system of recipient mice (Blank *et al.*, 2012). However, I also noticed inter-experimental variations in engraftment similar to a previous study (Blank *et al.*, 2012). The inter-experimental variations could be caused by dissimilarities in cell source, expansion periods, or batch to batch variations of cytokines. A limiting dilution assay would be helpful to verify if also low cell doses are able to reconstitute the hematopoietic system of recipients (Khoury *et al.*, 2011). Additionally, the variable engraftment may arise from a multitude of causes including how individual HSCs respond to growth factors and how they vary in their homing potential capabilities. Furthermore this study confirmed that after 7 days of culture, the human chimerism found in fresh CB-CD34⁺ grafts was maintained when CB-CD34⁺ cells were expanded under STFIA condition but not when they were expanded under STF condition (Zhang, 2008). However, engraftment levels of STFIA-cultured cells did not reach the 20-fold net expansion of repopulating HSPCs as earlier reported (Zhang *et al.*, 2008). Multilineage engraftment analyses revealed increased percentages of lymphocyte types such as CD19 and CD3 (Figure 5B) in STFIA- compared to STF-grafts indicating that the addition of Angptl5 and IGFBP2 boosts the hematopoietic progression of HSPCs towards the lymphoid lineage. Since multiple signals are known to interact within the HSC niche for establishing the balance between self-renewal and differentiation (Rice *et al.*, 2007), the importance of IGFBP2 and Angptl5 for HSC differentiation must be studied in greater detail. It was also reported that the use of Angptl5 greatly reconstituted both myeloid and lymphoid compartments (Khoury *et al.*, 2011), while I noticed an increased reconstitution of especially the lymphoid cell types. These

discrepancies could be explained by the use of different cell populations, cell dose, expansion periods and cell source in the above cited studies (Blank *et al.*, 2011; Khoury *et al.*, 2011; Zhang *et al.*, 2008). All these factors can affect the engrafting potential of HSCs.

In summary the data reported above indicate that CB-CD34⁺ cells expanded under STFIA condition compared to a standard cocktail show improved clonogenic and NSG engraftment potential. The *in vivo* assay reveals that lymphoid differentiation capacity is maintained in STFIA-grafts but not in STF-grafts when compared to fresh CB-CD34⁺-grafts. Due to the knowledge that post-engraftment infections are mostly related to an impaired reconstitution of B and T lymphocytes (Heining *et al.*, 2007), this finding may be of clinical relevance.

Several Angiopoietin-like (Angptl) proteins were shown to support the expansion of HSCs *in vitro* and *in vivo* (Zheng *et al.*, 2012). However the intracellular signal transduction pathways involved and further roles of these proteins in angiogenesis and in vascular as well as in tumor biology are poorly understood. Nevertheless, recent analyses proved the importance of Angptl proteins in supporting HSC expansion, metabolism, angiogenesis and inflammation (Morisada *et al.*, 2006; Hato *et al.*, 2008). Recent studies have aimed at finding the receptors of these so far called “orphan ligands”. Interestingly, the immune-inhibitory receptor human leukocyte immunoglobulin-like receptor B2 (LILRB2) showed enhanced binding to Angptl2 and Angptl5 (Zheng *et al.*, 2012). LILRB2 was found to be expressed on the surface of 40-95% of human CB-CD34⁺CD38⁻CD90⁺ cells, a population enriched in HSCs, and the silencing of LILRB2 resulted in decreased repopulation capabilities of human CB-HSCs (Zheng *et al.*, 2012). Therefore Angptl5-mediated CB-CD34⁺ expansion could act *via* the surface receptor LILRB2. The HSC niche is the microenvironment that maintains and controls the balance between survival, self-renewal ability and cell fate decision of HSCs (Orkin *et al.*, 2008; Carlesso *et al.*, 2010). Because Angptl proteins are widely expressed in many cell types including cells of endocrine organs and in the BM niche (Zheng *et al.*, 2011; Hato *et al.*, 2008), they are candidates for direct or indirect effects on HSCs expansion. It was reported that *ex vivo* culture significantly modulates the immunogenicity of HSCs, and therefore contribute to the “immune privilege” of HSCs, *via* changes in the expression of immune proteins such as MHC-I and MHC-II (Zheng *et al.*, 2011b) and other immune molecules. The Angptl-LILRB2 network may be involved in this process and may be fundamental for the maintenance of HSC stemness upon culture.

6.2 Global levels of H3K4me³ and H3K27me³ change upon expansion of CB-CD34⁺ cells

The limitations to expand HSCs *ex vivo* may be due to an altered control of the balance between survival and self-renewal (Srouf *et al.*, 2005). The importance of epigenetic mechanisms on whether HSCs proceed to either symmetrical or asymmetrical cell division has been validated (Araki *et al.*, 2007; Li *et al.*, 2011). The maintenance of HSC function and the differentiation potential of HSCs are both influenced by epigenetic regulation (Weishaupt *et al.*, 2010). Therefore I examined the epigenetic changes between fresh CB-CD34⁺ and CB-CD34⁻ cells, and CB-CD34⁺ cells expanded under different culture conditions. This work focuses on the analysis of H3K4me³ and H3K27me³ histone tail modifications. The simultaneous presence of these 2 marks characterizes bivalent domains which are regulatory regions associated with cell fate decision (Bernstein *et al.*, 2006). The co-occupancy by active and repressive marks is known to silence developmental genes and to keep them poised for activation (Mikkelsen *et al.*, 2007; Bernstein *et al.*, 2006). Chromatin flow cytometry and Western blot analysis were chosen for evaluating the global histone modification levels of fresh and expanded human CB cells. The two methodologies showed that H3K4me³ and H3K27me³ levels differed between CB-CD34⁺ and CB-CD34⁻ cells. Both methods found higher global H3K4me³ levels in fresh CB-CD34⁺ than in CB-CD34⁻ cells, which is in line with previously published data (Navakauskiene *et al.*, 2014). We next studied active or repressive histone modification remodeling upon expansion, and we observed that culturing CB-CD34⁺ was paralleled by global changes in H3K27me³ while H3K4me³ levels were less altered. Recent studies have revealed that Polycomb-group proteins are required not only for maintaining pluripotency and lineage potential in ES cells but also for a strict control of gene expression during differentiation (Shen *et al.*, 2008; Chamberlain *et al.*, 2008). It was also reported that the active modification H3K4me³ is stable in distinct stem cell lines while H3K27me³ varies in abundance and genome-wide distribution (Rugg-Gunn *et al.*, 2010). In line with these findings our data suggest that for the maintenance of HSC properties during CB-CD34⁺ expansion the H3K27me³ gene silencing promoted by Polycomb-group proteins seems to be functionally more relevant than Trithorax-group-mediated gene activation. Human CB-CD34⁺ cells are a heterogeneous cell population consisting of quiescent LT-HSCs, but also cycling short-term HSCs and multipotent progenitors with different potentials. I am aware of the fact that a more stringent HSC purification including an extended range of surface markers, which characterize the HSPCs population, would be beneficial (Wisniewski *et al.*, 2011). The data collected from the mixed population of CB-CD34⁺ cells may overestimate

the epigenetic complexity of cell populations with similar potentials and the results obtained with pure LT-HSCs would most probably be different. It is important to optimize chromatin profiling methods for even lower cell numbers to dissect epigenetic profiles in subtle cell populations. Nevertheless, the study of epigenetic changes during CB-CD34⁺ cell expansion contributes to clarify the histone modification dynamics in HSPC maintenance and development. The understanding of the chromatin status alterations linked to *ex vivo* expansion may provide instruments for finding new epigenetic drugs able to improve HSC transplantation potential, given that altered histone modification patterns have been proved to be reversible for instance in AML cells (Paul *et al.*, 2010).

6.3 Ex vivo expansion of CB-CD34⁺ cells remodels the distribution of H3K4me³ and H3K27me³ histone modification marks

Several studies revealed that epigenomic landscapes differ between different cell types (Hawkins *et al.*, 2010, Meissner *et al.*, 2008) and that these differences are crucial for defining cell-type specific gene expression patterns and functions (Creyghton *et al.*, 2010; Heintzman *et al.*, 2009). We therefore performed ChIP-seq experiments focusing on the genome-wide redistribution of H3K4me³ and H3K27me³ marks upon CB-CD34⁺ cell expansion.

ChIP-seq analyses identified that upon *ex vivo* expansion CB-CD34⁺ cells overall lost H3K27me³ marks at the TSSs and over gene bodies. Moreover it was found that in cultured cells the size of H3K4me³-enriched regions increased independently of the cytokine cocktail. Stem and mature cells have distinct epigenomic landscapes and differentiation is paralleled by large-scale expansion of H3K27me³ but less H3K4me³ domains (Hawkins *et al.*, 2010, Zuh *et al.*, 2013). Our analysis confirmed previous observations (Abraham *et al.*, 2013; Cui *et al.*, 2009; Hawkins *et al.*, 2010) showing that H3K4me³-enriched regions were narrower than H3K27me³-enriched regions irrespective of which dataset was analysed. The H3K27me³ histone modification appeared to be a very dynamic chromatin mark as previously reported (Hawkins *et al.*, 2010). It is shown that H3K27me³ distribution progresses from a more focal state in ESCs to expanded domains in differentiated cells, and is found in an intermediate state in adult stem cells (Rugg-Gunn *et al.*, 2010, Chen *et al.*, 2014). H3K27me³-enriched regions maintained the size distribution of fresh CB-CD34⁺ cells following STFIA expansion, but showed a relevant enlargement of H3K27me³ domains following STF expansion similar to the spatial distribution found in differentiated CB-CD34⁺ cells. Considering that H3K4me³ island

size distributions were maintained in human HSPCs while H3K27me³ island sizes increased during differentiation (Jones *et al.*, 2014; Hawkins *et al.*, 2010), noticeably STFIA- but not STF-cytokine cocktail was able to preserve the size distribution of H3K27me³-enriched regions. The ChIP-seq data further pointed out that the genome-wide H3K27me³ peak distribution occupied broad domains while H3K4me³ signals were confined to mainly promoter regions, in line with published observations (Cui *et al.*, 2009, Heintzman *et al.*, 2007). It was reported that human blood cells presented a high degree of intergenic regions covered by H3K27me³ (Zhu *et al.*, 2013). Also, H3K4me³ is mostly found in focal peak-like structures within promoters while the majority of H3K27me³ peaks is found in intergenic regions and forms broad local enrichments (BLOCs) (Cui *et al.*, 2009; Pauler *et al.*, 2009; Brinkman *et al.*, 2012). Our data are consistent with the above cited reports. We found different H3K4me³ and H3K27me³ distributions over specific gene regions and different enriched-island sizes.

The distribution of H3K27me³ modification is highly variable across different cell types and especially certain regions such as Hox gene clusters are associated with a high-degree of variability (Pinello *et al.*, 2014). To examine whether the extended H3K27me³ repressive mark domains are a pivotal feature of differentiated cells we examined specific gene loci. Our analysis of the HoxA and HoxB loci showed the predicted H3K4me³ and H3K27me³ landscapes as previously published (Abraham *et al.*, 2013). We also noticed expanded domains of H3K27me³ in the differentiated cells that were not found in fresh CB-CD34⁺ and CB-CD34⁻ cells.

To verify the correlation between gene expression data and ChIP-seq analysis we assessed H3K4me³ and H3K27me³ profiles around the TSSs of sets of genes that exhibited high or low expression levels in fresh CB-CD34⁺ cells. Our analyses revealed that the chromatin maps precisely reflected the true patterns of H3K4me³ histone modification with the typical nucleosome gap at the TSSs of the utmost expressed genes (Adli *et al.*, 2010, Rugg-Gunn *et al.*, 2010). The integration of gene expression profiles and ChIP-seq data confirmed the expected correlation between H3K27me³ and the transcriptional status of lowly expressed genes.

The subset of loci enriched with either H3K4me³, H3K27me³ or both chromatin modifications could give us insights on new genes with critical functions in hematopoietic progenitors (Azura *et al.*, 2006; Orford *et al.*, 2008). Therefore, we looked at lists of genes with marked promoters. The Venn diagrams in Figure 15 show a high degree of exclusivity of promoters that were H3K4me³- or H3K27me³-marked depending on whether samples from fresh, STF- or STFIA-cultured cells were analysed. We noticed that one third of the enriched

promoters was unique in each of the samples. The lists of H3K27me³ enriched promoters were used to view how Polycomb-repressive complex is specifically reorganizing chromatin to prepare different gene loci for silencing. These patterns may provide an epigenetic memory to keep lineage-specific expression or repression of defined sets of genes. The exclusively marked promoters of fresh and STFIA-expanded CB-CD34⁺ cells showed similar GO-terms revealing that genes linked to the same biological processes have the same chromatin structure. This finding supports the hypothesis that epigenetics and environmental cues are able to maintain certain lineage specific transcriptional programs.

The analysis of the correlation between histone modifications on promoters and gene expression indicates little transcriptional changes between STF- and STFIA-cultured cells while visible changes of H3K27me³ and H3K4me³ levels are apparent upon culture. I observed a higher remodelling of H3K27me³-enriched promoters compared to H3K4me³-enriched promoters without transcriptomic changes. Interestingly, Factor *et al.* showed marginal changes in gene expression when mouse ESCs and epiblast stem cells were analysed *via* high resolution genome-wide assay but significant alterations of global histone modifications (Factor *et al.*, 2014). These distinctive transcriptome and epigenome characteristics found in naive and primed pluripotent cells show that also closely related developmental stages with similar gene expression profiles can possess diverse epigenotypes, possibly priming but not yet resulting in transcriptional changes. This could indicate that STF and STFIA cocktails primarily act on the epigenomic and less on transcriptomic regulatory systems and that epigenomic properties on HSPCs are sensitive to whether the cells are exposed to *in vivo* or *in vitro* environments. The enrichment patterns of H3K4me³ and H3K27me³ have been shown to be highly variable among different cell types due to the cellular and developmental context (Zhu *et al.*, 2013, Young *et al.*, 2011). However the dynamic of how the distribution of these epigenetic modifications changes is still under investigation. Recently Masaki *et al.* claimed that changes in H3K27me³ status are consequence rather than cause of transcriptional regulation (Hosogane *et al.*, 2013).

Promoters marked with H3K4me³ and H3K27me³ are known to belong to poised key genes important for development and differentiation. We therefore tested how bivalency reorganizes upon expansion. Bivalency at promoter regions in HSCs primes for subsequent transcriptional activation of genes and is critical during differentiation (Voigt *et al.*, 2013). Moreover, bivalency is important for stem cell maintenance implying a critical role for chromatin modifications in HSC fate (Roh *et al.*, 2006). I observed a considerable redistribution of

bivalent domains upon culture. However, I am aware that the bivalent genes showed a heterogeneous enrichment for the two histone modifications, which can translate into important differences in the gene expression patterns (De Gobbi *et al.*, 2011). On the basis of the ratio between H3K4me³ and H3K27me³ enrichment it would be possible to separate the bivalent genes in several groups as the ratio between the two chromatin modifications can be important when translated into gene expression regulation (Roh *et al.*, 2006; Gibson *et al.*, 2009).

As previously published, we found nearly double the number of bivalent genes in CB-CD34⁺ cells, both fresh and expanded, in comparison with differentiated CB-CD34⁻ cells (Cui *et al.*, 2009, Bernstein *et al.*, 2006). Although the total number of bivalent promoters was similar in fresh and cultured CB-CD34⁺ cells, only about one third of the genes marked with both modifications in fresh CB-CD34⁺ cells maintained the bivalent mark upon STF or STFIA expansion. Moreover, we found newly established bivalent promoters in each of the samples. Thus, although transcriptomic changes are minor between the STF and STFIA culture conditions, different sets of genes are set up for being expressed (or definitely silenced) at a later stage, which subsequently may cause differences in engraftment potential. GO-term analysis revealed a cocktail-specific reorganization of the bivalency status. GO analysis also showed that genes involved in hematopoietic cell differentiation and development were occupied by bivalent marks in both fresh and expanded CB-CD34⁺ cells. However, I found that only in CB-CD34⁺ cells expanded under STFIA condition GO analysis showed genes involved in blood vessel development and morphogenesis. The appearance of these GO terms may relate to the activity of Angptl proteins (Oike *et al.*, 2004) or the angiogenic signatures may be relevant for HSC expansion.

For a better understanding of the process of epigenetic gene activation, repression and priming with respect to cell fate commitment upon *ex vivo* expansion of HSCs it will be important to genome-wide analyse other histone modifications. For instance, it would be relevant to study histone acetylation and H3K4 mono-/dimethylation characterizing active enhancers and promoters, as well as other repressive histone marks such as H3K9me³ or DNA methylation that may or may not overlap with H3K27me³. In particular, the colocalization of H3K9me³ and H3K27me³ has already drawn the attention of other groups (Bilodeau *et al.*, 2009) due to the dual repression at specific regulatory regions (Hawkins *et al.*, 2010) that may be fundamental for the maintenance of silencing during differentiation.

6.4 The treatment of STF-cultured CB-CD34⁺ cells with two different EZH2 inhibitors increases hematopoietic engraftment

I found a culture-associated chromatin remodelling and a genome-wide increase of especially H3K27me³ marks after analysing the chromatin organization and dynamics of fresh and expanded CB-CD34⁺ cells.

I therefore studied the protein responsible for PRC2's catalytic activity to deposit H3K27me³ mark, i.e. EZH2. The results of this analysis revealed increased culture-induced EZH2 protein and RNA levels in STF- compared to STFIA-cultured cells. EZH2 is less expressed in STFIA-cultured cells leading to lower H3K27 trimethylation levels in these cells. EZH2 plays an essential role in stem cell maintenance and lineage differentiation (Wei *et al.*, 2011; Chen *et al.*, 2012). Moreover, the involvement of EZH2 overexpression in cancer stem cells and tumor development and progression has been shown (Chang *et al.*, 2012). Both activating and inactivating mutations of EZH2 are associated with certain malignancies (Sauvageau *et al.*, 2010; Chase *et al.*, 2011), suggesting that EZH2 probably acts *via* positive and negative regulation of cell activity in a cell-context dependent manner. Numerous highly potent and selective small molecule inhibitors of EZH2 have been developed (Helin *et al.*, 2013), as EZH2 is a novel therapeutic target for human malignancies. Therefore I assessed if specific EZH2 inhibitors could block the activity of EZH2 in STF-cultured cells, and I analysed the consequences of this treatment. In the context of HSPCs expansion, epigenetic inhibitors have previously been shown to support expansion of CD34⁺ cells and combination of azaC with trichostatin A was shown to support the maintenance of NSG mice repopulating cells (Obier *et al.*, 2010, Milheim *et al.*, 2004). I could observe that treating STF-cultured cells with two EZH2 inhibitors counteracted the culture-induced loss of engraftment potential, indicating that EZH2 activity may be key to culture-associated loss of engraftment potential. Notably, multilineage engraftment analyses revealed increased percentages of lymphocyte types in STF-treated- compared to STF-untreated-grafts, as reported for STFIA-grafts. A strict regulation of the expression of PRC1 and PRC2 complexes has been shown to be crucial for HSCs identity (Kamminga *et al.*, 2006; Mochizuki-Kashio *et al.*, 2011; Van den Boom *et al.*, 2013). Being a subject of studies, the increased engraftment potential of EZH2 inhibitor-treated cells was not entirely unexpected as loss of function mutations of the PRC2 core components Suz12, Eed and EZH2 display enhanced hematopoietic progenitor cell activities following transplants in mice (Majewski *et al.*, 2010). Inhibition of histone methyltransferase activity by small molecule approaches is an active area of research (Verma *et al.*, 2012). Thus,

inhibitors of chromatin factors and chromatin-modifying agents provide potential strategies for the expansion of HSPCs. A more detailed knowledge of EZH2 target genes in the HSPC compartment will enable a better understanding of the role of this protein and PRC2 complex during HSPCs expansion and differentiation. The interplay between cell-extrinsic and –intrinsic factors involved in HSC expansion and self renewal potential vary depending on the combinations of environmental stimuli applied to the culture system. Knowing that the function and maintenance of HSCs *in vivo* as well as *in vitro* are controlled by transcriptional and epigenetic regulation, I suggest a model (Figure 22) in which *ex vivo* expansion strategies using the inhibition of chromatin factors are fundamental for retaining the characteristic biological properties of HSCs.

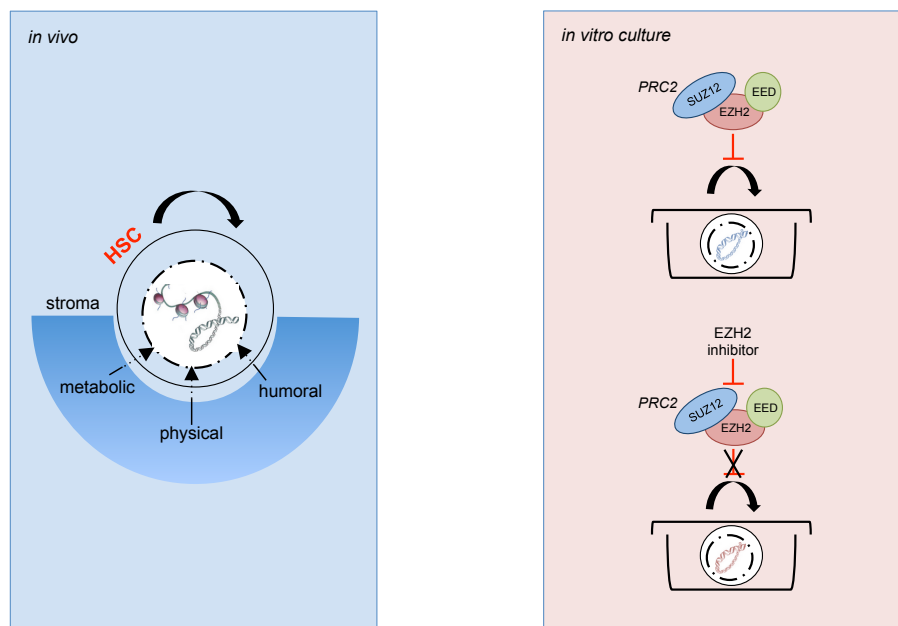


Figure 22: Proposed model for HSCs chromatin remodeling.

HSCs in the native niche are tightly regulated by specific stromal interactions that provide appropriate humoral, physical and metabolic signals. All these interactions feed HSC chromatin. When HSCs are out of their natural location, these environmental stimuli change, and with them the chromatin of HSCs. HSCs in culture show elevated PRC2 expression and reduced engraftment potential. The data shown here indicate that the use of EZH2 inhibitors increase the engraftment potential of HSCs. I hypothesize that a strict regulation of PRC2 complex is fundamental for HSCs expansion and that especially EZH2 activity is key to culture-associated loss of engraftment potential of HSCs.

In summary, this work provides genome-wide maps of H3K4 and H3K27 trimethylation changes upon expansion of CB-HSPCs and shows that the H3K4me³ but less the H3K27me³ landscape is stable. These findings suggest a model (see Figure 22) in which growth stimuli in culture media alter chromatin architecture. *Ex vivo* culture results in chromatin modification changes associated with a specific engraftment potential. H3K27me³ mediated gene repression rather than H3K4me³ may be critical to establish a specific transcriptional program. However H3K27me³ mediated influences on specific genomic loci remain to be understood. Our data further show that inhibition of the PRC2 component EZH2 counteracts the culture-associated loss of engraftment potential. These data may lead to new therapeutic tools and rational protocols for robust expansion of this clinically important adult stem cell type.

7 MATERIALS AND METHODS

7.1 Materials

7.1.1 Cell culture media and supplements

STF medium

Contents	Final concentration	Distributor
StemSpan serum-free medium	filled to 100%	StemCell Technologies
Penicillin and streptomycin	10 U/ml, 0,1 mg/ml	PAA
Heparin	10 µg/ml	Sigma Aldrich
Recombinant stem cell factor (SCF)	10ng/ml	Peprtech
Recombinant fibroblast growth factor 1 (FGF-1)	10ng/ml	Peprtech
Recombinant Thrombopoietin (TPO)	20ng/ml	Peprtech

STFIA medium

Contents	Final concentration	Distributor
StemSpan serum-free medium	filled to 100%	StemCell Technologies
Penicillin and streptomycin	10 U/ml, 0,1 mg/ml	PAA
Heparin	10 µg/ml	Sigma Aldrich
Recombinant stem cell factor (SCF)	10ng/ml	Peprtech
Recombinant fibroblast growth factor 1 (FGF-1)	10ng/ml	Peprtech
Recombinant Thrombopoietin (TPO)	20ng/ml	Peprtech
Angiopoietin-like 5 (Angptl5)	500ng/ml	Tebu-Bio
Insulin-like growth factor-binding protein-2 (IGFBP2)	100ng/ml	R&D Systems

Methylcellulose medium for CFU assay

Contents	Final concentration	Distributor
MethoCult SF H4236 Methylcellulose in Iscove's Modified Dulbecco's Media	40%	StemCell Technologies
Fetal Bovine Serum	25%	Gibco, Lot#41Q2105K
Bovine Serum Albumin	2%	PAA
L-Glutamine	2mM	PAA
2-Mercaptoethanol	5x10 ⁻⁵ M	PAA
Recombinant Human SCF	50 ng/mL	PAA
Recombinant Human GM-CSF	10 ng/mL	Miltenyi Biotec
Recombinant Human IL-3	10 ng/mL	Miltenyi Biotec
Recombinant Human Epo	3 IU/mL	Invitrogen
Recombinant Human SCF	1,4%	PepróTech

7.1.2 Antibodies**Primary antibodies**

Specificity	Species	Distributor
H3	Rabbit polyclonal	Abcam
H3K9me ³	Rabbit polyclonal	Diagenode
H3K4me ³	Rabbit polyclonal	Abcam
H3K27me ³	Rabbit polyclonal	Diagenode
H3K79me ³	Rabbit polyclonal	Abcam
EZH2	Rabbit polyclonal	Diagenode
IgG isotype control	Rabbit polyclonal	Abcam
CD34-FITC	Mouse monoclonal	Miltenyi Biotec
CD34-PE	Mouse monoclonal	Miltenyi Biotec
CD45FITC	Mouse monoclonal	Miltenyi Biotec
CD133-PE	Mouse monoclonal	Miltenyi Biotec
CD38-PE	Mouse monoclonal	Miltenyi Biotec
CD90-PE	Mouse monoclonal	Miltenyi Biotec
CD14-PE	Mouse monoclonal	Miltenyi Biotec
CD19-PE	Mouse monoclonal	Miltenyi Biotec
CD3-PE	Mouse monoclonal	Miltenyi Biotec
IgG2a-PE	Mouse monoclonal	Miltenyi Biotec
IgG2a-FITC	Mouse monoclonal	Miltenyi Biotec
IgG1-FITC	Mouse monoclonal	Miltenyi Biotec

Secondary antibodies

Specificity	Label	Distributor
Mouse	Cy2	Dianova
Mouse	Cy3	Dianova
Rabbit	Cy2	Dianova
Rabbit	APC	Dianova
Rat	goat, microbeads	Miltenyi Biotec
Rabbit	ECL- HRP	Ge Healthcare

7.1.3 Primers

All primers were ordered from Eurofins MWG Operon.

Gene expression primers

Gene	Sequence forward primer	Sequence reverse primer
CD34	CATCACAGAAACGACAGTCAA	ACTCCGCACAGCTGGAGG
RUNX1	CCACCTACCACAGAGCCATCAA	TTCCTGAGCCGCTCGGAAAAG
EZH2	AGGAGTTTGCTGCTGCTCTC	CCGAGAATTTGCTTCAGAGG
MLL	GTGGGATGTTACCAAACGCAG	ACTGTCTTCTCGACTCCTATCAG
LMO2	GCGCCTCTACTACAAACTGGGC	CTCATAGGCACGAATCCGCTTG
TAL1	CCACCAACAATCGAGTGAAGAGG	GTTTACATTCTGCTGCCGCCAT
cMYC	CTCCTGGCAAAGGTCAGAG	TCGGTTGTTGCTGATCTGTC
UTX	CTTCAGCCATTTCAACAGCA	GCTGAGCTGGGGTATATGGA
GATA2	TGACGGAGAGCATGAAGATG	GCCTTCTGAACAGGAACGAG
PU.1	GAAGCACTGGTGCCCTATGA	GGGGTGGAAAGTCCCAGTAAT
C/EBPa	TGGACAAGAACAGCAACGAG	TTGTCACTGGTCAGCTCCAG
C/EBPb	TTTCGAAGTTGATGCAATCG	CAACAAGCCCGTAGGAACAT
SUZ12	TGCAGTTCCTCTTCGTTGG	GAACCAGGCTTGTTCCTG
EED	TGGCCATGGAAATGCTATC	CCTCCAAATATTGCCACCAG
RPL27	ATCGCCAAGAGATCAAAGATAA	TCTGAAGACATCCTTATTGACG
BETA		
ACTIN	GCTATCCCTGTACGCCTCTG	CTCCTTCTGCATCCTGTCGG

ChIP primers

Gene	Sequence forward primer	Sequence reverse primer
CD34	GCTTCTCTCCTCCCCAGTCT	ACGACTGGTCCAATGGACT
RUNX1	AAGGAAGGGCATTGCTCAGA	ACCCTGTGGTTTGCAATTCAG
EZH2	CCGTGTGTTTCAGCGAAAGA	GCTGTAAGGGACGCCACTG
MLL	GAGGCCGCTATACAGATTGC	GAGAGGGAGAGGCGACAAC

LMO2	CTGCTTCCTGCCGACTTC	CAGATACAGACAGAACACTTGC
TAL1	ACTCCCTCCGGTGAAATTG	CGCTGTAATCCCACTCACG
cMYC	CACTCTCCCTGGGACTCTTG	TCTCCCTTTCTCTGCTGCTC
UTX	GCCCTACTGGGCAAGGTAAG	GAAAAGAGCGATTTTCGCAAG
GATA2	CCTGGAAGTGGGTGGAAGAC	ACCCGTGTCATCCCACTC
C/EBPa	GCCGGGAGAACTCTAACTCC	CTCTGCAGGTGGCTGCTC
C/EBPb	GGCCGCCCTTATAAATAACC	TATTAGTGAGGGGGCTGGTG
SUZ12	GGTCCTTCTCTCCCCACAAT	GATTCCCCCGTCAGTCAC
EED	GGTAGCGCTTTGAAATCCAC	TCTGGCGAATGAAAAGTACC

7.1.4 Kits and reagents

Kits	Distributor
CD34 progenitor cell isolation kit	Miltenyi Biotec
CD34 diamond cell isolation kit	Miltenyi Biotec
RNeasy Micro Kit	Qiagen
High Sensitivity DNA kit	Agilent Technologies

Reagents	Distributor
ABsolute qPCR SybrGreen Mix	Thermo Scientific
Agilent High Sensitivity DNA Kit	Agilent
BSA	Sigma-Aldrich
Chloroform	Applichem
DAPI	Sigma-Aldrich
DEPC	Applichem
DMSO	Applichem
Ethidium Bromid	Merck
ECL Select Western Blotting Detection Kit	Amersham
Ethanol	Applichem
First Strand cDNA Synthesis Kit	Thermo Scientific
GSK126	Chemie Tek
GSK343	Kindly provided from the SGC, University of Toronto
Isopropanol	Applichem
Laminin	Sigma-Aldrich
Methanol	Applichem
MethoCult SF H4236	Stem Cell Technologies
PageRuler Prestained Protein Ladder	Fermentas
Paraformaldehyd	Applichem
peqGold RNAPure	Peqlab
Phenol/Chloroform	Applichem

Propidiumiodid	Sigma-Aldrich
Proteinase K	Applichem
RNase	Sigma-Aldrich
Tris	Applichem

7.1.5 Consumables

Consumables	Distributor
Irradiation box	Greiner
Cell culture flasks	Nunc
Centrifuge tubes (15 mL & 50 mL)	Greiner Bio One
Cover slip	Hartenstein Laborbedarf
Blood collection bags	Kimberly-Clark
Multi-well cell culture plates	Nunc
Parafilm M	Hartenstein Laborbedarf
Scalpels	Ratiomed
Sterile filter	Schleicher & Schuell
Syringes	B. Braun
Tissue culture plates	Greiner Bio One

7.1.6 Buffers and solutions

1X PBS:

137 mM NaCl; 2,7 mM KCl; 10 mM Na₂HPO₄; 1,76 mM KH₂PO₄, pH 7,4.

DEPC-H₂O:

200 µl C₆H₁₀O₅ in 200 ml ddH₂O.

10X TBE Buffer:

0,9 M Tris-HCL (pH 8); 0,9 M Boric Acid; 20 mM EDTA.

Gel Loading Dye:

0,25 g Bromophenol Blue; 1,25 ml of 10% SDS; 12,5 ml of glycerol.

They are dissolved in 6,25 ml of ddH₂O.

1X Sample Solution:

0,01% Bromophenol Blue; 5% β-mercaptoethanol; 25% Glycerin; 2% of 20% SDS; 0,5 M Tris-HCL (pH 6,8).

Upper Tris:

0,5 M Tris-HCL; 10 ml of 20X SDS.

They are dissolved in 500 ml of ddH₂O (pH 6,8).

Lower Tris:

1,5 M Tris-HCL; 10 ml of 20X SDS.

They are dissolved in 500 ml of ddH₂O (pH 8,8).

Stacking gel:

1,5 ml of 30% PAA; 6,5 ml of ddH₂O; 2,5 ml Upper Tris; 40 µl TEMED; 70 µl 10% APS.

Running gel:

5 ml of 30% PAA; 4 ml of ddH₂O; 3 ml Lower Tris; 20 µl TEMED; 60 µl 10% APS.

10X Lamkli:

30 g Tris-HCL; 144 g Glycin; They are dissolved in 1 l of ddH₂O (pH 8,7).

Electrophoresis Buffer:

100 ml 10X Lamkli; 5 ml 10% SDS; 895 ml ddH₂O.

Transfer Buffer:

200 ml Methanol; 100 ml 10X Lamkli; 700 ml ddH₂O.

Blocking solution:

5% Nonfat dried milk powder; 0,1% Tween 20.

They are dissolved in 1X PBS.

Stripping solution:

10% SDS in ddH₂O; 1 M Tris-HCl (pH 6,5); 100 mM β-Mercaptoethanol.

FACS Buffer:

1000 ml of 1X PBS; 0,4% BSA; 0,02% NaN₃ (pH 7,4).

MACS Buffer:

1000 ml of 1X PBS; 0,3% BSA.

Gey's Solution:

20% Stock A: NH₄Cl 35,0 g; KCl 1,85 g; Na₂HPO₄-12 ·H₂O 1,5 g; KH₂PO₄ 0,12 g; Glucose 5,0 g; Phenol red 50 mg, bring to 1 liter with water.

5% Stock B: MgCl₂-6 ·H₂O 0,42 g, MgSO₄-7 ·H₂O 0,14 g, CaCl₂ 0,34g, bring to 100 ml with water.

5% Stock C: NaHCO₃ 2,25 g, bring to 100 ml 70% water.

Lysis buffer:

50 mM Tris–HCl, pH 8,0; 10 mM EDTA; 1% (wt/vol) SDS; protease inhibitor mix (1:100 dilution from stock); 1 mM PMSF. Protease inhibitor mix and PMSF should be added immediately before use.

RIPA buffer:

10 mM Tris–HCl, pH 7,5; 140 mM NaCl; 1 mM EDTA; 0,5 mM EGTA; 1% (vol/vol) Triton X-100; 0,1% (wt/vol) SDS; 0,1% (wt/vol) Na-deoxycholate.

RIPA ChIP buffer:

10 mM Tris–HCl, pH 7,5; 140 mM NaCl; 1 mM EDTA; 0,5 mM EGTA, 1% (vol/vol) Triton X-100; 0,1% (wt/vol) SDS; 0,1% (wt/vol) Na-deoxycholate; protease inhibitor mix (1:100 dilution from stock); 1 mM PMSF. Protease inhibitor mix and PMSF should be added immediately before use.

TE buffer:

10 mM Tris–HCl, pH 8,0; 10 mM EDTA.

Elution buffer:

20 mM Tris–HCl, pH 7,5; 5 mM EDTA; 50 mM NaCl.

Complete elution buffer:

20 mM Tris–HCl, pH 7,5; 5 mM EDTA; 50 mM NaCl; 20 mM Na-butyrate; 1% (wt/vol) SDS; 50 µg/mL proteinase K.

Buffer A:

10 mM Hepes pH 8; 10 mM EDTA pH 8; 0,5 mM EGTA pH 8; 0,25% TritonX100; protease inhibitor mix (1:100 dilution from stock); diluted in ddH₂O.

Buffer B:

10 mM Hepes pH8; 200 mM NaCl; 1 mM EDTA; 0,5 mM EGTA; 0,01% TritonX100; protease inhibitor mix (1:100 dilution from stock); diluted in ddH₂O.

7.1.7 Animals

For all animal experiments NOD.Cg-Prkdc^{scid} Il2rg^{tm1Wjl}/SzJ mice (NSG) were used. NSG mice were purchased from JAX (The Jackson Laboratory) and the colony was maintained at the ZEMM institute (in house-bred colony) at the University Würzburg, Germany.

7.1.8 Equipment

Instrument	Distributor
Cell culture microscope EVOS	Life Technologies
Cytospin 4 Zentrifuge	Thermo Scientific
FACS Canto I	BD
Gel Imaging System	Biorad
Confocal microscope	Leica SP5
Light Cycler 480 II	Roche
M220 Focused-ultrasonicator	Covaris
2100 Bioanalyzer	Agilent Technologies

7.1.9 Softwares

Software	Distributor
FACS Diva	BD
FlowJo	Tree Star, Inc.
ImageJ	NIH
Integrative Genomics Viewer	Broad Institute

7.2 Methods

7.2.1 Informed consent and CB collection

Written informed consents for umbilical cord blood collection, storage and donation were obtained from all the parents. The CB units were collected without alteration of safe Caesarean section deliveries. The CB units were always collected *ex utero* after the delivery of the placenta under strict sterile conditions. Blood samples were collected into sterile 250 ml blood collection bags containing 25 ml of anticoagulant (heparin, 30 U/ml) from the performing surgeon. The umbilical cord was clamped at one end, a needle was inserted into the umbilical vein on the unclamped end, and the blood was allowed to flow through the needle into the collection bag.

7.2.2 Criteria for the storage of samples prior to processing

Pre-processing CB storage temperature was maintained between 4°C and room temperature. The samples utilized for this thesis were all transported at room temperature and processed within 24 hours of collection. Time and temperature play an important role in the potential decline of cell viability in cord blood samples.

7.2.3 Isolation of CD34⁺ cells from CB

The mononuclear cell (MNC) fraction was obtained from whole CB using a density gradient method of cell separation. The blood samples were transferred from the sterile collection bags to sterile graduated beakers and diluted 1:4 with Dulbecco's Phosphate buffered salt solution (PBS). Ficoll-Paque PLUS was used for the MNC isolation procedure. 15 ml of Ficoll were transferred into 50 ml centrifuge tubes and 35 ml of diluted blood were then overlaid onto the Ficoll. The 50 ml tubes were centrifugated at 400 g (1350 rpm) for 35 minutes (20°C, acceleration 1, deceleration 0). Centrifugation accelerates the density gradient separation. A different migration through the Ficoll during centrifugation results in the formation of layers of different cell types: the bottom layer contains erythrocytes, whereas the MNCs are at the

interface between the plasma and Ficoll. The MNC layer was collected with a sterile Pasteur pipette and washed twice with ice cold PBS at 400 g (1350 rpm) for 10 minutes (4°C, acceleration 1, deceleration 0). Cell aliquots were taken for viability and enumeration using Trypan blue. Cells were counted with a Neubauer standard haemocytometer. The Trypan blue solution allows discrimination between dead cells (staining blue due to impaired membrane integrity) and viable cells (remaining translucent). CD34⁺ progenitor cells were isolated using the CD34 progenitor cell isolation kit from Miltenyi Biotec. 10⁸ MNCs were incubated with 100 µl FcR blocking reagent together with 100 µl microbeads conjugated to the anti-human CD34 antibody for 30 minutes at 4°C. CD34⁺ progenitor cells were obtained after two cycles of immunomagnetic bead selection according to the manufacturer's instructions. CD34⁺Lin⁻ progenitor cells were isolated using the Diamond CD34 isolation kit from Miltenyi Biotec. Magnetic cell separation was used to separate Lin⁺ from Lin⁻ human mononuclear cells. For this purpose 10⁸ freshly isolated MNCs were first incubated with microbeads conjugated to a cocktail of biotin-conjugated monoclonal anti-human antibodies against CD2, CD3, CD11b, CD14, CD15, CD16, CD19, CD56, CD61, and CD235a. According to the manufacturer, labeled MNCs were passed through a magnetic field with Lin⁺ cells remaining inside the column and with Lin⁻ cells passing through. The flow-through fraction was subsequently incubated with 100 µl microbeads conjugated to the anti-human CD34 antibody for 30 minutes at 4°C. After cell count, CD34⁺Lin⁻ purity was analysed by flow cytometry. The purity of the microbeads selection was ranging from 90% to 98 %.

7.2.4 Culture of CD34⁺ cells

CD34⁺ progenitor cells were cultured using serum-free StemSpan medium supplemented with 1X penicillin and streptomycin, and two different cytokine cocktails (see section 7.1.1). The two cytokine cocktails used were: STF consisting of SCF, TPO, FGF-1 and heparin, and STFIA consisting of SCF, TPO, FGF-1, IGFBP2, Angptl5 and heparin. Cells were cultured in 4-well polystyrene plates for all experiments. Cells were maintained at 37°C in a 20% O₂ and 5% CO₂ humidified atmosphere. Fresh medium was added every two days and cell density was maintained at 2×10⁵ cells/ml. Cell counting was performed by using a hemocytometer and an inverse microscope. At designed culture time points, expanded cells were harvested and used for analysis.

7.2.5 Immunostainings of fresh and cultured CD34⁺ cells

Cover slips with 100.000 fresh or expanded CD34⁺ cells were washed with PBS once. After removal of PBS, cells were permeabilised with 1 ml MSP buffer each well for 30 seconds. Afterwards, cells were fixed with 1 ml Methanol for 3 minutes at -20°C and washed three times with 1 ml PBS + 0,1 % Triton X-100. For blocking unspecific binding, cells were treated with 0,1 % Triton X-100, 5 % goat serum in PBS. Then cells were incubated for 30 minutes with 250 µl of different primary antibodies. Slides were stained with the following primary antibodies: rabbit anti-H3K4me³ (1:200), rabbit anti-H3K27me³ (1:500). After washing three times with 1 ml 0,1 % Triton X-100 in PBS for 5 minutes, 250 µl of secondary antibodies (anti-rabbit Cy3 and Cy5) were used. The cells were incubated for 1 hour in the dark at room temperature. Cells were then washed three times with 0,1 % Triton X-100 in PBS and after that, nuclei were stained with 1 ml DAPI-solution (5 mg/ml DAPI stock solution was diluted 1:500 in PBS with 0,1 % Triton X-100, yielding a DAPI concentration of 10 µg/ml) for 5 minutes. Then cells were washed with PBS and cover slips were put upside down on a drop of Fluorescent Mounting Medium on slides. Fluorescent imaging was done using a SP5 Confocal Microscope.

7.2.6 Inhibitor treatment

For EZH2 inhibitor treatment experiments, CD34⁺ cells expanded under STF conditions were treated with either GSK343 EZH2 inhibitor or GSK126 EZH2 inhibitor at the indicated concentrations. Cells were cultured in 4-well polystyrene plates. Fresh medium was added every second day and cell density was maintained at 2×10^5 cells/ml.

7.2.7 Colony-forming unit (CFU) assays

For analysis of clonogenicity 35-mm Petri dishes containing serum-free MethoCult SF H4236 were used. Cells were seeded on methylcellulose supplemented with the growth factors contained in the Materials section 7.1.1 (three triplicates per condition), and incubated in a humidified atmosphere at 37°C and 5% CO₂ for 14 days. Cell seeding numbers and

supplementation of methylcellulose medium are the following: for experiments of HPSC expansion using cytokine supplementation, 400 expanded cells (day 7) were plated per dish, the cells were expanded in either STFIA or STF conditions; for experiments of HPSC expansion using EZH2 inhibitors, aliquots of 400 expanded cells from each condition were seeded per dish. After 14 days of incubation, the number of granulopoietic colonies (colony-forming unit granulocyte-macrophage or CFU-GM), multilineage colonies (colony-forming unit granulocyte-erythrocyte-macrophage-megakaryocyte or CFU-GEMM) and erythroid colonies (burst forming unit-erythrocyte or BFU-E) were scored using an inverted light microscope. 400 freshly isolated CD34⁺ cells/plate (in triplicates) were cultured for 14 days in methylcellulose for control.

7.2.8 Hematoxylin & Eosin staining

14 days after methylcellulose culture the hematopoietic colonies were washed twice for 5 minutes and resuspended in 200 µl PBS and then cytocentrifuged onto glass slides 4 minutes at 200 g using Cytospin 4. The slides were stained with Hematoxylin & Eosin (HE). For HE staining the glass slides were shortly allowed to dry and, in order to better preserve the hematopoietic precursor cell morphology, the cells were fixed for 5 minutes with ice-cold Methanol. Subsequently, the samples were stained as follows: after an incubation of 5 minutes in H₂O, they were incubated for 5 minutes with Hematoxylin. The slides were washed with tap water (change several times). The slides were incubated for 2 minutes with Eosin, then washed short with demineralized H₂O, incubated first with 70% EtOH for 1 minute and then with 100% EtOH for 7 - 8 minutes. The slides were then directly incubated for 5 minutes with Xylene. Cover slips were put upside down on a drop of Vitroclud and the samples were then dried and photographed with an EVOS microscope.

7.2.9 Flow cytometry membrane staining

For the detection of cellular surface antigens on living cells, fluorochrome conjugated antibodies were used. Approximately 100.000 cells were used and washed once in 1 ml of FACS buffer before staining. The cells were incubated with the antibodies of interest in FACS buffer for 45 minutes at 4°C. The fluorochrome conjugated antibodies used were against CD45, CD34, CD133, CD90, CD38, CD14, CD19, CD8 which were used at a concentration of 2 µl per antibody in 100 µl FACS buffer at 4°C. All the antibodies were conjugated with either PE fluorochrome or FITC fluorochrome. After 2 washing steps with FACS buffer, cells stained with monoclonal antibodies were resuspended in 100 µl FACS buffer and were ready for analysis. For all the washing steps the cells were spun down for 5 minutes at 1350 rpm. Approximately 10.000 events were gated for each sample.

7.2.10 Intranuclear staining

For chromatin flow cytometry analysis, cells were counted and 250.000 cells were used for each staining: cells were washed in 1X PBS, the supernatant was discarded and the pellet was resuspended in 100 µl of 1X PBS. 1 ml of icecold 88% Methanol solution in 1X PBS was added to the FACS tubes, and 100 µl of the cell suspension was added dropwise and slowly into the FACS tubes, while vortexing them. Cells were incubated for 30 minutes at -20°C for fixation and permeabilization. The alcohol was then discarded after a spinning step of 5 min at 1700 rpm, and the cells, after vortexing, were washed twice with FACS buffer for 5 min at 1700 rpm. Primary antibodies in the corresponding dilutions were added into the FACS tubes in a final volume of 100 µl and the samples were incubated for one hour at 4°C in the dark. For the characterization of epigenetic patterns primary antibodies against H3K4me³ (0,5µg/100µl), H3K27me³ (0,5µg/100µl), H3K9me³ (0,5µg/100µl) and H3K79me³ (0,5µg/100µl) were used. Primary antibodies against H3 (0,48µg/100µl) were used as controls. After one hour of incubation with the primary antibodies, 1 ml of FACS buffer was added into the FACS tubes, the cells were spun down for 5 min at 1700 rpm and washed again in 1 ml of FACS buffer. The samples were incubated with the secondary antibody α -rabbit-APC (1:500) in FACS buffer in a final volume of 100 µl for 45 min and kept in the dark. After

washing with FACS buffer, the cells were resuspended in 120 μ l of FACS buffer and measured using BD FACS Canto I flow cytometer.

7.2.11 FACS data analysis

For every FACS analysis 10,000 events were collected in a BD FACSCanto I flow cytometer. The cell populations were identified at first on the basis of the composite pattern of forward scatter (FSC) and side scatter (SSC) and non viable cells were excluded from analysis based on scatter properties. The samples were then observed and analysed for the used fluorochrome. Data were further analysed by FACSDiva software and then by FlowJo FACS data analysis software that applies compensation corrections.

7.2.12 RNA isolation

An RNase-free work environment was used for all molecular methodology. RNA isolation from cell pellets was performed either using peqGOLD RNA Pure or Rneasy Micro kit, both supplied by Qiagen. The Micro kit was applied when the cell numbers were 3×10^5 and below. The kit was used according to the manufacturer's instructions. When the cell numbers were greater than 4×10^5 , cells were washed once in 1X PBS by centrifuging for 5 minutes at 1350 rpm. The cell pellet was resuspended in 500 μ l of RNA peqGOLD, mix by gentle pipetting and then incubated for 5 minutes at RT. 100 μ l of Chloroform (without Isoamil alcohol) was added and mixed by vortexing. Next, samples were incubated for 10 minutes on ice and then were centrifuged for 10 minutes at 4°C 12,000 g. The upper phases were transferred into fresh tubes and equal volumes of isopropanol at RT were added to the aqueous phase and mixed gently by inverting. The samples were incubated for 5 minutes at RT. The nucleic acid was then left to precipitate at 4°C for 15 minutes. Following precipitation, samples were centrifuged for 10 minutes at 4°C at 12,000 g. Following centrifugation, the supernatant was discarded and the pellet was resuspended in 1 ml of 75% icecold Ethanol. Samples were centrifuged for 10 minutes at 4°C at 12,000 g. The supernatant was discarded, and the pellet was again resuspended with 1 ml of icecold 75% Ethanol for a second wash and centrifuged for 10 minutes at 4°C at 12,000 g. Finally, the supernatant was decanted carefully and the pellet was air dried and resuspended in 25 μ l of DEPC-treated water. Samples were incubated

for 30 minutes at 4°C and were subsequently stored at -20°C. To evaluate the purity and the integrity of the mRNA produced, the extracted amounts of RNA were photometrically quantified using an Eppendorf BioPhotometer.

7.2.13 DNase treatment and cDNA synthesis

To remove any contaminating genomic DNA from total RNA, RNA samples were treated with RNase-free recombinant DNase. Between 0,5 and 1,5 µg of RNA was mixed with 1,3 µl of 10X DNase buffer, DEPC treated water was added to a final volume of 12 µl, and 1 µl (2U) of DNase I was added. Samples were incubated for exactly 30 minutes at 37°C. DNase was inactivated by adding 1 µl of 25 mM EDTA and 10 minutes incubation at 65°C. Samples were kept on ice for previous cDNA synthesis or were stored at -20°C. Half of the reaction mix containing 0,5 µg RNA was used for cDNA synthesis.

Purified RNA was reverse transcribed by the M-MLV reverse transcriptase (200 U/µl). 1 µl of oligo dT primers (5' TTT TTT TTT TTT TTT T 3') was added to the DNase treated RNA. DEPC treated water was added to a final volume of 16,5 µl. The oligo dT primers were allowed to anneal to the poly-A RNA at 65°C for 5 min, followed by rapid chill down on ice. Subsequently, RNA was incubated with 1 µl dNTPs (10 mM), 5 µl first-strand buffer, 2 µl of 0,1 M DTT, and 0,6 µl M-MLV reverse transcriptase at 37°C for 1 hour. Samples were incubated at -20°C for at least 20 minutes. The resulting cDNA was then either used directly or stored at -20°C until further application. The purity of the cDNA produced was tested photospectrometrically. The ratio of absorbance values at 260 nm and 280 nm gives an estimate of DNA. An A_{260}/A_{280} ratio of 1,8 - 2,0 was considered as pure cDNA.

7.2.14 Primer design and quantitative realtime PCR

A list of the primers used during the course of this study is elaborated in the section 7.1.3. All primers were self-designed using the following web provided programmes:

NCBI (National Centre for Biotechnology Information): the primers were designed ensuring that the mRNA sequence selected included a segment of two exons (<http://www.ncbi.nlm.nih.gov/nucore>).

Primer 3: the selected mRNA sequence was used for designing primers ranging in length between 100-200 bp (<http://bioinfo.ut.ee/primer3-0.4.0/primer3/>).

USCS in Silico PCR: once primers were designed they were checked for efficiency and selectivity (<http://genome.ucsc.edu/cgi-bin/hgPcr?org=Human>).

Oligo Calc (Oligonucleotide Properties Calculator): the PCR primers were checked for potential hairpin interactions and self complementarity (<http://www.basic.northwestern.edu/biotools/oligocalc.html>).

Real-time PCR allowing detection and quantification of nucleic acid sequences was performed using Sybr-Green Mix in the Corbett RG-3000. For general gene expression analyses, 1 μ l cDNA (~50 ng) was mixed with 10 μ l 2x Sybr-Green Mix, 8,5 μ l water and each 0,25 μ l of 100 pM primers. Sybr-Green Mix was used as a fluorescent DNA binding dye, that binds all double-stranded DNA and detection is monitored by measuring the increase in fluorescence throughout the cycle. All primers used are listed in the section 7.1.3. Analyses were referred to beta-actin and RPL27 by the delta-delta Ct calculation. All reactions were carried out as duplicates with the following PCR program: 95°C for 15 min, 40x (95°C for 10 s, 60°C for 20 s, 72°C for 30 s, 80°C for 20 s), 50°C for 1 min.

7.2.15 Global gene expression analysis (Microarray)

RNA was isolated using RNeasy Mini Kit with DNase I digestion (Qiagen) and subjected to microarray analysis. The RNA quality was analysed using the Agilent RNA 6000 Pico Total RNA Kit with a 2100 Bioanalyzer. Microarray preparation and determination of gene expression levels were performed by Prof. M. Zenke, Qiong Lin and colleagues. Briefly, sample preparation was performed according to the Expression Analysis Technical Manual (Affymetrix). GeneChip One-cycle Target Labeling Kit (Affymetrix) and 1 μ g total RNA were used. Biotin-labeled cRNA was hybridized on Affymetrix Human Gene 1.0 ST Array. Arrays were stained, washed, and scanned according to the manufacturer's protocols. Gene expression levels were determined by RMA algorithm using Affymetrix power tools. Hierarchical clustering was performed using Pearson correlation coefficient and the average linkage method and represented by dendrogram and heatmap. The transcripts having a fold

change >2 were considered as being differentially expressed. Data sets were submitted to Gene Expression Omnibus database (www.ncbi.nlm.nih.gov/geo) under the accession number GSE58461.

7.2.16 Western blot

Protein samples were prepared from $0,5 \times 10^6$ cells which were lysed in 60 μ l protein lysis buffer and sheared by passing through a 21 gauge needle for several times. Samples were heated up to 95°C for 5 min and proteins were separated by SDS-PAGE in 12% SDS gels. Proteins were blotted onto nitrocellulose membranes. Subsequently, after blocking unspecific binding sites in 5% milk in PBS with 0,1% Tween20 at room temperature for 30 min, the membranes were incubated with primary antibodies in 1X PBS containing 1% milk and 0,1% Tween20 at 4°C over night. After three washes secondary HRP-coupled antibodies were incubated for 2 h at RT in 1X PBS 0,1% Tween20, before proteins were detected by ECL addition and chemiluminescence measurement, either by X-ray film or by Biorad Imaging system. Membranes were stripped from antibodies by 30 min incubation with stripping solution at 50°C. Primary antibodies used were anti-H3K4me³, anti-H3K27me³, anti-H3 and anti-EZH2.

7.2.17 Chromatin immunoprecipitation (ChIP) low cell number

ChIP was done with adjustments to the protocol described by Dahl and Collas (Dahl *et al.*, 2009). 2×10^5 cells were crosslinked for 8 min at RT by 1% Formaldehyde in 500 μ l 1X PBS. The Formaldehyde was quenched by adding 1/10 of volume of 2 M freshly prepared Glycine followed by incubation for 5 minutes at RT, and the cells were washed twice in ice cold 1X PBS for 10 minutes at 4°C at 500 rcf. The cell pellet was gently resuspended in 500 μ l of buffer A and mixed well by pipetting followed by incubation on ice for 10 minutes. Nuclei were subsequently collected by centrifuging at 500 rcf for 5 minutes at 4°C. After removing the supernatant, the nuclei were resuspended in 500 μ l of buffer B followed by incubation on ice for 10 minutes. After nuclei isolation the pellets were resuspended in 120 μ l SDS lysis buffer. The chromatin was sheared with a Covaris M220 Focused-ultrasonicator for 15 minutes with 10% duty factor. The DNA fragment size and quantitation was analysed using

the Agilent High Sensitivity DNA kit with a 2100 Bioanalyzer. After sonication, the chromatin was diluted to reduce SDS concentration to 0,1% in a final volume of 1 ml RIPA ChIP buffer. 10% of the chromatin was used as input material and the remaining chromatin was suitable for 8 parallel ChIPs. 2,5 µg of H3K4me³, H3K27me³, H3 or 1 µg of IgG isotype control antibodies were used for 100 µl chromatin. The antibodies were incubated on a rotator for 2 h at 4°C with 10 µl Dynabeads protein A in a final volume of 100 µl RIPA buffer for the antibody-beads complex preparation. 100 µl chromatin was incubated with the antibody-beads complex on a rotator for 2h at 4°C. The DNA recovery and purification from the ChIP material was done by phenol chloroform extraction and ethanol precipitation. The DNA was dissolved in 40 µl TE buffer and used for real time PCR. 2 µl of ChIP-DNA and input DNA were used per PCR reaction together with Absolute SybrGreen Mix and ChIP-specific primers. All reactions were carried out on a Corbett RG-3000 machine as triplicates with the following PCR parameters: 15 min, 95°C 40x (10 s, 95°C; 20 s 60°C, 30 s, 72°C, 20 s, 80°C), 50°C for 1 min. Analyses were referred to non-precipitated input DNA by delta-delta Ct calculation. Values were normalized for H3 ChIP-DNA levels. All primers used were specific for the promoter regions of selected genes.

7.2.18 ChIP primer design and ChIP-seq analyses

A list of the ChIP primers designed according to methylation patterns during the course of this study is elaborated in the section 7.1.3. All primers were self-designed using the following web provided programmes:

Integrative Genomics Viewer (IGV): IGV is a visualization tool for interactive exploration of large genomic datasets, including array-based and next-generation sequence data. IGV was used for selecting the desired sequence with the use of annotated ChIPseq datasets of histone modifications of interest (<http://www.broadinstitute.org/igv/Genomes>).

Human BLAT search: After choosing the right genome, the primers were designed ensuring that the selected sequence was immediately upstream the transcription start site (TSS) or within the first exon. The primers were designed ensuring the presence of CpG islands and of annotated histone modifications of interest (<http://genome.ucsc.edu>).

Primer 3: the selected sequence was used for designing primers ranging in length between 100-200 bp (<http://bioinfo.ut.ee/primer3-0.4.0/primer3/>).

Oligo Calc (Oligonucleotide Properties Calculator): the PCR primers were checked for potential hairpin interactions and self complementarity (<http://www.basic.northwestern.edu/biotools/oligocalc.html>).

DNA from ChIP (10-30 ng) was used for library preparation (Illumina). Adapter ligated and amplified fragments were sequenced on an Illumina HiSeq 2000 sequencing system using 50 bp single end reads. Sequence tags were mapped to the human reference sequence version GRCh37/hg19 using BWA (Li *et al.*, 2010). Reads were filtered for unique mapping and mapping quality. Duplicate reads were removed. Sequence tags from biological replicates were analysed for correlation/reproducibility using ENCODE criteria (Landt *et al.*, 2014). Peaks were called separately in replicate samples, peak areas of replicates were then merged, and sequence tags in merged peak regions were finally correlated between replicates. The distribution of log-transformed ChIP-seq tags in replicates was plotted as a color-coded tag count density map. Tags from replicates were combined and normalized to 10^7 tags per sample. The fraction of reads falling within peak regions (fraction of reads in peaks, FRiP) was used as a measure for global ChIP enrichment. For global similarity analyses, tags were counted into 500 bp genomic bins and unsupervised hierarchical clustering was applied using Ward's minimum variance method. As H3K4me³ and H3K27me³ were expected to cover larger sized regions of the genome, SICER version 1.1 (Zang *et al.*, 2009) was used for peak detection with a fragment size estimate of 150 bp, a window size of 200 bp and a gap size of 400 bp for H3K4me³ and 600 bp for H3K27me³. FDR cut-off for statistical enrichment was set to 1×10^{-2} . Genomic locations of peaks were defined relative to RefSeq transcription start sites (TSSs) and annotated using HOMER (Heinz *et al.*, 2010). Promoters were defined from -1kb to +100bp. Promoters were considered to be bivalent if they had significant enrichment for both H3K4me³ and H3K27me³ within the narrow promoter window. The enrichment of Gene Ontology terms was calculated using DAVID tools (Huang *et al.*, 2009) and sorted by term enrichment p-value. Histograms of tag densities were calculated with position-corrected, normalized tag counts using the ngs.plot software (Shen *et al.*, 2014). We used MeV (Saeed *et al.*, 2003) to generate heatmaps, and area-proportional Venn diagrams were created (VennDiagram package in R, <http://cran.r-project.org/web/packages/VennDiagram>). UCSC browser tracks were created with a resolution of 1 bp window and normalized to 10^7 reads using HOMER. For relating changes of chromatin modifications and mRNA expression data,

approximately 26.000 transcripts with unique genomic representation and processable mRNA expression data read out on the Affymetrix arrays were chosen and respective promoter regions were retrieved using the BiomaRt package (Durinck *et al.*, 2009). Genomic intervals 1.000 bp upstream and 500 bp downstream the transcriptional start sites of those transcripts were defined and sequence tags from normalized ChIP-seq data were counted into the intervals. Log2-fold changes were calculated for ChIP-seq reads and for Affymetrix based expression data. Heatmaps were created using the Multiple Experiment Viewer (MeV, <http://www.tm4.org>). Data sets were submitted to Gene Expression Omnibus database (www.ncbi.nlm.nih.gov/geo) under accession number GSE58461.

7.2.19 NSG Mouse line

NSG (NOD.Cg-Prkdc^{scid} Il2rg^{tm1Wjl}/SzJ) mice were purchased from Jackson Laboratory (Bar Harbor, ME, USA), and have been bred and maintained under defined conditions in ventilated cages with irradiated food and filtered water. NSG mice were bred, housed and handled at the Animal Facility of the ZEMM Institute at the University of Würzburg, according to institutional regulations.

7.2.20 Primary and secondary NSG transplantation

Mice at 8-12 weeks of age were placed into the irradiation box and were irradiated with 2 Gray (Gy) (Faxitron CP-160 X-ray radiation cabinet (160 kV, 6.3 mA, 0.4 Gray/min, filter: 0.5mm Cu)) of whole-body irradiation at the ZEMM institute at the University of Würzburg. Within 8 hours mice were injected *via* tail vein with approximately $0,5 \times 10^5$ freshly isolated CD34⁺ cells or with their expanded progeny together with 2×10^5 freshly isolated NSG splenocytes. For experiments of HSPC expansion using cytokine supplementation, transplantation included two groups of mice injected with 7 days expanded cells using either STF or STFIA. Three to four mice per group were used in each experiment. Groups of four unmanipulated and four irradiated uninjected mice were used as negative controls. For experiments of HSPC expansion using EZH2 inhibitors, transplantation included three groups of mice injected with the progeny of 2×10^5 CD34⁺ cells expanded for 7 days using either STF or STFIA, or with the progeny of 2×10^5 CD34⁺ cells expanded for 7 days with STF cocktail plus either GSK 343 (1

mM) or GSK 126 (1 mM). Three to four mice per group were used in each experiment. Groups of four irradiated uninjected mice were used as negative controls. Eight to ten weeks post-transplantation (short-term engraftment) mice were sacrificed for a first engraftment assay analysis. 16 weeks post-transplantation (long-term engraftment) mice were sacrificed for a second engraftment assay analysis. Peripheral blood (PB), spleen (SP) and bone marrow (BM) were harvested for further analyses and analysed by flow cytometry. Secondary transplantations were carried out at 16 weeks post-primary transplantation. The BM cells of both tibias and femurs of a primary recipient together with 2×10^5 freshly isolated NSG splenocytes were injected into two sub-lethally irradiated secondary recipients.

7.2.21 Organs preparation and analysis of human cell engraftment

The mice were sacrificed by cervical dislocation. Blood samples were collected in 1,5 ml eppendorf tubes containing 500 μ l of 0.5 mM EDTA. 4 drops of blood were collected by heart puncture with a 27G sterile syringe. The samples were then incubated for 30 minutes in the water-bath at 37°C together with 1 ml of 2% Dextran in 1X PBS solution. The supernatants were spun down for 7 minutes at 1350 rpm and the pellets were then washed twice with 1X PBS. Spleens were scraped off and successively flushed through a 70 μ m cell strainer in MACS buffer. The pellets were washed twice with 1X PBS for 5 minutes at 1350 rpm. The BM cells of both tibias and femurs of a recipient were collected flushing the bones with MACS buffer. The BM cells were then flushed through a 70 μ m cell strainer and the pellets were washed twice with 1X PBS. PB, SP and BM cells were then resuspended in red blood cell (RBC) lysis solution (Gey's solution) and were incubated for 5 minutes on ice. The white blood cells were centrifuged in FCS for 7 minutes at 1350 rpm. After 2 washing steps with FACS buffer, cells were ready for staining with the antibodies of interest. For all the washing steps the cells were spun down for 5 minutes at 1350 rpm. Peripheral blood, spleen and bone marrow of the recipients were collected 4, 8 and 16 weeks post-transplantation and cells were analysed *via* FACS analysis for human chimerism using antibodies against human CD45 surface marker. The multilineage differentiation capacity of transplanted cells was analysed by staining the spleen and BM of the recipient animals for different FITC- or PE-labelled Lin markers and matching isotype antibodies (CD19, CD14, CD3, CD45). At least

10.000 events were acquired per probe and successful engraftment of human transplanted CD34⁺ cells was set to higher values than 0,1% of human CD45 cells in mouse PB.

7.2.22 Statistical analysis

All results are indicated with standard error of the average of independent experiments (number indicated per figure). To estimate the probability of difference, analyses were done by two-tailed Students t-test. Probability value of $p < 0,05$ denoted statistical significance.

8 BIBLIOGRAPHY

- Abraham, B. J., K. Cui, Q. Tang and K. Zhao (2013). "Dynamic regulation of epigenomic landscapes during hematopoiesis." *BMC Genomics* 14: 193.
- Adams, G. B. and D. T. Scadden (2006). "The hematopoietic stem cell in its place." *Nat Immunol* 7(4): 333-337.
- Adli, M., J. Zhu and B. E. Bernstein (2010). "Genome-wide chromatin maps derived from limited numbers of hematopoietic progenitors." *Nat Methods* 7(8): 615-618.
- Alakel, N., D. Jing, K. Muller, M. Bornhauser, G. Ehninger and R. Ordemann (2009). "Direct contact with mesenchymal stromal cells affects migratory behavior and gene expression profile of CD133+ hematopoietic stem cells during ex vivo expansion." *Exp Hematol* 37(4): 504-513.
- Allison, R. D., A. Katsounas, D. E. Koziol, D. E. Kleiner, H. J. Alter, R. A. Lempicki, B. Wood, J. Yang, B. Fullmer, K. J. Cortez, M. A. Polis and S. Kottlil (2009). "Association of interleukin-15-induced peripheral immune activation with hepatic stellate cell activation in persons coinfecting with hepatitis C virus and HIV." *J Infect Dis* 200(4): 619-623.
- Aloia, L., B. Di Stefano and L. Di Croce (2013). "Polycomb complexes in stem cells and embryonic development." *Development* 140(12): 2525-2534.
- Antonchuk, J., G. Sauvageau and R. K. Humphries (2002). "HOXB4-induced expansion of adult hematopoietic stem cells ex vivo." *Cell* 109(1): 39-45.
- Arai, F., A. Hirao and T. Suda (2005). "Regulation of hematopoietic stem cells by the niche." *Trends Cardiovasc Med* 15(2): 75-79.
- Arai, F. and T. Suda (2007). "Maintenance of quiescent hematopoietic stem cells in the osteoblastic niche." *Ann N Y Acad Sci* 1106: 41-53.
- Araki, H., N. Mahmud, M. Milhem, R. Nunez, M. Xu, C. A. Beam and R. Hoffman (2006). "Expansion of human umbilical cord blood SCID-repopulating cells using chromatin-modifying agents." *Exp Hematol* 34(2): 140-149.
- Araki, H., K. Yoshinaga, P. Boccuni, Y. Zhao, R. Hoffman and N. Mahmud (2007). "Chromatin-modifying agents permit human hematopoietic stem cells to undergo multiple cell divisions while retaining their repopulating potential." *Blood* 109(8): 3570-3578.
- Aslam, M. I., S. Hettmer, J. Abraham, D. Latocha, A. Soundararajan, E. T. Huang, M. W. Goros, J. E. Michalek, S. Wang, A. Mansoor, B. J. Druker, A. J. Wagers, J. W. Tyner and C. Keller (2013). "Dynamic and nuclear expression of PDGFRalpha and IGF-1R in alveolar Rhabdomyosarcoma." *Mol Cancer Res* 11(11): 1303-1313.
- Aziz, Z., S. Sana, S. Saeed and M. Akram (2003). "Institution based tumor registry from Punjab: five year data based analysis." *J Pak Med Assoc* 53(8): 350-353.
- Azuara, V., P. Perry, S. Sauer, M. Spivakov, H. F. Jorgensen, R. M. John, M. Gouti, M. Casanova, G. Warnes, M. Merkenschlager and A. G. Fisher (2006). "Chromatin signatures of pluripotent cell lines." *Nat Cell Biol* 8(5): 532-538.

- Bahceci, E., E. J. Read, S. Leitman, R. Childs, C. Dunbar, N. S. Young and A. J. Barrett (2000). "CD34+ cell dose predicts relapse and survival after T-cell-depleted HLA-identical haematopoietic stem cell transplantation (HSCT) for haematological malignancies." *Br J Haematol* 108(2): 408-414.
- Ballen, K. K., E. Gluckman and H. E. Broxmeyer (2013). "Umbilical cord blood transplantation: the first 25 years and beyond." *Blood* 122(4): 491-498.
- Barker, J. N., D. J. Weisdorf, T. E. DeFor, B. R. Blazar, P. B. McGlave, J. S. Miller, C. M. Verfaillie and J. E. Wagner (2005). "Transplantation of 2 partially HLA-matched umbilical cord blood units to enhance engraftment in adults with hematologic malignancy." *Blood* 105(3): 1343-1347.
- Barker, J. N., D. J. Weisdorf, T. E. DeFor, B. R. Blazar, J. S. Miller and J. E. Wagner (2003). "Rapid and complete donor chimerism in adult recipients of unrelated donor umbilical cord blood transplantation after reduced-intensity conditioning." *Blood* 102(5): 1915-1919.
- Bartling, B., A. Koch, A. Simm, R. Scheubel, R. E. Silber and A. N. Santos (2010). "Insulin-like growth factor binding proteins-2 and -4 enhance the migration of human CD34+/CD133+ hematopoietic stem and progenitor cells." *Int J Mol Med* 25(1): 89-96.
- Benedikt, A., S. Baltruschat, B. Scholz, A. Bursen, T. N. Arrey, B. Meyer, L. Varagnolo, A. M. Muller, M. Karas, T. Dingermann and R. Marschalek (2011). "The leukemogenic AF4-MLL fusion protein causes P-TEFb kinase activation and altered epigenetic signatures." *Leukemia* 25(1): 135-144.
- Benjamini, Y., Hochberg, Y. (1995). "Controlling the False Discovery Rate - a Practical and Powerful Approach to Multiple Testing." *Journal of the Royal Statistical Society Series B-Methodological* 57: 289-300.
- Bensinger, W., J. Singer, F. Appelbaum, K. Lilleby, K. Longin, S. Rowley, E. Clarke, R. Clift, J. Hansen, T. Shields and *et al.* (1993). "Autologous transplantation with peripheral blood mononuclear cells collected after administration of recombinant granulocyte stimulating factor." *Blood* 81(11): 3158-3163.
- Bernstein, B. E., T. S. Mikkelsen, X. Xie, M. Kamal, D. J. Huebert, J. Cuff, B. Fry, A. Meissner, M. Wernig, K. Plath, R. Jaenisch, A. Wagschal, R. Feil, S. L. Schreiber and E. S. Lander (2006). "A bivalent chromatin structure marks key developmental genes in embryonic stem cells." *Cell* 125(2): 315-326.
- Bhatia, M. (2001). "AC133 expression in human stem cells." *Leukemia* 15(11): 1685-1688.
- Bhatia, M., J. C. Wang, U. Kapp, D. Bonnet and J. E. Dick (1997). "Purification of primitive human hematopoietic cells capable of repopulating immune-deficient mice." *Proc Natl Acad Sci U S A* 94(10): 5320-5325.
- Bilodeau, S., M. H. Kagey, G. M. Frampton, P. B. Rahl and R. A. Young (2009). "SetDB1 contributes to repression of genes encoding developmental regulators and maintenance of ES cell state." *Genes Dev* 23(21): 2484-2489.
- Blank, U., B. Ehrnstrom, N. Heinz, E. Nilsson, A. Brun, C. Baum, B. Schiedlmeier and S. Karlsson (2012). "Angptl4 maintains in vivo repopulation capacity of CD34+ human cord blood cells." *Eur J Haematol* 89(3): 198-205.
- Boitano, A. E., J. Wang, R. Romeo, L. C. Bouchez, A. E. Parker, S. E. Sutton, J. R. Walker, C. A. Flaveny, G. H. Perdew, M. S. Denison, P. G. Schultz and M. P. Cooke (2010). "Aryl hydrocarbon receptor antagonists promote the expansion of human hematopoietic stem cells." *Science* 329(5997): 1345-1348.
- Bonifer, C., M. Hoogenkamp, H. Krysinska and H. Tagoh (2008). "How transcription factors program chromatin--lessons from studies of the regulation of myeloid-specific genes." *Semin Immunol* 20(4): 257-263.
- Bracken, A. P., D. Pasini, M. Capra, E. Prosperini, E. Colli and K. Helin (2003). "EZH2 is downstream of the pRB-E2F pathway, essential for proliferation and amplified in cancer." *EMBO J* 22(20): 5323-5335.
- Bracken, A. P., D. Pasini, M. Capra, E. Prosperini, E. Colli and K. Helin (2003). "EZH2 is downstream of the pRB-E2F pathway, essential for proliferation and amplified in cancer." *EMBO J* 22(20): 5323-5335.

- Bradley, M. B. and M. S. Cairo (2005). "Cord blood immunology and stem cell transplantation." *Hum Immunol* 66(5): 431-446.
- Brinkman, A. B., H. Gu, S. J. Bartels, Y. Zhang, F. Matarese, F. Simmer, H. Marks, C. Bock, A. Gnirke, A. Meissner and H. G. Stunnenberg (2012). "Sequential ChIP-bisulfite sequencing enables direct genome-scale investigation of chromatin and DNA methylation cross-talk." *Genome Res* 22(6): 1128-1138.
- Broske, A. M., L. Vockentanz, S. Kharazi, M. R. Huska, E. Mancini, M. Scheller, C. Kuhl, A. Enns, M. Prinz, R. Jaenisch, C. Nerlov, A. Leutz, M. A. Andrade-Navarro, S. E. Jacobsen and F. Rosenbauer (2009). "DNA methylation protects hematopoietic stem cell multipotency from myeloerythroid restriction." *Nat Genet* 41(11): 1207-1215.
- Brownlee, J. M., B. Heinz, J. Bates and G. R. Moran (2010). "Product analysis and inhibition studies of a causative Asn to Ser variant of 4-hydroxyphenylpyruvate dioxygenase suggest a simple route to the treatment of Hawkinsinuria." *Biochemistry* 49(33): 7218-7226.
- Broxmeyer, H. E., M. R. Lee, G. Hangoc, S. Cooper, N. Prasain, Y. J. Kim, C. Mallett, Z. Ye, S. Witting, K. Cornetta, L. Cheng and M. C. Yoder (2011). "Hematopoietic stem/progenitor cells, generation of induced pluripotent stem cells, and isolation of endothelial progenitors from 21- to 23.5-year cryopreserved cord blood." *Blood* 117(18): 4773-4777.
- Butler, J. S. and S. Y. Dent (2013). "The role of chromatin modifiers in normal and malignant hematopoiesis." *Blood* 121(16): 3076-3084.
- Cancer Genome Atlas Research, N. (2013). "Genomic and epigenomic landscapes of adult de novo acute myeloid leukemia." *N Engl J Med* 368(22): 2059-2074.
- Cao, R., L. Wang, H. Wang, L. Xia, H. Erdjument-Bromage, P. Tempst, R. S. Jones and Y. Zhang (2002). "Role of histone H3 lysine 27 methylation in Polycomb-group silencing." *Science* 298(5595): 1039-1043.
- Cao, R., L. Wang, H. Wang, L. Xia, H. Erdjument-Bromage, P. Tempst, R. S. Jones and Y. Zhang (2002). "Role of histone H3 lysine 27 methylation in Polycomb-group silencing." *Science* 298(5595): 1039-1043.
- Carlesso, N. and A. A. Cardoso (2010). "Stem cell regulatory niches and their role in normal and malignant hematopoiesis." *Curr Opin Hematol* 17(4): 281-286.
- Catlin, S. N., L. Busque, R. E. Gale, P. Guttery and J. L. Abkowitz (2011). "The replication rate of human hematopoietic stem cells in vivo." *Blood* 117(17): 4460-4466.
- Chamberlain, S. J., D. Yee and T. Magnuson (2008). "Polycomb repressive complex 2 is dispensable for maintenance of embryonic stem cell pluripotency." *Stem Cells* 26(6): 1496-1505.
- Chang, C. J. and M. C. Hung (2012). "The role of EZH2 in tumour progression." *Br J Cancer* 106(2): 243-247.
- Chao, N. J., S. G. Emerson and K. I. Weinberg (2004). "Stem cell transplantation (cord blood transplants)." *Hematology Am Soc Hematol Educ Program*: 354-371.
- Chase, A. and N. C. Cross (2011). "Aberrations of EZH2 in cancer." *Clin Cancer Res* 17(9): 2613-2618.
- Chen, T. and S. Y. Dent (2014). "Chromatin modifiers and remodellers: regulators of cellular differentiation." *Nat Rev Genet* 15(2): 93-106.
- Chen, Y. H., M. C. Hung and L. Y. Li (2012). "EZH2: a pivotal regulator in controlling cell differentiation." *Am J Transl Res* 4(4): 364-375.
- Chou, S., P. Chu, W. Hwang and H. Lodish (2010). "Expansion of human cord blood hematopoietic stem cells for transplantation." *Cell Stem Cell* 7(4): 427-428.
- Chung, Y. S., H. J. Kim, T. M. Kim, S. H. Hong, K. R. Kwon, S. An, J. H. Park, S. Lee and I. H. Oh (2009). "Undifferentiated hematopoietic cells are characterized by a genome-wide undermethylation dip around the transcription start site and a hierarchical epigenetic plasticity." *Blood* 114(24): 4968-4978.

- Civin, C. I., L. C. Strauss, C. Brovall, M. J. Fackler, J. F. Schwartz and J. H. Shaper (1984). "Antigenic analysis of hematopoiesis. III. A hematopoietic progenitor cell surface antigen defined by a monoclonal antibody raised against KG-1a cells." *J Immunol* 133(1): 157-165.
- Creyghton, M. P., A. W. Cheng, G. G. Welstead, T. Kooistra, B. W. Carey, E. J. Steine, J. Hanna, M. A. Lodato, G. M. Frampton, P. A. Sharp, L. A. Boyer, R. A. Young and R. Jaenisch (2010). "Histone H3K27ac separates active from poised enhancers and predicts developmental state." *Proc Natl Acad Sci U S A* 107(50): 21931-21936.
- Cui, K., C. Zang, T. Y. Roh, D. E. Schones, R. W. Childs, W. Peng and K. Zhao (2009). "Chromatin signatures in multipotent human hematopoietic stem cells indicate the fate of bivalent genes during differentiation." *Cell Stem Cell* 4(1): 80-93.
- Da, H. X., Z. Q. Huang and Z. Y. Li (2009). "Electrically controlled optical Tamm states in magnetophotonic crystal based on nematic liquid crystals." *Opt Lett* 34(11): 1693-1695.
- Da, H. X., Z. Q. Huang and Z. Y. Li (2009). "Voltage-controlled Kerr effect in magnetophotonic crystal." *Opt Lett* 34(3): 356-358.
- Dahl, J. A. and P. Collas (2009). "MicroChIP: chromatin immunoprecipitation for small cell numbers." *Methods Mol Biol* 567: 59-74.
- Dahlberg, A., C. Delaney and I. D. Bernstein (2011). "Ex vivo expansion of human hematopoietic stem and progenitor cells." *Blood* 117(23): 6083-6090.
- De Gobbi, M., D. Garrick, M. Lynch, D. Vernimmen, J. R. Hughes, N. Goardon, S. Luc, K. M. Lower, J. A. Sloane-Stanley, C. Pina, S. Soneji, R. Renella, T. Enver, S. Taylor, S. E. Jacobsen, P. Vyas, R. J. Gibbons and D. R. Higgs (2011). "Generation of bivalent chromatin domains during cell fate decisions." *Epigenetics Chromatin* 4(1): 9.
- de Lima, M., J. McMannis, A. Gee, K. Komanduri, D. Couriel, B. S. Andersson, C. Hosing, I. Khouri, R. Jones, R. Champlin, S. Karandish, T. Sadeghi, T. Peled, F. Grynszpan, Y. Daniely, A. Nagler and E. J. Shpall (2008). "Transplantation of ex vivo expanded cord blood cells using the copper chelator tetraethylenepentamine: a phase I/II clinical trial." *Bone Marrow Transplant* 41(9): 771-778.
- Delaney, C., S. Heimfeld, C. Brashem-Stein, H. Voorhies, R. L. Manger and I. D. Bernstein (2010). "Notch-mediated expansion of human cord blood progenitor cells capable of rapid myeloid reconstitution." *Nat Med* 16(2): 232-236.
- Delaney, C., M. Z. Ratajczak and M. J. Laughlin (2010). "Strategies to enhance umbilical cord blood stem cell engraftment in adult patients." *Expert Rev Hematol* 3(3): 273-283.
- Devine, S. M., H. M. Lazarus and S. G. Emerson (2003). "Clinical application of hematopoietic progenitor cell expansion: current status and future prospects." *Bone Marrow Transplant* 31(4): 241-252.
- Diaz, E., C. A. Machutta, S. Chen, Y. Jiang, C. Nixon, G. Hofmann, D. Key, S. Sweitzer, M. Patel, Z. Wu, C. L. Creasy, R. G. Kruger, L. LaFrance, S. K. Verma, M. B. Pappalardi, B. Le, G. S. Van Aller, M. T. McCabe, P. J. Tummino, A. J. Pope, S. H. Thrall, B. Schwartz and M. Brandt (2012). "Development and validation of reagents and assays for EZH2 peptide and nucleosome high-throughput screens." *J Biomol Screen* 17(10): 1279-1292.
- Doulatov, S., F. Notta, E. Laurenti and J. E. Dick (2012). "Hematopoiesis: a human perspective." *Cell Stem Cell* 10(2): 120-136.
- Drake, A. C., M. Khoury, I. Leskov, B. P. Iliopoulou, M. Fragoso, H. Lodish and J. Chen (2011). "Human CD34+ CD133+ hematopoietic stem cells cultured with growth factors including Angptl5 efficiently engraft adult NOD-SCID Il2rgamma-/- (NSG) mice." *PLoS One* 6(4): e18382.
- Dupont, C., D. R. Armant and C. A. Brenner (2009). "Epigenetics: definition, mechanisms and clinical perspective." *Semin Reprod Med* 27(5): 351-357.
- Durinck, S., P. T. Spellman, E. Birney and W. Huber (2009). "Mapping identifiers for the integration of genomic datasets with the R/Bioconductor package biomaRt." *Nat Protoc* 4(8): 1184-1191.

- Egger, G., G. Liang, A. Aparicio and P. A. Jones (2004). "Epigenetics in human disease and prospects for epigenetic therapy." *Nature* 429(6990): 457-463.
- Ehninger, A. and A. Trumpp (2011). "The bone marrow stem cell niche grows up: mesenchymal stem cells and macrophages move in." *J Exp Med* 208(3): 421-428.
- Ernst, J., P. Kheradpour, T. S. Mikkelsen, N. Shores, L. D. Ward, C. B. Epstein, X. Zhang, L. Wang, R. Issner, M. Coyne, M. Ku, T. Durham, M. Kellis and B. E. Bernstein (2011). "Mapping and analysis of chromatin state dynamics in nine human cell types." *Nature* 473(7345): 43-49.
- Factor, D. C., O. Corradin, G. E. Zentner, A. Saiakhova, L. Song, J. G. Chenoweth, R. D. McKay, G. E. Crawford, P. C. Scacheri and P. J. Tesar (2014). "Epigenomic comparison reveals activation of "seed" enhancers during transition from naive to primed pluripotency." *Cell Stem Cell* 14(6): 854-863.
- Fernandez-Sanchez, V., R. Pelayo, P. Flores-Guzman, E. Flores-Figueroa, J. Villanueva-Toledo, E. Garrido, E. Ruiz-Sanchez, E. Alvarez-Sanchez and H. Mayani (2011). "In vitro effects of stromal cells expressing different levels of Jagged-1 and Delta-1 on the growth of primitive and intermediate CD34(+) cell subsets from human cord blood." *Blood Cells Mol Dis* 47(4): 205-213.
- Ferreira, M. S., W. Jahnen-Dechent, N. Labude, M. Bovi, T. Hieronymus, M. Zenke, R. K. Schneider and S. Neuss (2012). "Cord blood-hematopoietic stem cell expansion in 3D fibrin scaffolds with stromal support." *Biomaterials* 33(29): 6987-6997.
- Flores-Guzman, P., V. Fernandez-Sanchez and H. Mayani (2013). "Concise review: ex vivo expansion of cord blood-derived hematopoietic stem and progenitor cells: basic principles, experimental approaches, and impact in regenerative medicine." *Stem Cells Transl Med* 2(11): 830-838.
- Fuhrmann, D. R., M. I. Krzywinski, R. Chiu, P. Saeeedi, J. E. Schein, I. E. Bosdet, A. Chinwalla, L. W. Hillier, R. H. Waterston, J. D. McPherson, S. J. Jones and M. A. Marra (2003). "Software for automated analysis of DNA fingerprinting gels." *Genome Res* 13(5): 940-953.
- Gammaitoni, L., K. C. Weisel, M. Gunetti, K. D. Wu, S. Bruno, S. Pinelli, A. Bonati, M. Aglietta, M. A. Moore and W. Piacibello (2004). "Elevated telomerase activity and minimal telomere loss in cord blood long-term cultures with extensive stem cell replication." *Blood* 103(12): 4440-4448.
- Garcia-Pineros, A. J., A. Hildesheim, L. Dodd, T. J. Kemp, J. Yang, B. Fullmer, C. Harro, D. R. Lowy, R. A. Lempicki and L. A. Pinto (2009). "Gene expression patterns induced by HPV-16 L1 virus-like particles in leukocytes from vaccine recipients." *J Immunol* 182(3): 1706-1729.
- Garderet, L., N. Dulphy, C. Douay, N. Chalumeau, V. Schaeffer, M. T. Zilber, A. Lim, J. Even, N. Mooney, C. Gelin, E. Gluckman, D. Charron and A. Toubert (1998). "The umbilical cord blood alphabeta T-cell repertoire: characteristics of a polyclonal and naive but completely formed repertoire." *Blood* 91(1): 340-346.
- Gibson, J. D., C. M. Jakuba, N. Boucher, K. A. Holbrook, M. G. Carter and C. E. Nelson (2009). "Single-cell transcript analysis of human embryonic stem cells." *Integr Biol (Camb)* 1(8-9): 540-551.
- Giebel, B., D. Corbeil, J. Beckmann, J. Hohn, D. Freund, K. Giesen, J. Fischer, G. Kogler and P. Wernet (2004). "Segregation of lipid raft markers including CD133 in polarized human hematopoietic stem and progenitor cells." *Blood* 104(8): 2332-2338.
- Glimm, H., W. Eisterer, K. Lee, J. Cashman, T. L. Holyoake, F. Nicolini, L. D. Shultz, C. von Kalle and C. J. Eaves (2001). "Previously undetected human hematopoietic cell populations with short-term repopulating activity selectively engraft NOD/SCID-beta2 microglobulin-null mice." *J Clin Invest* 107(2): 199-206.
- Gluckman, E., H. A. Broxmeyer, A. D. Auerbach, H. S. Friedman, G. W. Douglas, A. Devergie, H. Esperou, D. Thierry, G. Socie, P. Lehn and *et al.* (1989). "Hematopoietic reconstitution in a patient with Fanconi's anemia by means of umbilical-cord blood from an HLA-identical sibling." *N Engl J Med* 321(17): 1174-1178.
- Gluckman, E., V. Rocha, W. Arcese, G. Michel, G. Sanz, K. W. Chan, T. A. Takahashi, J. Ortega, A. Filipovich, F. Locatelli, S. Asano, F. Fagioli, M. Vowels, A. Sirvent, J. P. Laporte, K. Tiedemann, S. Amadori, M. Abecassis, P. Bordigoni, B. Diez, P. J. Shaw, A. Vora, M. Caniglia, F. Garnier, I. Ionescu, J. Garcia, G. Koegler, P. Rebull,

- S. Chevret and G. Eurocord (2004). "Factors associated with outcomes of unrelated cord blood transplant: guidelines for donor choice." *Exp Hematol* 32(4): 397-407.
- Gluckman, E., A. Ruggeri, F. Volt, R. Cunha, K. Boudjedir and V. Rocha (2011). "Milestones in umbilical cord blood transplantation." *Br J Haematol* 154(4): 441-447.
- Godfrey, W. R., D. J. Spoden, Y. G. Ge, S. R. Baker, B. Liu, B. L. Levine, C. H. June, B. R. Blazar and S. B. Porter (2005). "Cord blood CD4(+)CD25(+)-derived T regulatory cell lines express FoxP3 protein and manifest potent suppressor function." *Blood* 105(2): 750-758.
- Goessling, W., T. E. North, S. Loewer, A. M. Lord, S. Lee, C. L. Stoick-Cooper, G. Weidinger, M. Puder, G. Q. Daley, R. T. Moon and L. I. Zon (2009). "Genetic interaction of PGE2 and Wnt signaling regulates developmental specification of stem cells and regeneration." *Cell* 136(6): 1136-1147.
- Gratwohl, A., H. Baldomero, M. Aljurf, M. C. Pasquini, L. F. Bouzas, A. Yoshimi, J. Szer, J. Lipton, A. Schwendener, M. Gratwohl, K. Frauendorfer, D. Niederwieser, M. Horowitz, Y. Kodera, B. Worldwide Network of and T. Marrow (2010). "Hematopoietic stem cell transplantation: a global perspective." *JAMA* 303(16): 1617-1624.
- Gurdon, J. B., T. R. Elsdale and M. Fischberg (1958). "Sexually mature individuals of *Xenopus laevis* from the transplantation of single somatic nuclei." *Nature* 182(4627): 64-65.
- Haddad, R., F. Pflumio, I. Vigon, G. Visentin, C. Auvray, S. Fichelson and S. Amsellem (2008). "The HOXB4 homeoprotein differentially promotes ex vivo expansion of early human lymphoid progenitors." *Stem Cells* 26(2): 312-322.
- Hato, T., M. Tabata and Y. Oike (2008). "The role of angiopoietin-like proteins in angiogenesis and metabolism." *Trends Cardiovasc Med* 18(1): 6-14.
- Hatzimichael, E. and M. Tuthill (2010). "Hematopoietic stem cell transplantation." *Stem Cells Cloning* 3: 105-117.
- Hawkins, R. D., G. C. Hon, L. K. Lee, Q. Ngo, R. Lister, M. Pelizzola, L. E. Edsall, S. Kuan, Y. Luu, S. Klugman, J. Antosiewicz-Bourget, Z. Ye, C. Espinoza, S. Agarwahl, L. Shen, V. Ruotti, W. Wang, R. Stewart, J. A. Thomson, J. R. Ecker and B. Ren (2010). "Distinct epigenomic landscapes of pluripotent and lineage-committed human cells." *Cell Stem Cell* 6(5): 479-491.
- Heining, C., A. Spyridonidis, E. Bernhardt, J. Schulte-Monting, D. Behringer, C. Grulich, A. Jakob, H. Bertz and J. Finke (2007). "Lymphocyte reconstitution following allogeneic hematopoietic stem cell transplantation: a retrospective study including 148 patients." *Bone Marrow Transplant* 39(10): 613-622.
- Heintzman, N. D., G. C. Hon, R. D. Hawkins, P. Kheradpour, A. Stark, L. F. Harp, Z. Ye, L. K. Lee, R. K. Stuart, C. W. Ching, K. A. Ching, J. E. Antosiewicz-Bourget, H. Liu, X. Zhang, R. D. Green, V. V. Lobanenko, R. Stewart, J. A. Thomson, G. E. Crawford, M. Kellis and B. Ren (2009). "Histone modifications at human enhancers reflect global cell-type-specific gene expression." *Nature* 459(7243): 108-112.
- Heintzman, N. D., R. K. Stuart, G. Hon, Y. Fu, C. W. Ching, R. D. Hawkins, L. O. Barrera, S. Van Calcar, C. Qu, K. A. Ching, W. Wang, Z. Weng, R. D. Green, G. E. Crawford and B. Ren (2007). "Distinct and predictive chromatin signatures of transcriptional promoters and enhancers in the human genome." *Nat Genet* 39(3): 311-318.
- Heinz, S., C. Benner, N. Spann, E. Bertolino, Y. C. Lin, P. Laslo, J. X. Cheng, C. Murre, H. Singh and C. K. Glass (2010). "Simple combinations of lineage-determining transcription factors prime cis-regulatory elements required for macrophage and B cell identities." *Mol Cell* 38(4): 576-589.
- Helin, K. and D. Dhanak (2013). "Chromatin proteins and modifications as drug targets." *Nature* 502(7472): 480-488.
- Herrera-Merchan, A., L. Arranz, J. M. Ligos, A. de Molina, O. Dominguez and S. Gonzalez (2012). "Ectopic expression of the histone methyltransferase Ezh2 in haematopoietic stem cells causes myeloproliferative disease." *Nat Commun* 3: 623.

- Hosogane, M., R. Funayama, Y. Nishida, T. Nagashima and K. Nakayama (2013). "Ras-induced changes in H3K27me3 occur after those in transcriptional activity." *PLoS Genet* 9(8): e1003698.
- Huang da, W., B. T. Sherman and R. A. Lempicki (2009). "Systematic and integrative analysis of large gene lists using DAVID bioinformatics resources." *Nat Protoc* 4(1): 44-57.
- Huang da, W., B. T. Sherman and R. A. Lempicki (2009). "Bioinformatics enrichment tools: paths toward the comprehensive functional analysis of large gene lists." *Nucleic Acids Res* 37(1): 1-13.
- Huang, H. T., K. L. Kathrein, A. Barton, Z. Gitlin, Y. H. Huang, T. P. Ward, O. Hofmann, A. Dibiase, A. Song, S. Tyekucheva, W. Hide, Y. Zhou and L. I. Zon (2013). "A network of epigenetic regulators guides developmental haematopoiesis in vivo." *Nat Cell Biol* 15(12): 1516-1525.
- Ishii, M., Y. Matsuoka, Y. Sasaki, R. Nakatsuka, M. Takahashi, T. Nakamoto, K. Yasuda, K. Matsui, H. Asano, Y. Uemura, T. Tsuji, S. Fukuhara and Y. Sonoda (2011). "Development of a high-resolution purification method for precise functional characterization of primitive human cord blood-derived CD34-negative SCID-repopulating cells." *Exp Hematol* 39(2): 203-213 e201.
- Ivanova, N. B., J. T. Dimos, C. Schaniel, J. A. Hackney, K. A. Moore and I. R. Lemischka (2002). "A stem cell molecular signature." *Science* 298(5593): 601-604.
- Iwama, A., H. Oguro, M. Negishi, Y. Kato, Y. Morita, H. Tsukui, H. Ema, T. Kamijo, Y. Katoh-Fukui, H. Koseki, M. van Lohuizen and H. Nakauchi (2004). "Enhanced self-renewal of hematopoietic stem cells mediated by the polycomb gene product Bmi-1." *Immunity* 21(6): 843-851.
- Jenq, R. R. and M. R. van den Brink (2010). "Allogeneic haematopoietic stem cell transplantation: individualized stem cell and immune therapy of cancer." *Nat Rev Cancer* 10(3): 213-221.
- Jenuwein, T. and C. D. Allis (2001). "Translating the histone code." *Science* 293(5532): 1074-1080.
- Jones, P. A. (2014). "At the tipping point for epigenetic therapies in cancer." *J Clin Invest* 124(1): 14-16.
- Jorgensen, H. F., S. Giadrossi, M. Casanova, M. Endoh, H. Koseki, N. Brockdorff and A. G. Fisher (2006). "Stem cells primed for action: polycomb repressive complexes restrain the expression of lineage-specific regulators in embryonic stem cells." *Cell Cycle* 5(13): 1411-1414.
- Kamani, N., S. Spellman, C. K. Hurley, J. N. Barker, F. O. Smith, M. Oudshoorn, R. Bray, A. Smith, T. M. Williams, B. Logan, M. Eapen, C. Anasetti, M. Setterholm, D. L. Confer and P. National Marrow Donor (2008). "State of the art review: HLA matching and outcome of unrelated donor umbilical cord blood transplants." *Biol Blood Marrow Transplant* 14(1): 1-6.
- Kamminga, L. M., L. V. Bystrykh, A. de Boer, S. Houwer, J. Douma, E. Weersing, B. Dontje and G. de Haan (2006). "The Polycomb group gene Ezh2 prevents hematopoietic stem cell exhaustion." *Blood* 107(5): 2170-2179.
- Kelly, S. S., C. B. Sola, M. de Lima and E. Shpall (2009). "Ex vivo expansion of cord blood." *Bone Marrow Transplant* 44(10): 673-681.
- Khoury, M., A. Drake, Q. Chen, D. Dong, I. Leskov, M. F. Fragoso, Y. Li, B. P. Iliopoulou, W. Hwang, H. F. Lodish and J. Chen (2011). "Mesenchymal stem cells secreting angiopoietin-like-5 support efficient expansion of human hematopoietic stem cells without compromising their repopulating potential." *Stem Cells Dev* 20(8): 1371-1381.
- Klipper-Aurbach, Y., M. Wasserman, N. Braunspeigel-Weintrob, D. Borstein, S. Peleg, S. Assa, M. Karp, Y. Benjamini, Y. Hochberg and Z. Laron (1995). "Mathematical formulae for the prediction of the residual beta cell function during the first two years of disease in children and adolescents with insulin-dependent diabetes mellitus." *Med Hypotheses* 45(5): 486-490.
- Knutson, S. K., N. M. Warholic, T. J. Wigle, C. R. Klaus, C. J. Allain, A. Raimondi, M. Porter Scott, R. Chesworth, M. P. Moyer, R. A. Copeland, V. M. Richon, R. M. Pollock, K. W. Kuntz and H. Keilhack (2013). "Durable tumor regression in genetically altered malignant rhabdoid tumors by inhibition of methyltransferase EZH2." *Proc Natl Acad Sci U S A* 110(19): 7922-7927.

- Kollet, O., A. Peled, T. Byk, H. Ben-Hur, D. Greiner, L. Shultz and T. Lapidot (2000). "beta2 microglobulin-deficient (B2m(null)) NOD/SCID mice are excellent recipients for studying human stem cell function." *Blood* 95(10): 3102-3105.
- Kottlil, S., M. Y. Yan, K. N. Reitano, X. Zhang, R. Lempicki, G. Roby, M. Daucher, J. Yang, K. J. Cortez, M. Ghany, M. A. Polis and A. S. Fauci (2009). "Human immunodeficiency virus and hepatitis C infections induce distinct immunologic imprints in peripheral mononuclear cells." *Hepatology* 50(1): 34-45.
- Kros, J., P. Austin, N. Beslu, E. Kroon, R. K. Humphries and G. Sauvageau (2003). "In vitro expansion of hematopoietic stem cells by recombinant TAT-HOXB4 protein." *Nat Med* 9(11): 1428-1432.
- Kustikova, O., B. Fehse, U. Modlich, M. Yang, J. Dullmann, K. Kamino, N. von Neuhoff, B. Schlegelberger, Z. Li and C. Baum (2005). "Clonal dominance of hematopoietic stem cells triggered by retroviral gene marking." *Science* 308(5725): 1171-1174.
- Lam, A. C., K. Li, X. B. Zhang, C. K. Li, T. F. Fok, A. M. Chang, A. E. James, K. S. Tsang and P. M. Yuen (2001). "Preclinical ex vivo expansion of cord blood hematopoietic stem and progenitor cells: duration of culture; the media, serum supplements, and growth factors used; and engraftment in NOD/SCID mice." *Transfusion* 41(12): 1567-1576.
- Landt, S. G. e. a. (2014). "CHIP-seq guidelines and practices of the ENCODE and modENCODE consortia." *Genome Research* 22: 1813-1831.
- Lanzkron, S. M., M. I. Collector and S. J. Sharkis (1999). "Homing of long-term and short-term engrafting cells in vivo." *Ann N Y Acad Sci* 872: 48-54; discussion 54-46.
- Larsson, J. and S. Karlsson (2005). "The role of Smad signaling in hematopoiesis." *Oncogene* 24(37): 5676-5692.
- Laughlin, M. J., M. Eapen, P. Rubinstein, J. E. Wagner, M. J. Zhang, R. E. Champlin, C. Stevens, J. N. Barker, R. P. Gale, H. M. Lazarus, D. I. Marks, J. J. van Rood, A. Scaradavou and M. M. Horowitz (2004). "Outcomes after transplantation of cord blood or bone marrow from unrelated donors in adults with leukemia." *N Engl J Med* 351(22): 2265-2275.
- Li, H. and R. Durbin (2010). "Fast and accurate long-read alignment with Burrows-Wheeler transform." *Bioinformatics* 26(5): 589-595.
- Li, J. (2011). "Quiescence regulators for hematopoietic stem cell." *Exp Hematol* 39(5): 511-520.
- Liao, Y., M. B. Geyer, A. J. Yang and M. S. Cairo (2011). "Cord blood transplantation and stem cell regenerative potential." *Exp Hematol* 39(4): 393-412.
- Ljungman, P., A. Urbano-Ispizua, M. Cavazzana-Calvo, T. Demirer, G. Dini, H. Einsele, A. Gratwohl, A. Madrigal, D. Niederwieser, J. Passweg, V. Rocha, R. Saccardi, H. Schouten, N. Schmitz, G. Socie, A. Sureda, J. Apperley, B. European Group for and Marrow (2006). "Allogeneic and autologous transplantation for haematological diseases, solid tumours and immune disorders: definitions and current practice in Europe." *Bone Marrow Transplant* 37(5): 439-449.
- Ma, S., J. Huang and M. S. Moran (2009). "Identification of genes associated with multiple cancers via integrative analysis." *BMC Genomics* 10: 535.
- Mahmud, N., B. Petro, S. Baluchamy, X. Li, S. Taioli, D. Lavelle, J. G. Quigley, M. Suphangul and H. Araki (2014). "Differential effects of epigenetic modifiers on the expansion and maintenance of human cord blood stem/progenitor cells." *Biol Blood Marrow Transplant* 20(4): 480-489.
- Majewski, I. J., M. E. Ritchie, B. Phipson, J. Corbin, M. Pakusch, A. Ebert, M. Busslinger, H. Koseki, Y. Hu, G. K. Smyth, W. S. Alexander, D. J. Hilton and M. E. Blewitt (2010). "Opposing roles of polycomb repressive complexes in hematopoietic stem and progenitor cells." *Blood* 116(5): 731-739.
- Margueron, R. and D. Reinberg (2011). "The Polycomb complex PRC2 and its mark in life." *Nature* 469(7330): 343-349.

- Marks, H., T. Kalkan, R. Menafra, S. Denissov, K. Jones, H. Hofemeister, J. Nichols, A. Kranz, A. F. Stewart, A. Smith and H. G. Stunnenberg (2012). "The transcriptional and epigenomic foundations of ground state pluripotency." *Cell* 149(3): 590-604.
- McCabe, M. T., H. M. Ott, G. Ganji, S. Korenchuk, C. Thompson, G. S. Van Aller, Y. Liu, A. P. Graves, A. Della Pietra, 3rd, E. Diaz, L. V. LaFrance, M. Mellinger, C. Duquenne, X. Tian, R. G. Kruger, C. F. McHugh, M. Brandt, W. H. Miller, D. Dhanak, S. K. Verma, P. J. Tummino and C. L. Creasy (2012). "EZH2 inhibition as a therapeutic strategy for lymphoma with EZH2-activating mutations." *Nature* 492(7427): 108-112.
- McKinney-Freeman, S., P. Cahan, H. Li, S. A. Lacadie, H. T. Huang, M. Curran, S. Loewer, O. Naveiras, K. L. Kathrein, M. Konantz, E. M. Langdon, C. Lengerke, L. I. Zon, J. J. Collins and G. Q. Daley (2012). "The transcriptional landscape of hematopoietic stem cell ontogeny." *Cell Stem Cell* 11(5): 701-714.
- Medvinsky, A., S. Rybtsov and S. Taoudi (2011). "Embryonic origin of the adult hematopoietic system: advances and questions." *Development* 138(6): 1017-1031.
- Meissner, A., T. S. Mikkelsen, H. Gu, M. Wernig, J. Hanna, A. Sivachenko, X. Zhang, B. E. Bernstein, C. Nusbaum, D. B. Jaffe, A. Gnirke, R. Jaenisch and E. S. Lander (2008). "Genome-scale DNA methylation maps of pluripotent and differentiated cells." *Nature* 454(7205): 766-770.
- Mendez-Ferrer, S., T. V. Michurina, F. Ferraro, A. R. Mazloom, B. D. Macarthur, S. A. Lira, D. T. Scadden, A. Ma'ayan, G. N. Enikolopov and P. S. Frenette (2010). "Mesenchymal and haematopoietic stem cells form a unique bone marrow niche." *Nature* 466(7308): 829-834.
- Mikkelsen, T. S., M. Ku, D. B. Jaffe, B. Issac, E. Lieberman, G. Giannoukos, P. Alvarez, W. Brockman, T. K. Kim, R. P. Koche, W. Lee, E. Mendenhall, A. O'Donovan, A. Presser, C. Russ, X. Xie, A. Meissner, M. Wernig, R. Jaenisch, C. Nusbaum, E. S. Lander and B. E. Bernstein (2007). "Genome-wide maps of chromatin state in pluripotent and lineage-committed cells." *Nature* 448(7153): 553-560.
- Milhem, M., N. Mahmud, D. Lavelle, H. Araki, J. DeSimone, Y. Sauntharajah and R. Hoffman (2004). "Modification of hematopoietic stem cell fate by 5aza 2'deoxyctidine and trichostatin A." *Blood* 103(11): 4102-4110.
- Miranda, T. B., C. C. Cortez, C. B. Yoo, G. Liang, M. Abe, T. K. Kelly, V. E. Marquez and P. A. Jones (2009). "DZNep is a global histone methylation inhibitor that reactivates developmental genes not silenced by DNA methylation." *Mol Cancer Ther* 8(6): 1579-1588.
- Mochizuki-Kashio, M., Y. Mishima, S. Miyagi, M. Negishi, A. Saraya, T. Konuma, J. Shinga, H. Koseki and A. Iwama (2011). "Dependency on the polycomb gene Ezh2 distinguishes fetal from adult hematopoietic stem cells." *Blood* 118(25): 6553-6561.
- Moran-Crusio, K., L. Reavie, A. Shih, O. Abdel-Wahab, D. Ndiaye-Lobry, C. Lobry, M. E. Figueroa, A. Vasanthakumar, J. Patel, X. Zhao, F. Perna, S. Pandey, J. Madzo, C. Song, Q. Dai, C. He, S. Ibrahim, M. Beran, J. Zavadil, S. D. Nimer, A. Melnick, L. A. Godley, I. Aifantis and R. L. Levine (2011). "Tet2 loss leads to increased hematopoietic stem cell self-renewal and myeloid transformation." *Cancer Cell* 20(1): 11-24.
- Morisada, T., Y. Kubota, T. Urano, T. Suda and Y. Oike (2006). "Angiopoietins and angiopoietin-like proteins in angiogenesis." *Endothelium* 13(2): 71-79.
- Muller, A. M., A. Medvinsky, J. Strouboulis, F. Grosveld and E. Dzierzak (1994). "Development of hematopoietic stem cell activity in the mouse embryo." *Immunity* 1(4): 291-301.
- Muller-Sieburg, C. E., R. H. Cho, M. Thoman, B. Adkins and H. B. Sieburg (2002). "Deterministic regulation of hematopoietic stem cell self-renewal and differentiation." *Blood* 100(4): 1302-1309.
- Navakauskiene, R., V. V. Borutinskaite, G. Treigyte, J. Savickiene, D. Matuzevicius, D. Navakauskas and K. E. Magnusson (2014). "Epigenetic changes during hematopoietic cell granulocytic differentiation--comparative analysis of primary CD34+ cells, KG1 myeloid cells and mature neutrophils." *BMC Cell Biol* 15: 4.
- Neff, T. and S. A. Armstrong (2013). "Recent progress toward epigenetic therapies: the example of mixed lineage leukemia." *Blood* 121(24): 4847-4853.

- Neokleous, N., A. Sideri and C. Peste-Tsilimidis (2011). "Double cord blood transplantation: co-operation or competition?" *Hematol Rep* 3(1): e6.
- Ning, Y., T. Wei, C. Defu, X. Yonggang, H. Da, C. Dafu, S. Lei and G. Zhizhong (2009). "The research of degradability of a novel biodegradable coralline hydroxyapatite after implanted into rabbit." *J Biomed Mater Res A* 88(3): 741-746.
- Nitsche, A., M. Zhang, T. Clauss, W. Siegert, K. Brune and A. Pahl (2007). "Cytokine profiles of cord and adult blood leukocytes: differences in expression are due to differences in expression and activation of transcription factors." *BMC Immunol* 8: 18.
- Novershtern, N., A. Subramanian, L. N. Lawton, R. H. Mak, W. N. Haining, M. E. McConkey, N. Habib, N. Yosef, C. Y. Chang, T. Shay, G. M. Frampton, A. C. Drake, I. Leskov, B. Nilsson, F. Pfeffer, D. Dombkowski, J. W. Evans, T. Liefeld, J. S. Smutko, J. Chen, N. Friedman, R. A. Young, T. R. Golub, A. Regev and B. L. Ebert (2011). "Densely interconnected transcriptional circuits control cell states in human hematopoiesis." *Cell* 144(2): 296-309.
- Obier, N. and A. M. Muller (2010). "Chromatin flow cytometry identifies changes in epigenetic cell states." *Cells Tissues Organs* 191(3): 167-174.
- Obier, N., C. F. Uhlemann and A. M. Muller (2010). "Inhibition of histone deacetylases by Trichostatin A leads to a HoxB4-independent increase of hematopoietic progenitor/stem cell frequencies as a result of selective survival." *Cytotherapy* 12(7): 899-908.
- Orford, K., P. Kharchenko, W. Lai, M. C. Dao, D. J. Worhunsky, A. Ferro, V. Janzen, P. J. Park and D. T. Scadden (2008). "Differential H3K4 methylation identifies developmentally poised hematopoietic genes." *Dev Cell* 14(5): 798-809.
- Orkin, S. H. and L. I. Zon (2002). "Hematopoiesis and stem cells: plasticity versus developmental heterogeneity." *Nat Immunol* 3(4): 323-328.
- Orkin, S. H. and L. I. Zon (2008). "Hematopoiesis: an evolving paradigm for stem cell biology." *Cell* 132(4): 631-644.
- Park, I. K., D. Qian, M. Kiel, M. W. Becker, M. Pihalja, I. L. Weissman, S. J. Morrison and M. F. Clarke (2003). "Bmi-1 is required for maintenance of adult self-renewing haematopoietic stem cells." *Nature* 423(6937): 302-305.
- Paul, T. A., J. Bies, D. Small and L. Wolff (2010). "Signatures of polycomb repression and reduced H3K4 trimethylation are associated with p15INK4b DNA methylation in AML." *Blood* 115(15): 3098-3108.
- Pauler, F. M., M. A. Sloane, R. Huang, K. Regha, M. V. Koerner, I. Tamir, A. Sommer, A. Aszodi, T. Jenuwein and D. P. Barlow (2009). "H3K27me3 forms BLOCs over silent genes and intergenic regions and specifies a histone banding pattern on a mouse autosomal chromosome." *Genome Res* 19(2): 221-233.
- Peled, T., J. Mandel, R. N. Goudsmid, C. Landor, N. Hasson, D. Harati, M. Austin, A. Hasson, E. Fibach, E. J. Shpall and A. Nagler (2004). "Pre-clinical development of cord blood-derived progenitor cell graft expanded ex vivo with cytokines and the polyamine copper chelator tetraethylenepentamine." *Cytotherapy* 6(4): 344-355.
- Piacibello, W., F. Sanavio, L. Garetto, A. Severino, D. Bergandi, J. Ferrario, F. Fagioli, M. Berger and M. Aglietta (1997). "Extensive amplification and self-renewal of human primitive hematopoietic stem cells from cord blood." *Blood* 89(8): 2644-2653.
- Pinello, L., J. Xu, S. H. Orkin and G. C. Yuan (2014). "Analysis of chromatin-state plasticity identifies cell-type-specific regulators of H3K27me3 patterns." *Proc Natl Acad Sci U S A* 111(3): E344-353.
- Probst, A. V., E. Dunleavy and G. Almouzni (2009). "Epigenetic inheritance during the cell cycle." *Nat Rev Mol Cell Biol* 10(3): 192-206.
- Purton, L. E. and D. T. Scadden (2008). *The hematopoietic stem cell niche*. StemBook. Cambridge (MA).

- Reitano, K. N., S. Kottlilil, C. M. Gille, X. Zhang, M. Yan, M. A. O'Shea, G. Roby, C. W. Hallahan, J. Yang, R. A. Lempicki, J. Arthos and A. S. Fauci (2009). "Defective plasmacytoid dendritic cell-NK cell cross-talk in HIV infection." *AIDS Res Hum Retroviruses* 25(10): 1029-1037.
- Rice, K. L., I. Hormaeche and J. D. Licht (2007). "Epigenetic regulation of normal and malignant hematopoiesis." *Oncogene* 26(47): 6697-6714.
- Rocha, V. and H. E. Broxmeyer (2010). "New approaches for improving engraftment after cord blood transplantation." *Biol Blood Marrow Transplant* 16(1 Suppl): S126-132.
- Rocha, V., A. Crotta, A. Ruggeri, D. Purtill, K. Boudjedir, A. L. Herr, I. Ionescu, E. Gluckman and R. Eurocord (2010). "Double cord blood transplantation: extending the use of unrelated umbilical cord blood cells for patients with hematological diseases." *Best Pract Res Clin Haematol* 23(2): 223-229.
- Roh, T. Y., S. Cuddapah, K. Cui and K. Zhao (2006). "The genomic landscape of histone modifications in human T cells." *Proc Natl Acad Sci U S A* 103(43): 15782-15787.
- Rountree, M. R., K. E. Bachman, J. G. Herman and S. B. Baylin (2001). "DNA methylation, chromatin inheritance, and cancer." *Oncogene* 20(24): 3156-3165.
- Rugg-Gunn, P. J., B. J. Cox, A. Ralston and J. Rossant (2010). "Distinct histone modifications in stem cell lines and tissue lineages from the early mouse embryo." *Proc Natl Acad Sci U S A* 107(24): 10783-10790.
- Saeed, A. I., V. Sharov, J. White, J. Li, W. Liang, N. Bhagabati, J. Braisted, M. Klapa, T. Currier, M. Thiagarajan, A. Sturn, M. Snuffin, A. Rezantsev, D. Popov, A. Ryltsov, E. Kostukovich, I. Borisovsky, Z. Liu, A. Vinsavich, V. Trush and J. Quackenbush (2003). "TM4: a free, open-source system for microarray data management and analysis." *Biotechniques* 34(2): 374-378.
- Sauvageau, G., U. Thorsteinsdottir, C. J. Eaves, H. J. Lawrence, C. Largman, P. M. Lansdorp and R. K. Humphries (1995). "Overexpression of HOXB4 in hematopoietic cells causes the selective expansion of more primitive populations in vitro and in vivo." *Genes Dev* 9(14): 1753-1765.
- Sauvageau, M. and G. Sauvageau (2010). "Polycomb group proteins: multi-faceted regulators of somatic stem cells and cancer." *Cell Stem Cell* 7(3): 299-313.
- Schiedlmeier, B., A. C. Santos, A. Ribeiro, N. Moncaut, D. Lesinski, H. Auer, K. Kornacker, W. Ostertag, C. Baum, M. Mallo and H. Klump (2007). "HOXB4's road map to stem cell expansion." *Proc Natl Acad Sci U S A* 104(43): 16952-16957.
- Schuettengruber, B., D. Chourrout, M. Vervoort, B. Leblanc and G. Cavalli (2007). "Genome regulation by polycomb and trithorax proteins." *Cell* 128(4): 735-745.
- Schuller, C. E., K. Jankowski and K. L. Mackenzie (2007). "Telomere length of cord blood-derived CD34(+) progenitors predicts erythroid proliferative potential." *Leukemia* 21(5): 983-991.
- Seet, L. F., E. Teng, Y. S. Lai, J. Laning, M. Kraus, S. Wnendt, S. Merchav and S. L. Chan (2009). "Valproic acid enhances the engraftability of human umbilical cord blood hematopoietic stem cells expanded under serum-free conditions." *Eur J Haematol* 82(2): 124-132.
- Seita, J. and I. L. Weissman (2010). "Hematopoietic stem cell: self-renewal versus differentiation." *Wiley Interdiscip Rev Syst Biol Med* 2(6): 640-653.
- Shen, L., N. Shao, X. Liu and E. Nestler (2014). "ngs.plot: Quick mining and visualization of next-generation sequencing data by integrating genomic databases." *BMC Genomics* 15(1): 284.
- Shen, X., Y. Liu, Y. J. Hsu, Y. Fujiwara, J. Kim, X. Mao, G. C. Yuan and S. H. Orkin (2008). "EZH1 mediates methylation on histone H3 lysine 27 and complements EZH2 in maintaining stem cell identity and executing pluripotency." *Mol Cell* 32(4): 491-502.
- Shilatifard, A. (2012). "The COMPASS family of histone H3K4 methylases: mechanisms of regulation in development and disease pathogenesis." *Annu Rev Biochem* 81: 65-95.

- Shmelkov, S. V., R. St Clair, D. Lyden and S. Rafii (2005). "AC133/CD133/Prominin-1." *Int J Biochem Cell Biol* 37(4): 715-719.
- Sideri, A., N. Neokleous, P. Brunet De La Grange, B. Guerton, M. C. Le Bousse Kerdilles, G. Uzan, C. Peste-Tsilimidos and E. Gluckman (2011). "An overview of the progress on double umbilical cord blood transplantation." *Haematologica* 96(8): 1213-1220.
- Srour, E. F., X. Tong, K. W. Sung, P. A. Plett, S. Rice, J. Daggy, C. T. Yiannoutsos, R. Abonour and C. M. Orschell (2005). "Modulation of in vitro proliferation kinetics and primitive hematopoietic potential of individual human CD34+CD38-/lo cells in G0." *Blood* 105(8): 3109-3116.
- Stanevsky, A., G. Goldstein and A. Nagler (2009). "Umbilical cord blood transplantation: pros, cons and beyond." *Blood Rev* 23(5): 199-204.
- Strahl, B. D. and C. D. Allis (2000). "The language of covalent histone modifications." *Nature* 403(6765): 41-45.
- Tadokoro, Y., H. Ema, M. Okano, E. Li and H. Nakauchi (2007). "De novo DNA methyltransferase is essential for self-renewal, but not for differentiation, in hematopoietic stem cells." *J Exp Med* 204(4): 715-722.
- Tarnani, M., L. Laurenti, P. Chiusolo, F. Sora, I. Innocenti, G. Leone and S. Sica (2008). "Simultaneous double mismatched cord blood transplantation in a young patient with secondary myelodysplastic syndrome: feasibility and complications." *Leuk Lymphoma* 49(4): 821-823.
- Till, J. E. and C. E. Mc (1961). "A direct measurement of the radiation sensitivity of normal mouse bone marrow cells." *Radiat Res* 14: 213-222.
- Trowbridge, J. J., J. W. Snow, J. Kim and S. H. Orkin (2009). "DNA methyltransferase 1 is essential for and uniquely regulates hematopoietic stem and progenitor cells." *Cell Stem Cell* 5(4): 442-449.
- van den Boom, V., M. Rozenveld-Geugien, F. Bonardi, D. Malanga, D. van Gosliga, A. M. Heijink, G. Viglietto, G. Morrone, F. Fusetti, E. Vellenga and J. J. Schuringa (2013). "Nonredundant and locus-specific gene repression functions of PRC1 paralog family members in human hematopoietic stem/progenitor cells." *Blood* 121(13): 2452-2461.
- Verma, S., Tian, X, LaFrance, LV, Duquenne, C, Suarez, DP, Newlander, KA, Romeril, SP, Burgess, JL, Grant, SW, Brackley, JA, Graves, AP, Scherzer, DA, Shu, A, *et al.* Miller WH (2012). "Identification of Potent, Selective, Cell-Active Inhibitors of the Histone Lysine Methyltransferase EZH2." *ACS Med. Chem. Lett.* 3: 1091-1096.
- Voigt, P., W. W. Tee and D. Reinberg (2013). "A double take on bivalent promoters." *Genes Dev* 27(12): 1318-1338.
- Waddington, C. H. (2012). "The epigenotype. 1942." *Int J Epidemiol* 41(1): 10-13.
- Wagner, J. E., J. N. Barker, T. E. DeFor, K. S. Baker, B. R. Blazar, C. Eide, A. Goldman, J. Kersey, W. Krivit, M. L. MacMillan, P. J. Orchard, C. Peters, D. J. Weisdorf, N. K. Ramsay and S. M. Davies (2002). "Transplantation of unrelated donor umbilical cord blood in 102 patients with malignant and nonmalignant diseases: influence of CD34 cell dose and HLA disparity on treatment-related mortality and survival." *Blood* 100(5): 1611-1618.
- Walasek, M. A., R. van Os and G. de Haan (2012). "Hematopoietic stem cell expansion: challenges and opportunities." *Ann N Y Acad Sci* 1266: 138-150.
- Walenda, T., G. Bokermann, M. S. Ventura Ferreira, D. M. Piroth, T. Hieronymus, S. Neuss, M. Zenke, A. D. Ho, A. M. Muller and W. Wagner (2011). "Synergistic effects of growth factors and mesenchymal stromal cells for expansion of hematopoietic stem and progenitor cells." *Exp Hematol* 39(6): 617-628.
- Wan, Y., X. Ren, Y. Ren, J. Wang, Z. Hu, X. Xie and J. Xu (2014). "As a genetic adjuvant, CTA improves the immunogenicity of DNA vaccines in an ADP-ribosyltransferase activity- and IL-6-dependent manner." *Vaccine* 32(19): 2173-2180.
- Wang, H., L. Wang, H. Erdjument-Bromage, M. Vidal, P. Tempst, R. S. Jones and Y. Zhang (2004). "Role of histone H2A ubiquitination in Polycomb silencing." *Nature* 431(7010): 873-878.

- Wang, J. C., M. Doedens and J. E. Dick (1997). "Primitive human hematopoietic cells are enriched in cord blood compared with adult bone marrow or mobilized peripheral blood as measured by the quantitative in vivo SCID-repopulating cell assay." *Blood* 89(11): 3919-3924.
- Watt, F. M. and B. L. Hogan (2000). "Out of Eden: stem cells and their niches." *Science* 287(5457): 1427-1430.
- Wei, Y., Y. H. Chen, L. Y. Li, J. Lang, S. P. Yeh, B. Shi, C. C. Yang, J. Y. Yang, C. Y. Lin, C. C. Lai and M. C. Hung (2011). "CDK1-dependent phosphorylation of EZH2 suppresses methylation of H3K27 and promotes osteogenic differentiation of human mesenchymal stem cells." *Nat Cell Biol* 13(1): 87-94.
- Weidner, C. I., T. Walenda, Q. Lin, M. M. Wolfler, B. Denecke, I. G. Costa, M. Zenke and W. Wagner (2013). "Hematopoietic Stem and Progenitor Cells Acquire Distinct DNA-Hypermethylation During in vitro Culture." *Sci Rep* 3: 3372.
- Weishaupt, H. and J. L. Attema (2010). "A Method to Study the Epigenetic Chromatin States of Rare Hematopoietic Stem and Progenitor Cells; MiniChIP-Chip." *Biol Proced Online* 12(1): 1-17.
- Weishaupt, H., M. Sigvardsson and J. L. Attema (2010). "Epigenetic chromatin states uniquely define the developmental plasticity of murine hematopoietic stem cells." *Blood* 115(2): 247-256.
- Wilson, A. and A. Trumpp (2006). "Bone-marrow haematopoietic-stem-cell niches." *Nat Rev Immunol* 6(2): 93-106.
- Wisniewski, D., M. Affer, J. Willshire and B. Clarkson (2011). "Further phenotypic characterization of the primitive lineage- CD34+CD38-CD90+CD45RA- hematopoietic stem cell/progenitor cell sub-population isolated from cord blood, mobilized peripheral blood and patients with chronic myelogenous leukemia." *Blood Cancer J* 1(9): e36.
- Xie, H., J. Xu, J. H. Hsu, M. Nguyen, Y. Fujiwara, C. Peng and S. H. Orkin (2014). "Polycomb repressive complex 2 regulates normal hematopoietic stem cell function in a developmental-stage-specific manner." *Cell Stem Cell* 14(1): 68-80.
- Yamagata, Y., V. Parietti, D. Stockholm, G. Corre, C. Poinson, N. Touleimat, D. Delafoy, C. Besse, J. Tost, A. Galy and A. Paldi (2012). "Lentiviral transduction of CD34(+) cells induces genome-wide epigenetic modifications." *PLoS One* 7(11): e48943.
- Yeoh, J. S., R. van Os, E. Weersing, A. Ausema, B. Dontje, E. Vellenga and G. de Haan (2006). "Fibroblast growth factor-1 and -2 preserve long-term repopulating ability of hematopoietic stem cells in serum-free cultures." *Stem Cells* 24(6): 1564-1572.
- Yip, M., D. Da He, E. Winokur, A. G. Balderrama, R. Sheridan and H. Ma (2009). "A flexible pressure monitoring system for pressure ulcer prevention." *Conf Proc IEEE Eng Med Biol Soc* 2009: 1212-1215.
- Young, M. D., T. A. Willson, M. J. Wakefield, E. Trounson, D. J. Hilton, M. E. Blewitt, A. Oshlack and I. J. Majewski (2011). "ChIP-seq analysis reveals distinct H3K27me3 profiles that correlate with transcriptional activity." *Nucleic Acids Res* 39(17): 7415-7427.
- Zang, C., D. E. Schones, C. Zeng, K. Cui, K. Zhao and W. Peng (2009). "A clustering approach for identification of enriched domains from histone modification ChIP-Seq data." *Bioinformatics* 25(15): 1952-1958.
- Zhang, C. C., M. Kaba, G. Ge, K. Xie, W. Tong, C. Hug and H. F. Lodish (2006). "Angiopoietin-like proteins stimulate ex vivo expansion of hematopoietic stem cells." *Nat Med* 12(2): 240-245.
- Zhang, C. C., M. Kaba, S. Iizuka, H. Huynh and H. F. Lodish (2008). "Angiopoietin-like 5 and IGFBP2 stimulate ex vivo expansion of human cord blood hematopoietic stem cells as assayed by NOD/SCID transplantation." *Blood* 111(7): 3415-3423.
- Zhang, C. C. and H. F. Lodish (2004). "Insulin-like growth factor 2 expressed in a novel fetal liver cell population is a growth factor for hematopoietic stem cells." *Blood* 103(7): 2513-2521.

Zhang, X., A. C. Frank, C. M. Gille, M. Daucher, J. Kabat, S. Becker, R. A. Lempicki, K. J. Cortez, M. A. Polis, G. M. Subramanian and S. Kottlil (2009). "Altered regulation of extrinsic apoptosis pathway in HCV-infected HCC cells enhances susceptibility to mapatumumab-induced apoptosis." *Hepatology* 39(12): 1178-1189.

Zheng, J., H. Huynh, M. Umikawa, R. Silvano and C. C. Zhang (2011). "Angiopoietin-like protein 3 supports the activity of hematopoietic stem cells in the bone marrow niche." *Blood* 117(2): 470-479.

Zheng, J., M. Umikawa, C. Cui, J. Li, X. Chen, C. Zhang, H. Huynh, X. Kang, R. Silvano, X. Wan, J. Ye, A. P. Canto, S. H. Chen, H. Y. Wang, E. S. Ward and C. C. Zhang (2012). "Inhibitory receptors bind ANGPTLs and support blood stem cells and leukaemia development." *Nature* 485(7400): 656-660.

Zheng, J., M. Umikawa, S. Zhang, H. Huynh, R. Silvano, B. P. Chen, L. Chen and C. C. Zhang (2011). "Ex vivo expanded hematopoietic stem cells overcome the MHC barrier in allogeneic transplantation." *Cell Stem Cell* 9(2): 119-130.

Zhu, J., M. Adli, J. Y. Zou, G. Verstappen, M. Coyne, X. Zhang, T. Durham, M. Miri, V. Deshpande, P. L. De Jager, D. A. Bennett, J. A. Houmard, D. M. Muoio, T. T. Onder, R. Camahort, C. A. Cowan, A. Meissner, C. B. Epstein, N. Shores and B. E. Bernstein (2013). "Genome-wide chromatin state transitions associated with developmental and environmental cues." *Cell* 152(3): 642-654.

9 ACKNOWLEDGMENTS

First of all, I would like to express my heartfelt thanks to Professor Albrecht Müller for his guidance, support, experience and encouragement during these years.

I also thank my second supervisor Prof. Dr. Ricardo Benavente, and I am especially grateful to Andrea Reusch, Dr. Rainer Claus, Dr. Nadine Obier and Dr. Matthias Becker for their scientific input into this study and for all the scientific discussions about my experiments.

I'm thankful to all the former and current members of AGM that made these last years so magical. My sincere gratitude goes to the dear friends that constantly encourage, help, trust and love me : Justyna, Vroni, Dr. Nadine Obier, Dr. Ruhel Amhad and Dr. Ankita Minhas.

I want to say thanks to all my true friends, my chosen family. For all the love, the power and the trust I always needed. Thank you Chiara, Nicola, Cla, Luca, Davide, Carla, Markus, Silvia, Sara, Anna, Marghe and Vazzo.

Most importantly, I want to give my loving gratitude to my Dad, my Mom and my Brother, for the constant support and because they are the most important people in my life.

10 AFFIDAVIT

I hereby declare that my thesis entitled:

PRC2 inhibition counteracts the culture-associated loss of engraftment potential of human cord blood-derived hematopoietic stem/progenitor cells

is the result of my own work except the analyses done by collaborators (see next page). I did not receive any help or support from commercial consultants.

All sources and / or materials used are listed or specified in the thesis.

Furthermore, I verify that this entire thesis or any part of its contents has not been submitted or is not under consideration for another examination process, neither in identical nor in similar form.

Würzburg, Date Signature

Hereby it is confirmed that I worked on my own on the following parts of my doctoral thesis:

CB-CD34⁺ cells isolation and expansion, immunphenotyping, chromatin FACS analysis, Western blot analysis, analysis of gene expression, immunofluorescence, CHIP assay, NSG mice transplantation and engraftment analyses.


Fig. 6: for global gene expression analysis, I performed CB-CD34⁺ cells isolation, expansion and mRNA isolation and quality check. Microarray preparation and determination of gene expression levels were performed by Prof. M. Zenke and Dr. Qiong Lin, RWTH Aachen.

Figs. 9 - 11, 14 - 17: for CHIP-seq analysis, I performed CB-CD34⁺ cell isolation, expansion, chromatin preparation, chromatin immunoprecipitation, and chromatin quality controls. Library preparation and sequencing was performed by PD Dr. Rainer Claus in collaboration with Professor Christoph Plass, DKFZ Heidelberg. CHIP-seq bioinformatics were discussed in a group comprising me, Albrecht Müller and Rainer Claus. The bioinformatic analyses were performed by Rainer Claus.

Linda Varagnolo

Place, Date 1h. Oct. 2014 Signature 

Prof. Dr. Albrecht Müller

Place, Date 14. Oct. 2014 Signature 

11 LIST OF PUBLICATIONS

Varagnolo L, Claus R, Lin Q, Plass C, Wagner W, Zenke M, Müller AM. (2014) “PRC2 inhibition counteracts the culture-associated loss of engraftment potential of human cord blood-derived hematopoietic stem/progenitor cells.” (Submitted).

Boussaad I, **Varagnolo L**, Hornich V, Rieger L, Krockenberger M, Stuehmer T, Kranzfelder D, Mueller AM, Schneider-Schaulies S. (2011) “Wild-type measles virus interferes with short-term engraftment of human CD34+ hematopoietic progenitor cells.” *J Virol.* 2011 Aug;85(15):7710-8.

Benedikt A, Baltruschat S, Scholz B, Bursen A, Arrey TN, Meyer B, **Varagnolo L**, Müller AM, Karas M, Dingermann T, Marschalek R. (2010) “The leukemogenic AF4-MLL fusion protein causes P-TEFb kinase activation and altered epigenetic signatures.” *Leukemia.* 2011 Jan;25(1):135-44.